

Technical Completion Report

to

University of California Water Resources Center

Long-term Nitrate Leaching Below the Root Zone in California Tree Fruit Orchards

**Michelle Denton
Sevim Onsoy
Thomas Harter
Jan W. Hopmans
William R. Horwath**



July 2004



TECHNICAL COMPLETION REPORT

to

University of California Water Resources Center, Project W-919

Project Title: Transport and Fate of Nitrate-Nitrogen in Heterogeneous, Unsaturated Sediments below the Root Zone

Project Location Kearney Agricultural Center, Parlier, California

Project Scientists Michelle Denton, Graduate Research Assistant, University of California, Davis;
Yuksel S. Onsoy, Ph.D. Candidate, Graduate Research Assistant, University of California, Davis;

Project Leaders

Thomas Harter, Ph.D.
Assoc. CE Specialist, Subsurface Hydrology
thharter@ucdavis.edu

William R. Horwath, Ph.D.
Assoc. Prof., Soil Biogeochemistry
wrhorwath@ucdavis.edu

Jan Hopmans, Ph.D.
Professor, Water Management
jwhopmans@ucdavis.edu

Department of Land, Air, and Water Resources
University of California
Davis, CA 95616-8628

Cooperators

Scott Johnson, Ph.D.
Pomology Specialist
Kearney Agricultural Center
9240 S. Riverbend Ave.
Parlier, CA 93648

Dick Rice, Ph.D.
Entomologist, AES
Kearney Agricultural Center
9240 S. Riverbend Ave.
Parlier, CA 93648

Funding Support

Fertilizer Research and Education Program, *Project 97—0365 M97-04*, 1998-2001
\$ 86,905

Fertilizer Research and Education Program, *Project 01—0584*, 2002-2004
\$ 58,468

Geoprobe Systems[®], 3 months in-kind services: soil drilling and sampling device GH-40, 1997
\$ 18,000

California Tree Fruit Agreement, 1997-2000
\$ 26,189

California Water Resources Center, *Project W-919*, 1999-2001
\$ 54,500

TABLE OF CONTENTS

LIST OF TABLES	4
LIST OF FIGURES	5
OBJECTIVES	9
EXECUTIVE SUMMARY	9
ACKNOWLEDGMENTS	11
1. INTRODUCTION.....	13
Problem Identification:.....	13
Current Approach:.....	13
Shortcomings of Current Approaches:.....	13
Past Research on Nitrate Flux in Deep Vadose Zones:.....	14
Research and Educational Needs:	14
2. SITE DESCRIPTION AND FIELD EXPERIMENTATION	15
2.1 Orchard Experiment Overview	15
2.2 Fertilizer Experiment and Nitrate Application	16
2.3 Irrigation	16
2.4 Weather Data	17
Precipitation	18
Reference Evapotranspiration	18
Air temperature	18
Solar radiation	19
Vapor pressure.....	19
Relative humidity	19
Dew point	20
Wind speed.....	20
Soil temperature	20
2.5 Plant yield, nutrient uptake, and soil water quality.....	20
2.6 Bromide tracer experiment, October 2, 1996.....	21
2.7 Core sampling, 1997	22
3. LABORATORY METHODS	24
3.1 Hydraulic characterization: Multi-step outflow experiment.....	24
3.2 Hydraulic characterization- inverse modeling	25
3.3 Scaling.....	27
4. RESULTS	29
4.1 Geologic Framework	29
4.2 Laboratory Measurements	31
4.3 Multi-step Outflow Experiment and Parameter Estimation.....	32
4.4 Generating Pedotransfer Functions: NeuroMultistep	34

4.5 Scaling.....	35
4.6 Nitrogen Field Scale Mass Balance, Nitrogen Spatial Variability, and Total Unsaturated Zone Nitrogen Storage.....	36
5. DISCUSSION AND CONCLUSIONS	37
Overcoming Site-Specificity:	40
Publications and New Products Generated by Project:.....	41
Extension Activities Related to This Project:	41
Technical/Scientific Conference Presentations:	42
6. REFERENCES.....	43

LIST OF TABLES

	<u>PAGE</u>
Table 2.2.1. Fertilizer amounts and application dates.	48
Table 2.3.1. Irrigation dates for the orchard. The date shown is the afternoon start date.	49
Table 2.4.1. Explanation of CIMIS report contents.	50
Table 2.4.2. Summary statistics for weather averages from 1983 to 1999. All values are monthly with exceptions noted.	50
Table 2.4.3. Department of Water Resources CIMIS Sensor Specifications	51
Table 2.5.1. Fruit yield, load and weight summary, including the 7 year average.	53
Table 2.5.2. Percent nitrogen in fruit on a dry mass basis (1983).	53
Table 2.5.3. Leaf nutrients.	54
Table 2.5.4. Soil nitrate concentration, in ppm, and pH in October, 1991.	55
Table 2.5.5. Soil nitrate concentration, in ppm, in January, 1995.	55
Table 3.3.1. Comparison of scaling subgroup assignments and data quality for each soil sample.	56
Table 4.2.1. Summary of DANR laboratory measurements.	59
Table 4.2.2. Summary statistics of DANR laboratory measurements	63
Table 4.3.1. Summary of the optimized van Genuchten parameters.	65
Table 4.3.2. Summary statistics of the van Genuchten parameters.	68
Table 4.5.1. Summary of percent reduction in sum of squares (SS) for subgroup "sandy loam" in groups 2, 3, and 4 using two scaling methods.	69

LIST OF FIGURES

	<u>PAGE</u>
Figure 2.1.1. Fantasia Nectarine Orchard Plot	71
Figure 2.2.1. Hand Application of Fertilizer	72
Figure 2.4.1. Average monthly precipitation from 1983 to 1999.	73
Figure 2.4.2. Average monthly ETo from 1983 to 1999.	73
Figure 2.4.3. Average monthly air temperature from 1983 to 1999.	73
Figure 2.4.4. Average monthly solar radiation from 1983 to 1999.	74
Figure 2.4.5. Average monthly vapor pressure from 1983 to 1999.	74
Figure 2.4.6. Average monthly relative humidity from 1983 to 1999.	74
Figure 2.4.7. Average monthly dew point from 1983 to 1999.	75
Figure 2.4.8. Average monthly wind speed from 1983 to 1999.	75
Figure 2.4.9. Average soil temperature from 1983 to 1999.	75
Figure 2.5.1a. Soil nitrate concentration measured in 1991 and 1995 for the 0 treatment subplot.	76
Figure 2.5.1b. Soil nitrate concentration for the 100 lbs N/acre subplot.	76
Figure 2.5.1c. Soil nitrate concentration for the 175 lbs N/acre subplot.	76
Figure 2.5.1d. Soil nitrate concentration for the 250 lbs N/acre subplot.	77
Figure 2.5.1e. Soil nitrate concentration for the 325 lbs N/acre subplot.	77
Figure 2.7.1. Fantasia Nectarine Soil Core Map	78
Figure 2.7.2. Deep Soil Profile Sampling Strategy	79
Figure 2.7.3. Soil Sample Numbering	80

	<u>PAGE</u>
Figure 3.1.1. Fantasia Nectarine Hydraulic Soil Core Map	81
Figure 4.1.1. Stratigraphic cross-section along a tree-row showing the major stratigraphic units.	82
Figure 4.2.1 a-i. Histograms for the nine laboratory measurements for 118 soil samples.	83-85
Figure 4.2.2a-b. Categorized box and whisker plots for bulk density.	86
Figure 4.2.3a-b. Categorized box and whisker plots for organic matter content.	87
Figure 4.2.4a-b. Categorized box and whisker plots for organic carbon content.	88
Figure 4.2.5a-b. Categorized box and whisker plots for porosity.	89
Figure 4.2.6a-b. Categorized box and whisker plots for saturated water content.	90
Figure 4.2.7a-b. Categorized box and whisker plots for the sand fraction.	91
Figure 4.2.8a-b. Categorized box and whisker plots for the silt fraction.	92
Figure 4.2.9a-b. Categorized box and whisker plots for the clay fraction.	93
Figure 4.2.10a-b. Categorized box and whisker plots for unsaturated hydraulic conductivity.	94
Figure 4.3.1a-b. Multi-step outflow experiment results and optimized curves for a sample with transient data.	95
Figure 4.3.2. Multi-step outflow results and optimized curve for a sample with steady state data.	96
Figure 4.3.3a-d. Histograms for the van Genuchten parameters for the 97 samples.	97-98
Figure 4.3.4a-h. Categorized box and whisker plot for the van Genuchten parameters.	99-102
Figure 4.5.1a-e. Soil water retention (a) unscaled, (b) scaled using method 1, and (c) scaled using method 2. Original and de-scaled soil water pressure head using method 1 (d) and method 2 (e). All curves represent Group 1, Population 1.	103-104

	<u>PAGE</u>
Figure 4.5.1f-j. Unsaturated hydraulic conductivity (f) unscaled, (g) scaled using method 1, and (h) scaled using method 2. Original and de-scaled unsaturated hydraulic conductivity using method 1 (i) and method 2 (j). All curves represent Group 1, Population 1.	105-106
Figure 4.5.2a-e. Soil water retention (a) unscaled, (b) scaled using method 1, and (c) scaled using method 2. Original and de-scaled soil water pressure head using method 1 (d) and method 2 (e). All curves represent Group 2, Population 2.	107-108
Figure 4.5.2f-j. Unsaturated hydraulic conductivity (f) unscaled, (g) scaled using method 1, and (h) scaled using method 2. Original and de-scaled unsaturated hydraulic conductivity using method 1 (i) and method 2 (j). All curves represent Group 2, Population 2.	109-110
Figure 4.5.3a-e. Soil water pressure head (a)unscaled,(b) scaled using method 1, and (c) scaled using method 2. Original and descaled soil water pressure head using method 1(d) and method 2 (e). All curves represent Group 2, Population 1, subgroup sandy loam.	111-112
Figure 4.5.3f-j. Unsaturated hydraulic conductivity (f) unscaled, (g) scaled using method 1, and (h) scaled using method 2. Original and de-scaled unsaturated hydraulic conductivity using method 1 (i) and method 2 (j). All curves represent Group 2, Population 1, subgroup sandy loam.	113-114
Figure 4.5.4a-e. Soil water pressure head (a) unscaled (b) scaled using method 1,and (c) scaled using method 2. Original and descaled soil water pressure head curves using method 1 (d) and method 2 (e). All curves represent Group 3, Population 1, subgroup sandy loam.	115-116
Figure 4.5.4f-j. Unsaturated hydraulic conductivity (f) unscaled, (g) scaled using method 1,and (h) scaled using method 2. Original and descaled unsaturated hydraulic conductivity using method 1 (i) and method 2 (j). All curves represent Group 3, Population 1, subgroup sandy loam.	117-118
Figure 4.5.5a-e. Soil water pressure head (a) unscaled, (b) scaled using method 1, and (c) scaled using method 2. Original and descaled soil water pressure head curves using method 1 (d) and method 2 (e). All curves represent Group 4, Population 1, subgroup Sandy loam.	119-120

	<u>PAGE</u>
Figure 4.5.5f-j. Unsaturated hydraulic conductivity (f) unscaled, (g) scaled using method 1, and (h) scaled using method 2. Original and descaled unsaturated hydraulic conductivity (i-j) for Group 4, Population 1, subgroup sandy loam.	121-122
Photos 1 – 11. Flood irrigation of tree-row basins after bromide application.	123-125

OBJECTIVES

The objective of our work is to provide a better understanding of the processes governing the transport and fate of nitrate-nitrogen in deep alluvial unsaturated zones. Such unsaturated zones occur throughout the eastern San Joaquin Valley and many other agricultural production regions of the Southwestern United States. We develop and analyze an intensive field dataset to determine the geologic, hydrologic, and geochemical framework that controls the long-term rate of nitrate leaching to groundwater under various fertilizer application rates. For this project, a site with a well-controlled fertilization trial was chosen. The project site is located on top of a 16-m thick alluvial unsaturated sediment sequence that is part of the Kings River alluvial fan in Fresno County. Our specific objectives in this report are:

- to provide a detailed overview of the water and nitrogen conditions during a 12-year controlled fertilization experiment.
- to describe the heterogeneity of unsaturated alluvial sediments typical of the eastern San Joaquin Valley.
- to determine the physical and hydraulic properties of the deep unsaturated zone, and their relationship to sedimentary facies and soil texture.
- to develop a pedotransfer function tool that can be used to quickly determine soil hydraulic properties from inexpensively measured textural data.
- to provide an analysis of the spatial variability of hydraulic properties by the similar-media scaling concept, for later use in modeling studies.
- to provide an analysis and assessment of the nitrogen distribution in the unsaturated zone and a comparison to the nitrogen load predicted from an agronomic mass balance.

The field and laboratory characterization of the site provides the foundation for the development and validation of various modeling tools to assess the fate of nitrogen in the deep, heterogeneous vadose zone at the site. In an on-going follow-up project, the soil hydraulic database generated for the site is utilized to develop modeling strategies to quantitatively address the effect of physical heterogeneity on flow and nitrate transport throughout the deep vadose zone and to assess the long-term impact of various nitrate fertilizer management practices on groundwater quality. The site database in conjunction with the modeling results provide not only an important resource for further research, but also an educational component for growers, farm advisors, and personnel from irrigation districts, water districts, and regulatory agencies on the leaching potential and attenuation rates of agricultural chemicals in similar areas.

EXECUTIVE SUMMARY

Nitrate-nitrogen in groundwater is the most widespread contaminant causing up to ten times as many well closures in the State of California as all other industrial contamination combined. While a large amount of research has focused on nitrogen cycling in the root zone (to depths of 6-10 feet), little is known about the fate of nitrogen between the root zone and the groundwater table. Unlike in other agricultural regions of the United States,

however, groundwater levels in many areas of Central and Southern California and elsewhere in the Southwestern United States are from 30 feet to over 100 feet deep. Therefore, the deep vadose zone is a critical link between agricultural sources and groundwater. Few studies have surveyed the hydrology and the fate of nitrogen at such depths or monitored leaching of nitrogen to a deep water table. Field-scale spatial variability of nitrate due to natural variability of soils and vadose zone sediments also remains unaccounted for in most work on groundwater quality impacts of agricultural nitrogen management.

In this study, field, laboratory, and modeling research was carried out in conjunction with an eastern San Joaquin Valley orchard site (near Reedley, Fresno County). The site was subject to a unique long-term nitrogen fertilizer study that investigated crop impacts of several alternative management practices, with fertilization rates ranging from 0 to 325 pounds of nitrogen per acre. Groundwater levels at the orchard site are approximately 50 feet below the surface, which is typical for many areas in the southern and eastern San Joaquin Valley. The unsaturated zone at the site has a heterogeneous profile that is characteristic for many alluvial soils and sediments found in the San Joaquin Valley and other alluvial basins in the southwestern United States.

Sixty continuous cores to 52 feet were obtained with the Geoprobe Systems Macrocore[®] direct push sampling technique. We identified ten major facies ranging in thickness from less than 1 foot to over 10 feet. Most of the identified facies are laterally continuous across the site. Sediment textures in these unsaturated zone facies range from clean medium sand (remnant of a former channel bed) to finely laminated clayey-silt loam (flood-plain deposits). The facies identification provides an overall framework of the unsaturated zone geology. Significant textural and structural variability was observed on the cores within each facies unit.

Over 1,000 samples were collected from the continuous cores for analysis of water content, pH, and nitrate. Undisturbed cores were collected for determination of unsaturated hydraulic properties using a multi-step outflow technique that we successfully modified to fit the relatively small diameter Macrocore[®] samples. For the approximately 100 undisturbed core samples, parameters of the hydraulic functions were obtained by inverse modeling of each individual multi-step experiment. All of the directly and indirectly measured sediment and hydraulic parameters are found to be highly variable within facies and across facies. For example, saturated hydraulic conductivity is log-normal distributed with a variance of over 5. The van Genuchten α and n parameters also have a skewed and highly variable distribution. Much of the variability is observed within facies, although between facies variability of hydraulic properties is also significant.

The hydraulic property database was used to develop pedotransfer functions from a neural network analysis of the observed relationship between textural sample composition and hydraulic properties of the samples. The pedotransfer functions are implemented within a simple-to-use computer program that can be used for other sites in the San Joaquin Valley to estimate hydraulic properties from the percent sand, silt, and clay content of individual soils or sediment facies. This tool provides the basis for site-specific unsaturated zone hydraulic analysis without the time-consuming step of measuring hydraulic functions.

We also determined scaling factors from the hydraulic property database. Scaling factors are a pseudo-geometric measure of the pore-space variability and have been used to capture the spatial variability of multiple hydraulic parameters (e.g., the van Genuchten parameters describing unsaturated hydraulic conductivity and soil water retention functions) into a single parameter. We found that scaling indeed captures a significant amount of the observed variability. Including information about textural or facies membership into the scaling process significantly improves the capability of the scaling factor to describe the spatial variability of the unsaturated hydraulic properties.

Little empirical evidence exists about the spatial distribution of nitrate ($\text{NO}_3\text{-N}$) in deep vadose zones and about the associated fate and transport of $\text{NO}_3\text{-N}$ between the root zone and the water table. Statistical and geostatistical analyses were used to determine spatial variability of $\text{NO}_3\text{-N}$ and water content. Vadose zone nitrate was highly variable and lognormally distributed. Fertilizer treatment had a significant effect on $\text{NO}_3\text{-N}$ levels in the vadose zone. Total $\text{NO}_3\text{-N}$ mass in the vadose zone was estimated beneath each of three fertilizer treatments by kriging interpolation of measured nitrate and water content data to characterize the differences in nitrate and water flux distributions among the three subplots. The total $\text{NO}_3\text{-N}$ mass was then compared with that predicted from standard agronomic analysis of nitrogen and water flux mass balances in the orchard. In all cases, deep vadose zone nitrogen mass estimated by kriging the measured data totaled only one-sixth to one-third of the mass predicted by the nitrogen and water flux mass balance approach. Vadose zone denitrification estimates could not account for this discrepancy. Instead, the discrepancy was attributed to highly heterogeneous flux conditions, which were not accounted for by the mass-balance approach. The results suggest that spatially variable vadose-zone flow conditions must be accounted for in order to better estimate the potential for groundwater nitrate loading. In ongoing further work, we are currently testing this hypothesis by implementing a detailed stochastic flow and nitrate transport model of the site that builds upon the extensive database of hydraulic properties, historic data, and scaling factors obtained for this site.

The database, analyses, and modeling tools developed during this project are not only important for further research, but are also used to educate growers, farm advisors, irrigation and water districts, and regulatory agency personnel about nitrate leaching potential and attenuation rates and its time-frame in areas where the water table is substantially deeper than the root zone and where significant soil layering and spatial variability is observed.

ACKNOWLEDGMENTS

Under the supervision of the principal investigators, this project was implemented primarily by students and technical staff at University of California Davis and the Kearney Agricultural Center. The project would not have been possible without their incredible enthusiasm, hard work, and dedication:

- Katrin Heeren was the field geologist in charge of the field operation in 1997 and completed a preliminary geologic report on the site geology in 1998.

- Anthony Cole, Chad Pyatt, and Rigo Rios, all undergraduate students from CSU Fresno, successfully implemented the drilling operations during the summer and fall of 1997 under the supervision of Katrin Heeren and Thomas Harter. Chad Pyatt later also completed all of the pH analyses.
- Kevin Pope with Geoprobe Systems[®] suggested and arranged for the use of the Geoprobe Direct Push drilling rig used for collecting the sediment cores. He provided invaluable and enthusiastic support and advice during the process of recovering 3,000 feet of undisturbed sediment cores.
- Andrea DeLisle completed the nitrate analyses in 1997 on over 1,000 samples. Briefly, Cindy Bergens and Michael Ridolfi worked on chemical analyses. More recently, Tad Doane is in charge of the isotope and other chemical analyses (all under the supervision of Dr. William Horwath).
- Jim MacIntyre, hired for this project out of retirement, successfully adopted the multi-step outflow experiment in 1998 to work in conjunction with the Geoprobe Systems Macrocore[®] samples; and implemented all of the laboratory multi-step outflow experiments in 1998-1999.
- Michelle Denton is completing her M.S. thesis (1999-2003), which focuses on the inverse modeling of the multi-step outflow experiments, documentation of the updated experimental and modeling protocols, and interpretation of the soil hydraulic data she obtained from the computer modeling of the lab experiments. She is the main author of this final report.
- Dr. Budi Minasny, Faculty of Agriculture, Food and Natural Resources, The University of Sydney, Australia, in collaboration with Dr. Jan Hopmans used Michelle's dataset together with two similar datasets developed in Dr. Hopmans laboratory for the western San Joaquin Valley and the Sacramento Valley to generate a neural network based prediction tool for Central Valley soils.
- In a follow-up project (2002-2004), funded by FREP, Yuksel S. Onsoy, as part of her Ph.D. studies at UC Davis, has taken the rich database generated for the Kearney site to perform advanced statistical and geostatistical analyses to quantify the observed spatial variability of physical and biochemical properties in the subsurface and to develop flow and nitrate transport modeling strategies within a stochastic framework. The framework allows us to account for the tremendous heterogeneity encountered at the site.

We also thank all of the funding agencies and sponsors that have and still are supporting this multi-faceted project: The University of California Water Resources Center, the California Department of Food and Agriculture Fertilizer Research and Education Program, the California Tree Fruit Agreement, and Geoprobe Systems[®].

1. INTRODUCTION

Problem Identification:

Pollution of groundwater from agricultural fertilization practices has become one of the largest groundwater quality issues in the intensively used agricultural areas of California. The number of well closures due to contamination with nitrate is almost ten times greater than the number of well closures due to industrial contamination (Metropolitan Water District of Southern California, 1987). Nitrate contamination of groundwater is particularly widespread in Southern California and along the east side of the San Joaquin Valley. High nitrate levels in groundwater are caused by leaking septic systems, percolation of animal waste, and leaching of nitrogen fertilizer in agricultural fields. In a USDA document (Kellogg et al., 1992), it was estimated that 14 percent of California's rural lands have significant potential for nitrate leaching. The same report also concludes that more research is needed to understand the physical and biogeochemical processes dictating the fate of chemicals applied to crops and their transport in soil and water systems.

Current Approach:

Minimizing the impact on groundwater quality is an important aspect of fertilizer research and management. Commonly, nitrate leaching is evaluated by monitoring root zone nitrate levels with a small number of soil or lysimeter samples over one to several crop periods. Nutrients are rarely monitored below a depth of six feet. Tanji et al. (1977) and Tanji et al. (1979) presented a conceptual model for estimating nitrogen emissions from cropped lands, which was tested for a corn crop. Their model considers fluxes to and from the root zone and assumes that both water and nitrate fluxes are at steady-state. Similar but somewhat less sophisticated nitrogen balance models are typically used in many nitrogen field studies to estimate fertilizer nitrogen impact on groundwater quality (e.g., Hartz and Costa, 1995; Lovatt, 1995; Lovatt and Morse, 1995; Meyer, 1995; Miller and Friedman, 1995; Weinbaum and Goldhamer, 1995). The common assumption is that nitrate losses to below approximately six feet represent the amount of nitrate leached into groundwater. This assumption is justified for many areas in the United States, where groundwater is found at depths of less than 10 to 20 feet.

Shortcomings of Current Approaches:

In many agricultural areas of California, in contrast, groundwater levels are 30 to 100 feet deep and little is known about the fate of nutrients between the root zone and the groundwater table. Few studies have surveyed nitrate levels at such depths or monitored leaching of nitrate to deep water tables or related it to the hydraulic and geochemical properties of the unsaturated zone. Also, most of the intensively used agricultural areas in California are located in large to very large basins filled with alluvial deposits (Central Valley, Salinas Valley, Southern California and Mojave Desert basins) adding further complication to real time assessment of nitrate leaching to groundwater. Vertical stratification of the alluvial soils and horizontal discontinuity of both coarse and fine grained soil material causes significant spatial variability in water percolation rates, nitrate concentrations, and denitrification rates (intrinsic variability). Spatial variability in both the horizontal and vertical direction limits the value of composite root zone soil samples

with respect to predicting nitrate leaching rates. Our current understanding of the spatial variability of hydraulic properties and their impact on nitrate fate and transport below the root zone is therefore limited and based on greatly simplified models.

Past Research on Nitrate Flux in Deep Vadose Zones:

Pioneering work on nitrate in deep soil profiles was presented by Pratt et al. (1972), who investigated nitrate profiles in a southern California citrus orchard to depths of 100 feet. The experimental site was subject to differential nitrogen treatment for 35 years from 1927 to 1962. Nitrogen treatments ranged from 50 to 350 lbs/ac. During the period from 1963 to the time of sampling in 1969, uniform treatment was applied at a rate of 150 lbs/ac. The soil under the orchard was classified as a Greenfield sandy loam. From their observations, the authors estimated that it would take between 10 and 50 years to leach nitrate to a depth of 100 feet. Average nitrate-nitrogen levels below the root zone varied from 15 to 35 ppm under the 50 lbs/acre treatment and from 35 to 55 ppm under the 350 lbs/acre treatment. Estimated differences between nitrate applied and the sum of nitrate uptake in the fruit and nitrate remaining in the soil profile increased with application rates, suggesting that denitrification may account for up to 50% of nitrate losses in the soil profile when application rates are high. Not enough data was available to further confirm that denitrification was occurring. Lund et al. (1974) argued that differences in unaccounted nitrate losses (presumed to be due to denitrification) are strongly correlated with the textural properties of the soil. High losses were found in soils with pans or textural discontinuities, while losses were limited in relatively homogeneous, well draining soils. Later work by Gilliam et al. (1978), Klein and Bradford (1979), and Rees et al. (1995) in other areas of southern California supported these observations. No such studies are available for tree fruit orchards or vineyards. More importantly, none of these studies explicitly account for spatial variability in either the horizontal or vertical direction to quantify the risk for groundwater pollution from fertilizer applications. Recently, Fogg et al. (1995) estimated the residence time of nitrate in groundwater of the Salinas valley, where vegetable crops are dominant. Their work, which accounted for spatial variability only in the saturated zone, demonstrated that it may take decades before changes in agricultural practices have a significant impact on groundwater quality. They pointed out the need to better understand nitrogen transport processes in the deep vadose zone as a key to assessing the long-term impact of agricultural management practices on groundwater quality.

Research and Educational Needs:

Recently, geostatistical and stochastic methods have been developed to evaluate spatial variability of soil characteristics and to assess its effect upon solute transport. It has been shown, theoretically and in field experiments, that spatial variability can significantly impact the amount of solute leaching in soils and that concentrations of nitrate may vary significantly over short distances as a result of soil heterogeneity (e.g., Lund et al., 1974; Harter and Yeh, 1996). This may lead to large amounts of nitrate being leached quickly in some portions of the soil profile, while others retain nitrate for very long periods of time. The geostatistical-stochastic approach provides a well-suited framework to better understand the fate of nitrogen in California's deep, heterogeneous vadose zones. The Kearney Agricultural Center research orchard provides a unique, extensively sampled and

characterized field site with a well controlled, long-term field research experiment completed prior to our intensive deep vadose zone sampling campaign. Our goal in developing the site is to better understand the degree of spatial variability in hydraulic, transport, and chemical properties in the unsaturated zone below the root zone and to provide the basis for adapting the stochastic approach specifically for nitrogen fate and transport. In a current follow-up project we demonstrate its utility for the assessment of nitrogen fluxes in deep vadose zones under irrigated agriculture. Ultimately, this project will provide significant information to better understand the risk of groundwater pollution and the associated costs and benefits of fertilizer treatments in tree orchards.

2. SITE DESCRIPTION AND FIELD EXPERIMENTATION

2.1 Orchard Experiment Overview

The research site, a former nectarine orchard, is located on the east side of the San Joaquin Valley, approximately 30 km southeast of Fresno, California, at the University of California Kearney Research Center. The orchard was planted by Marvin Gertz in 1975 and had four varieties of nectarines, each covering approximately 2 acres. A controlled fertilization management experiment was conducted in the orchard over a period of 12 years (Johnson et al., 1995) beginning in September 1982 and continuing through 1995. The experiment was conducted only on the Fantasia variety of nectarine. The ID number assigned to the experimental site was KAC #92-74 and was later renumbered to KAC #663. Trees were planted in a 15-tree by 15-tree matrix spaced 20 feet apart on berms approximately 4 feet wide and 1 foot high (Figure 2.1.1), creating 16 feet wide shallow furrows between tree rows.

As in many surrounding areas, groundwater levels at the orchard are significantly deeper than the root zone. Since 1970, water levels have fluctuated between 35 and 67 feet below the surface. In 1997, the unsaturated zone was approximately 50 feet thick. For the site, relatively high quality records about fertilization methods are available including exact dates and quantities. Dates and approximate amounts of applied irrigation water (flood irrigation) and climate conditions during the past 15 years are also available and are documented here. These data are important for the interpretation of any deep vadose zone hydrology and nitrogen data, because they define the water and nitrogen fluxes across the root zone of the orchard, which are driven by water applications, precipitation, and evapotranspiration.

The site is located on the Kings River alluvial fan, a highly heterogeneous sedimentary system consisting of coarse channel deposits, fine flood deposits, paleosols, and fine eolian deposits. Sedimentary layers exposed to the surface for sufficient amount of geologic time have developed soil profiles with distinguishable horizons. The type of sedimentary layering, the paleosols encountered, and the range of soil textural classes encountered at this site are rather typical for many areas in the San Joaquin Valley that have deep vadose zones (Weissmann and Fogg, 1999). Similar alluvial conditions are also found in the

Salinas Valley, in the desert basins of Southern and Southeastern California, and elsewhere in the southwestern United States.

2.2 Fertilizer Experiment and Nitrate Application

The fertilizer experiment consisted of five application treatments in a random block design. The five nitrogen application treatments (0, 100, 175, 250, and 325 lbs N/ac/yr, not including nitrogen applied via irrigation water) were applied in 3 replicates, with the exception of the 0 treatment having 2 replicates. This results in the orchard being divided into 14 subplots. Each subplot consists of a row of 5 trees. Two border trees and one border row on either side of a subplot separate treatments (Figure 2.2.1).

Except for the 0 lbs N/acre/year treatment plots, all trees received a broadcast application of 100 lbs N/acre nitrogen in September of each year. The fertilizer was applied from berm edge to berm edge using a tractor-mounted spreader. Application uniformity was not measured but anecdotal evidence indicates that greater amounts were applied near the edge of the furrows and less in the center of the furrows (Scott Johnson, personal communication). Generally, the fertilizer was not disked into the soil but was left at the soil surface.

In spring, additional fertilizer was applied by hand to the 175, 250, and 325 lbs N/acre plots in 75 lbs N/acre increments. It was applied 2-3 feet wide (normal to the berm) and about 12 feet in length, starting 6 feet on one side of a tree and ending 6 feet on the other side, leaving an 8-foot fertilizer-less gap between trees (Figure 2.2.2). Fertilizer application was repeated in this manner two or three times depending on the total treatment desired. These applications were separated by a few weeks.

Ammonium sulfate was used in the first application in September 1982. However, it was believed that the ammonium sulfate was acidifying the soil so ammonium nitrate and calcium nitrate were substituted for the remainder of the experiment. No fertilizer was applied in 1995. On September 11, 1996 a single application of 100 lbs N/acre was applied to the entire 20 year old orchard.

Fertilization records detailing the amount of fertilizer applied and the application dates are available from 1982 through 1994 and are shown in Table 2.2.1. Notice that the amount reported is on a per tree basis and is in reference to the amount of fertilizer and not the amount of nitrogen.

The orchard received further nitrogen from nitrate in precipitation (less than 5lbs N/acre) and from nitrate in irrigation water (30-50 lbs N/acre assuming 4-5 ppm of nitrate-N in 3-4 acre-feet/acre of irrigation water).

2.3 Irrigation

As is common for many orchards and vineyards in the area, the orchard was flood irrigated every 2-3 weeks from April through September. The orchard was irrigated from 1983 to

1997. The irrigation water was supplied by a pipe located at the east side of the orchard. The water was turned on to a low flow rate (described as a “trickle”) in the late afternoon (between 3 and 4 o’clock) and was left on overnight. In the morning the flow rate was increased and was shut off after 2-3 inches water depth was achieved at the opposite end of the row (around 1 pm). In 1997, the orchard received regular irrigations only through early July, when field sampling began. One additional irrigation was applied in late September 1997 (to facilitate coring through the hardpan at 10 feet depth), after approximately two-thirds of all cores were taken.

A typical irrigation applied approximately 4-6 inches of water with an average application rate of 16 gpm for roughly 21 hours (10-15 gpm for 15 hours (4pm – 7am) and 20-30 gpm for 6 hours (7 a.m. – 1 p.m.)). On average, 12 irrigations totaling 48 to 72 inches, or 4 to 6 feet, of water were applied to the orchard annually. This is slightly higher than the typical 45 inches/year applied for a well managed nectarine orchard under furrow irrigation. Photos 1-11 show an irrigation event from start to finish.

Average consumptive use of the mature orchard is estimated to be 3 feet per year. Average net infiltration to below the root zone is therefore estimated to be on the order of 1 to 3 feet. The groundwater level at the site varies from 45-60 feet below ground surface. Assuming an average effective water content of 15%, travel time to the water table is on the order of 3-8 years.

Unfortunately, irrigation records are only available for 1983 and 1990-1997. Records for 1984-1989 have not been found. These records also include dates for fertilization, mowing, rotovating, pruning, thinning, harvesting, and application of chemicals other than fertilizer, such as herbicides. It is important to remember that irrigation data come with some uncertainty. For example, sometimes the irrigation event would last 1 day and sometimes it would span 3 days. Also, uniformity of water application is thought to be low and the trees at the end of a row are likely to receive less water than those trees near the supply pipe. Table 2.3.1 shows the dates of the irrigation events. A detailed review and analysis of the water budget is described in Onsoy et al. (2004).

2.4 Weather Data

Climate records from June 1983 to December 1999 were obtained from the California Irrigation Management Information System (CIMIS) web site for the Parlier Station (#39) located near the site.

CIMIS is an integrated network of over 100 computerized weather stations located at key agricultural and municipal sites throughout California. By measuring values for various sensors, such as wind speed, air temperature, solar radiation, etc., we can calculate ETo and other useful factors. Providing information for improving water and energy management through efficient irrigation practices is the primary use of the CIMIS system. The URL for CIMIS is <http://www.cimis.water.ca.gov>.

Several types of reports are available from CIMIS including hourly, 7-day daily, and monthly reports. For each of these the values are averaged over the time period of the report. For example, the hourly report consists of hourly averages. Table 2.4.1 summarizes the various report contents. The values within this report are monthly averages.

The following nine sub-sections briefly describe the CIMIS weather data for 1983 to 1999. Table 2.4.2 summarizes the basic statistics for the weather data. The sensor specifications are summarized in Table 2.4.3. The information in this table was copied directly from the CIMIS web site.

Precipitation

With computations based on the water year from October 1 to September 30, average annual precipitation is 13 inches with a standard deviation of 4.7 inches. The range is from 3.9 to 22.6 inches with the driest year being 1996 (October 1995 to September 1996) and the wettest year being 1995.

In most years essentially no precipitation is recorded between late May and early October. For monthly averaged precipitation, the range is from 0 to 8.7 inches with a mean of 1.07 inches and a standard deviation of 1.5 inches, i.e., high variability. Figure 2.4.1 shows the 1983-1999 average monthly precipitation [in inches].

Reference Evapotranspiration

Evapotranspiration is the combined process of water loss by evaporation and water transfer to the air through plant tissues. Reference evapotranspiration (ET_o) is a term used to describe the evapotranspiration rate from a known surface, such as grass or alfalfa. ET_o is expressed in either inches or millimeters. Crop Coefficients, K_c, are used together with measured ET_o data to estimate specific crop evapotranspiration rates. The reference crop used here is grass, which is closely clipped, actively growing, completely shading the soil, and well watered.

The average annual ET_o is 53.3 inches with a standard deviation of 2.7 inches. The range is from 46.8 to 56.4 inches. The average monthly maximum ET_o occurs in July and the minimum occurs in December or January. The range is from 0.4 to 8.8 inches. The mean monthly ET_o is 4.5 inches with a standard deviation of 2.6 inches. Figure 2.4.2 shows the average monthly ET_o in inches from 1983 to 1999.

Air temperature

Maximum, minimum, and average air temperatures are reported on a monthly average basis (CIMIS web site). The maximum air temperature has 3 anomalous values that have been flagged. These occur during July 1983, December 1985, and December 1988 at values of 105.4, 71, and 83.6 °C, respectively (possibly a temperature conversion error). There is no notation as to which day or days the errors occur on nor is there any explanation as to why the errors occurred. The error message is “one or more daily values flagged”. It could be due to a variety of instrumentation errors.

Without the anomalies, the range for the maximum monthly air temperature is 8.4 to 37.2°C. The mean is 24.6 °C with a standard deviation of 7.9 °C. The range for the minimum monthly air temperature is -2.6 to 18.9 °C. The mean is 9.1 °C with a standard deviation of 5.3 °C. The range for the average monthly air temperature is 3.3 to 27.5 °C. The mean is 16.5 °C with a standard deviation of 6.7 °C. Figure 2.4.3 shows the maximum, minimum, and average monthly air temperatures from 1983 to 1999 and includes the anomalies.

Solar radiation

Net radiation at the earth's surface is the major energy input for evaporation of water (Chow, et. al., 1988). Solar radiation makes up one component of net radiation.

The average monthly maximum solar radiation occurs during the summer, in June or July, and the minimum occurs during the winter, in December or January. The range is from 51 to 355 Watts/m². The mean is 206.02 Watts/m² and standard deviation is 91.5 Watts/m². Figure 2.4.4 shows the average monthly solar radiation from 1983 to 1999.

Vapor pressure

Besides the supply of heat energy, the second factor controlling evaporation is the ability to transport vapor away from the surface (Chow, et. al., 1988). Vapor pressure is calculated from the relative humidity and the air temperature.

The average monthly maximum occurs in July or August. The minimum occurs mostly from December to February. The range is from 0.4 to 2 kPa. The mean is 1.23 kPa and the standard deviation is 0.35 kPa. Figure 2.4.5 shows the average monthly vapor pressure from 1983 to 1999.

Relative humidity

For a given air temperature there is a maximum moisture content the air can hold. The corresponding vapor pressure is called the saturation vapor pressure. The relative humidity is the ratio of the actual vapor pressure to its saturation vapor pressure (Chow, et. al., 1988).

Maximum, minimum, and average relative humidity are reported on the CIMIS site on a monthly average basis. There is a period, March 1990 to January 1994, during which the relative humidity seems to not follow the same trend that is exhibited during the leading and following years. The precipitation shows larger peaks during this time period (Figure 2.4.1). Also, the vapor pressure (Figure 2.4.5) and dew point (Figure 2.4.7) exhibit a different than usual trend during this period. Vapor pressure, dew point, and relative humidity are interdependent variables.

The range for the maximum relative humidity is from 40 to 100% with a mean value of 88.9% with a standard deviation of 11.2%. The range for the minimum relative humidity is from 17 to 84% with a mean value of 41.9% and a standard deviation of 16.7%. The range for the average relative humidity is from 27 to 95% with a mean value of 64.8% and a standard deviation of 14.6%. The maximums occur in winter and the minimums occur in

summer. Figure 2.4.6 shows the maximum, minimum, and average monthly relative humidity from 1983 to 1999.

Dew point

The temperature at which air would just become saturated at a given specific humidity is the dew-point temperature (Chow, et. al., 1988). The range is from -6.1 to 17.7 °C. The lows are mostly in December and January and the highs are in July and August. The mean is 9.2 °C and the standard deviation is 4.5 °C. Figure 2.4.7 shows the average monthly dew point temperature from 1983 to 1999.

Wind speed

It is windiest in April and May and the least windy in November. The range is from 1 to 2.5 m/s. Mean wind speed is 1.7 m/s with a standard deviation of 0.36 m/s. Figure 2.4.8 shows the average monthly wind speed from 1983 to 1999.

Soil temperature

Soil temperature values were not reported for April and May 1998. Soil temperature was at a minimum in December and January and at a maximum in July and August. The range is from 6.2 to 29.6 °C. The mean is 17.8°C with a standard deviation of 6.3°C. The point of measurement is 6 inches below the soil surface under irrigated grass. Figure 2.4.9 shows the average monthly soil temperature from 1983 to 1999.

2.5 Plant yield, nutrient uptake, and soil water quality

As part of the fertilizer management project implemented at the site the following were measured:

- fruit yield
- nitrogen concentration in fruit (flesh, pit, and seed)
- leaf nutrients (%N, %P, and %K)
- soil nitrate and pH

Table 2.5.1 shows the available fruit yield summary (in kg/tree) for 1983-1985 and 1991-1994 for all five treatment plots. Average individual fruit weight is obtained by dividing the total weight of fruit per tree by the number of fruit per tree. In 1983, at the beginning of the experiment, yield responded positively to the increasing fertilizer rate. The 7-year average yield, however, dropped in all subplots. A significant drop was seen in the control subplot (0 lbs N/acre): there, the N storage reserve was not consumed until after 1983. Once the reserve N was depleted the drop in yield became apparent. The yield from the so-called “high” subplot (325 lb N/ac) gave the second lowest yield after the control subplot, indicating a negative response to the high fertilizer application rate.

Percent nitrogen in fruit (flesh, pit, and seed) was measured in dry fruit mass in 1983 for each treatment group except the control treatment plots and is shown in Table 2.5.2. Dry weight is approximately 10% of wet fruit weight. Although fruit yields varied little between treatments, total fruit N levels varied greatly from treatment to treatment. There is

an increasing trend in nitrogen content in fruit flesh with nitrate application but there is no evident trend in nitrogen content in seeds or pits. For the 0, 100, and 325 lb N/acre treatments, fruit harvest is estimated to remove 22, 69, and 87 lbs N/acre (25, 77, and 98 kg N/ha), respectively (Onsoy et al., 2004).

Table 2.5.3 summarizes the measured leaf nutrients (%N, %P, and %K) for 1983-1985 and 1991-1994 for all five treatment plots. It is observed that nitrogen content in leaves increases with nitrate application. An opposite trend is seen in %P and %K. Leaf and cover crop N uptake are assumed to be returned to the soil via leaf fall, decomposition, and mechanical incorporation into the soil.

Average soil nitrate-N data are available for October 1991 and January 1995 to a depth of 10 feet at a measurement interval of 1 foot for each treatment subplot. Data for pH were measured to a depth of 1 foot with a measurement interval of 0.5 foot and are only available for October, 1991. The soil nitrate and soil pH data are shown in Table 2.5.4 and Table 2.5.5, respectively. The values reported for soil nitrate are arithmetic means of 6 to 9 soil samples. The time progression of soil nitrate through the soil profile from 1991 to 1995 for each subplot is illustrated in Figure 2.5.1a-e. Nitrogen concentration increases with time and depth as the nitrogen has an opportunity to transport through the soil. The peak concentration decreases due to N removal from the trees, possibly through denitrification, and perhaps lateral transport. The peak concentration depths for the 100, 175, 250, and 325 lb N/ac are 4, 6, 6, and 7 feet, respectively. Nitrogen concentration at the surface decreases from 1991 to 1995 because the 1991 measurement was taken shortly after a fertilizer application whereas the 1995 measurement was taken 5 months after the last fertilizer application. The greater concentration at the surface for this subplot in 1991 may be explained by lateral flow from the surrounding treatment plots. That is, during times of fertilization there may have been some lateral flow. When fertilization ceased we see a decrease in the nitrate concentration at the surface of the control plot. Also, some nitrogen is applied even to the control plot via irrigation water and in precipitation. Soil pH increases with depth from an average of 6.75 inches the upper 6 feet (Hanford fine sandy loam) to 7.19 at a depth of 40-50 feet. Differences in pH between fertilizer treatments are not significant.

2.6 Bromide tracer experiment, October 2, 1996

Dr. Johnson's fertilization trial was completed in 1994. No fertilizer was applied in 1995. A single 100 lbs N/acre broadcast was applied to the entire orchard on September 12, 1996. On October 2, 1996 a simple tracer experiment was conducted to follow solute movement from the fertilization. The tracer experiment covered approximately one-fifteenth of the orchard including two of the three subplots that were later used for core drilling. Lab-grade potassium bromide solution was filled into a hand sprayer (backpack type) and sprayed in length wise passes across the entire area between tree-rows ("basin") from tree 14 to tree 10 until all solution was used. The only exception is the southernmost treatment basin, where the application is from tree 14 to tree 9. The treatment basins are between tree rows 8-9, 9-10, 10-11, and 11-12. Tree-rows are counted starting from the southernmost row, the tree number is counted starting from the westernmost tree in a tree-

row. The bromide application rate averaged 13g/m². Prior to the bromide application, the orchard was mowed and rotovated to 6 inches depth. Following the application, the field was rotovated and irrigated.

2.7 Core sampling, 1997

During 1997, upon completion of the fertilizer experiment, three subplots were selected for detailed sampling and intensive data analysis (boxed areas in Figure 2.7.1). The three subplots were fertilized at the annual rates of 0, 100, 325 lb N/acre and are referred to henceforth as the “control”, “standard”, and “high” subplots. Approximately 3000 feet of geologic material were obtained from 62 continuous soil cores drilled to the water table (~52 feet). At each of the three subplots, 18-19 cores were collected. Spacing of the borehole locations varied from 4 to 10 feet in a transect that is approximately 300 feet long and 8 feet wide (Figure 2.7.1 and Figure 2.7.2). An additional north-south transect throughout the entire orchard, consisting of 6 cores spaced 40 feet apart, was sampled to obtain estimates of nitrate distribution at the scale of the entire orchard.

The drilling was implemented with the Geoprobe Systems® GH-40 direct push sampling device provided courtesy of the manufacturer. This method allows for highly efficient field sampling and comparatively less disturbed sediment cores than hollow-stem auger drilling. The cores were obtained in hard plastic liners in segments of 4 feet (1.2 m) length with a diameter of 1.6 inches (4.0 cm). The sampler (Macrocore®) consists of a stainless steel cutting shoe attached to a 4 feet (1.2 m) long stainless steel cylinder with an equally long plastic tube that receives the core sample. The inner diameter of the plastic liner is 2 mm larger than the inner diameter of the cutting shoe to minimize compression inside the liner. Before lowering the sampler to the desired depth the cutting shoe was plugged with a removable tip to prevent slough accumulating at the bottom of the borehole from entering the sample. Upon reaching the top of the depth interval to be sampled, the tip was removed and the sample collected by pushing the sampler 4 feet into undisturbed sediment. The sampler was then raised out of the borehole.

Following the extraction of the 4 feet core, the 1.6 inch (4.1 cm) diameter core liner was laid out horizontally, cut lengthwise, and the upper half of the liner removed to expose the entire length of the core. Immediately, a complete sedimentologic description by color, texture and moisture was made on the continuous core. We determined major textural classes using USDA-SCS 1994 Field Estimation, sediment color based on the Munsell Color Chart, and grain-size for sands and gravels. Major textural units identified within the predominantly horizontally stratified transect span a wide range from finely cross-bedded clayey silts to paleosols, hardpans, and uniform medium sand. Major identifiable stratigraphic units vary in thickness from a few centimeters to several meters across the transect.

Based on the sedimentologic description, (disturbed) samples were collected approximately every 2-3 feet. A total of 1,200 samples were collected. Samples consisted of 8.9 inch (22.5 cm) length of core, collected from as many identifiable sedimentologic strata or sub-strata as possible.

Each 8.9 inch (22.5 cm) sample was subdivided into sections for various analysis:

- Nitrate analysis: a 2 inch (5 cm) sample section
- Water content: a 0.5 inch (1.25 cm) sample section
- pH analysis: a 0.5 inch (1.25 cm) sample section
- Isotope and other chemical analysis: a 5.9 inch (15 cm) section

In approximately one third of the boreholes, a slightly different sampling protocol was applied to also collect undisturbed core samples for the analysis of soil hydraulic properties. In those boreholes, the sampling protocol for all samples was as follows:

Prior to cutting the core, sampling locations were determined from visual inspection of the core through the clear plastic liner. At each sampling location in the core, a 3.9 inch (10 cm) lined section was cut and sealed with caps on each end (black cap at the bottom, red cap at the top). The remaining core was then sliced open lengthwise. Sub-samples were collected from the core sampling locations in the following sequence:

- pH analysis: a 0.5 inch (1.25) cm sample section
- (soil hydraulic analysis: a 3.9 inch (10 cm) undisturbed core taken prior to taking disturbed samples)
- Water content: a 0.5 inch (1.25 cm) sample section
- Nitrate analysis: a 2 inch (5 cm) sample section
- Isotope and other chemical analysis: a 2 inch (5 cm) section

All disturbed soil samples were collected with a clean knife and spoon (rinsed with clean water in between different units) and stored in Ziploc® bags, envelopes and containers:

- Water content samples are put in tin boxes (21 grams) and immediately weighed. Samples were then oven-dried at 105 degrees Celsius for 2-3 days and weighed again for gravimetric determination of moisture content (Klute, 1986).
- pH samples: approximately 20 g are collected into a paper envelope and air-dried. Soil pH was later measured with KCl electrometric method using 10g of air-dry soil (see standard soil pH measurement, SSSA Book, Part 3, p. 487).
- Chemical analysis samples are collected into in Ziploc® bags and stored in ice-chests until the end of the field day

After every field day, soil samples for nitrate and hydraulic properties were moved to cold storage at -1° C. Soil samples for isotope and other chemical analysis were moved to a freezer (-10° C to -20° C).

Sample Numbering System: Soil cores are numbered in reference to the trees. The set of 6 cores to the east of a tree are associated with that tree. Soil cores are numbered with the tree column number first, then the row number, then the soil sample location (1-6). For example, the soil sample shown in Figure 2.7.3 is numbered 11-10-4. A fourth number, in reference to the 2.5 feet interval sub-sample is tagged on to the core number (increasing number with depth).

3. LABORATORY METHODS

3.1 Hydraulic characterization: Multi-step outflow experiment

In 19 of the 62 cores, samples were collected for hydraulic characterization (Figure 3.1.1). Hydraulic characterization was performed on 120 undisturbed core samples from those 19 core locations. Hydraulic characterization included determination of soil moisture content at the time of sampling (see above), determination of the saturated hydraulic conductivity, determination of grain size distribution, and measurement of the dependence between unsaturated hydraulic conductivity, moisture content, and soil water pressure. Additional measurements include bulk density and sand, silt, and clay fractions.

Saturated hydraulic conductivity was measured using the constant head method (Klute, 1986). The UC Agriculture and Natural Resources laboratory determined soil texture based on the percentages by weight of sand, silt, and clay (hydrometer method, ASTM, 1985). Bulk density was obtained gravimetrically from the undisturbed cores.

The soil-water retention and unsaturated hydraulic conductivity relations are basic elements necessary for the simulation and prediction of flow and transport in the vadose zone. We used the multi-step outflow (MSO) technique (Eching and Hopmans, 1993) to determine these relationships. The principle of the multistep outflow technique is to observe water outflow from and soil water suction changes in an initially saturated soil core sample at increasing steps of dryness. The method has two components: implementation of a laboratory experiment, and computer analysis of the laboratory experiment to determine the hydraulic parameters of unsaturated hydraulic conductivity function and of the soil water retention curve.

For the laboratory experiment, a saturated sample is placed into a specially developed pressure/suction chamber (Tempe cell) at atmospheric pressure conditions. During the experiment, air pressure is increased in several discrete steps over the course of several days (typical for sands) to several weeks (typical for clays). Each step-wise increase in air-pressure forces water to flow out of the soil core sample until soil water suction in the pores matches the applied air pressure. Using high-precision instrumentation, we monitor how quickly the soil pressure inside the core changes in response to each pressure step and we monitor the outflow rate from the core over time. The core is instrumented with a tensiometer at the center of the core measuring the soil water suction. A burette connected to the core captures the outflow. Soil pressure and outflow are recorded automatically with these sensors and the data are sent to a computer. After completion of each experiment, the measurement data are cleaned up and converted into meaningful units using laboratory-derived calibration curves.

For this project, the original multistep outflow technique was modified to accept the 1.6" (nearly 1.75" outer diameter) Geoprobe Macrocore[®] core samples such that they fit tightly inside the Tempe cell. The semi-permeable membrane on the outflow side of the Tempe cell was modified from a 1 bar ceramic plate to a 2 micron nylon filter. Various changes in the pressure and outflow tubing design have been made to allow for faster and safer

connections, simplified trouble-shooting, and superior system testing. Special attention had to be paid to the development of air-bubbles in the outflow tubing to avoid erroneous measurements. A standard protocol has been developed and tested for the uniform handling of all core samples in each texture class (Tuli and Denton, 2001).

To streamline the implementation of the multi-step laboratory experiments, the samples were arranged into 12 sets (or Runs) of 10 samples (or cells) per set resulting in 120 samples. The samples were identified using the naming convention described at the end of Section 2.7 and can also be identified by the run and cell number. The implementation of a single set of ten parallel laboratory multi-step experiments typically took 3-6 weeks including set-up and take-down, depending on the texture of the samples. Coarse textured samples are typically faster to run than fine textured samples due to their faster response to pressure changes. The multi-step outflow experiments were successfully completed for 118 undisturbed cores representing 9 major textural classes identified in the field cores: sand, loamy sand, sandy loam and silty loam to sandy loam, Hanford fine sandy loam (surface soil), loam, clay loam, clay, hardpan, deep paleosol. Due to a variety of experimental complications and errors, the multi-step outflow data for 21 soil cores were unusable resulting in 97 viable samples for the inverse modeling process.

3.2 Hydraulic characterization- inverse modeling

To compute the hydraulic properties of the soil core, the multi-step outflow experiment is reproduced in computer simulations. The hydraulic parameters of the computer model are adjusted until results from the computer simulation match the measurements from the outflow experiment. This process is referred to as “inverse modeling”, “parameter estimation” or “optimization”. The end product of the inverse modeling is a set of hydraulic parameters for the soil water retention and unsaturated hydraulic conductivity functions that can then be used to describe flow beneath the orchard. The computer model solves the one-dimensional Richards equation of unsaturated flow. In its one-dimensional form with the vertical coordinate, $z(L)$, taken positive upward Richard’s equation is written as:

$$C(h)\frac{\partial h}{\partial t} = \frac{\partial}{\partial z} \left[K(h) \left(\frac{\partial h}{\partial z} + 1 \right) \right]$$

where $C = d\theta/dh$ is the water capacity (L^{-1}), h is soil matric head (L), K is unsaturated hydraulic conductivity (LT^{-1}), and t denotes time (T).

An existing finite element code, SFOPT, has been adopted to simultaneously optimize the soil-water retention, $\theta(h)$, and unsaturated hydraulic conductivity, $K(\theta)$, parameters given our particular experimental setup. Several models have been developed that describe $\theta(h)$ and $K(\theta)$. We chose to use the soil water retention function proposed by van Genuchten (1980):

$$S_e = \left[1 + |\alpha h|^n\right]^{-m} \quad [1]$$

with

$$S_e = \frac{\theta(h) - \theta_r}{\theta_s - \theta_r}$$

and $m = 1 - 1/n$, where S_e is the effective water saturation ($0 \leq S_e \leq 1$), θ_s and θ_r are the saturated and residual water content (L^3 and L^{-3}), respectively, and $\alpha (L^{-1})$ and n are empirical parameters. Substituting Eq. [1] in the capillary model of Mualem (1976), van Genuchten (1980) derived the following unsaturated hydraulic conductivity model:

$$K(h) = K_s S_e^l \left[1 - (1 - S_e^{1/m})^m\right]^2$$

The parameters K_s and l denote saturated hydraulic conductivity (LT^{-1}) and tortuosity/connectivity coefficient, respectively. S_e and m are the same parameters as used in Eq. [1]. From the analysis of a variety of soils, Mualem (1976) proposed a value for $l = 0.5$, although l can be considered as another fitting parameter as well (Hopmans et al., 1994; Hopmans et al., 2002).

Other models describing these relationships that could be applied to interpret the experimental data are the lognormal model derived by Kosugi (1994) and the typical algebraic equations proposed by Brooks and Corey (1964), Gardner (1958), and Haverkamp and others (1977). The parameters necessary to mathematically describe the measured hydraulic conductivity and soil moisture retention curves are simultaneously determined in the computer model with an optimization algorithm using the Levenberg-Marquardt method. The inverse method is an iterative process that uses an initial guess for the parameters as a starting point. We repeated the optimization process with different initial guesses to ensure that the parameter estimates obtained from the computer model can be trusted (combined manual-automatic calibration).

Among the 97 samples, transient data were unavailable for all the samples in Runs 7 and 8 (20 samples). Due to transducer failure seven samples in Run 4 also had unusable transient data. The total number of samples for which we can implement the inverse modeling is now reduced to 71 samples. For the 27 samples with missing transient data there exists handwritten data for the equilibrium conditions between pressure steps during the outflow experiment. One sample in Run 10 (Cell 1 or sample 4-10-5 #13) did not converge using SF-OPT thus reducing the number of samples with transient data that will be considered in the remaining analyses (for example, scaling) to 70. Implementation of the inverse modeling for these 27 samples and the remaining 70 samples with transient data is described in detail in Chapter 6 in Tuli and Denton (2001).

The consequence of having a collection of samples with transient data and another with only equilibrium data is that the samples must be categorized into populations according to the information available for each sample. Those categorizations affect both the parameter estimation and the scaling as will be discussed below and in Section 4.3 and Section 4.5.

3.3 Scaling

Scaling is a technique used to simplify the analysis of hydraulic parameter datasets in heterogeneous unsaturated sediments. Scaling is based on the concept that various hydraulic parameters, e.g., K_s , α , n , θ_s , θ_r , are all related to the pore size distribution and pore geometry. Heterogeneity of sediments or soils is reflected in the heterogeneity of pore geometry and pore size. Coarse soils have large pores, while heavy, fine-grained soils or soils with a high content of fines have very small pores. As the pore geometry varies with the type of sediment, the various hydraulic parameters vary accordingly. The scaling factor is a measure of that change in pore geometry and relates the actual hydraulic function derived for a sample to the scaled hydraulic function. The variability of the hydraulic parameters can, with some limitations, be directly related to the variability of the scaling factor and vice versa. The scaling method is based on the similar media theory introduced by Miller and Miller (1956) which assumes that the structure of pore spaces is geometrically similar among different locations. That is, similar media differ only in the scale of their geometry. An existing model, SCALE, was used to scale the hydraulic data (Clausnitzer et al, 1990, 1992). There are several options in the program including (A) to scale either water retention data only; (B) to scale hydraulic conductivity data only; (C) simultaneous scaling of soil water pressure head, h , and the natural logarithm of hydraulic conductivity K ; and (D) simultaneous scaling of the logarithm of both h and K .

The soil water retention and unsaturated hydraulic conductivity curves obtained for the 97 samples (70 with transient data and 27 with equilibrium data) were scaled simultaneously using methods C and D. The scaling yields a single set of scale factors, λ , thus simplifying the description of heterogeneity from a set of multi-variate probability functions (K_s , α , n , θ_s , θ_r) to a single-variable probability function for λ that relates to a reference soil. That is, scale factors, λ , are conversion factors relating the characteristics of a system to those of another system. In the case of soil hydraulic parameters the scale factors relate the multi-variate functions of soil water retention and unsaturated hydraulic conductivity to a reference soil via a single factor. Take, for instance, a group of 10 soils whose hydraulic functions are to be scaled. The result would be 10 scale factors relating the original functions to one reference soil. The reference soil's hydraulic parameters are determined via the SCALE program using Powell's optimization (Powell, 1964) method in combination with a Newton-Raphson iterative procedure.

In our case there are 97 samples representing many texture classes and stratigraphic units. The samples were grouped in four ways (Table 3.3.1):

- Group 1.** Soils scaled all together. No a priori knowledge, such as texture, was used.
- Group 2.** Scaled within individual sub-groups, where sub-groups represent texture classes (USDA soil triangle) as determined in sieve analyses obtained by the UC ANR Analytical laboratory, without regard to the specific facies that the samples belonged to.

- Group 3.** Scaled within individual sub-groups, where sub-groups represent field determined texture classes (visual determination), but without regard to facies location.
- Group 4.** Scaled samples within individual sub-groups, where each sub-group is associated with a specific facies location (primarily texture-driven). See Figure 4.1.1.

Each group, except group 1, is a collection of subgroups. The subgroups for Group 2 are loamy sand, sand, sandy loam, silt loam, and silt. The subgroups for Group 3 are clay, hardpan, loam, loamy sand, paleosol, sand, sandy loam, silt loam, and Hanford sandy loam. The subgroups for Group 4 are sand, sandy loam (sL), silt/silt loam/loam/silty clay loam (CSiL), hardpan (HP1), paleosol (HP2), and two facies named “var1” and “var2” that contain various sedimentary structures within the unit but are distinguishable as a facies separate from the adjacent facies. Each soil sample was assigned to one of the subgroups of scaling groups 2-4 (group 1 has no subgroups). For example, sample 5-10-2 #20 is a sand in group 2, a loamy sand in group 3, and a sandy loam in group 4. Sometimes the subgroup designation is the same for all groups as is the case for sample 10-10-2 #8 (sand).

Additionally, each sample’s dataset was determined to be of good or poor quality. The samples were assigned to two populations according to the data quality for that sample. Data quality is defined as follows: 1) if transient data exist the quality is considered to be good, 2) if only equilibrium data exist then the quality is considered to be poor. The first population consists of a mixture of good and poor quality datasets (97 soil samples) and will be referred to as Population 1. The second population contains only good quality datasets (70 soil samples) and will be referred to as Population 2. The subgroup designations and data quality for each sample are shown in Table 3.3.1 where a “1” indicates a transient dataset and a “0” indicates an equilibrium dataset only.

Each population is scaled with two of the methods available in SCALE. Method 1 simultaneously scales soil-water pressure, h , and the log of unsaturated hydraulic conductivity, $\ln K$. Method 2 simultaneously scales $\ln h$ and $\ln K$. The results are presented in Section 4.5. Soil water retention curves were scaled over 11 equally spaced pressure increments (0, 50, ..., 500 cm) with the exception of the sands which were scaled over 16 steps (0, 10, ..., 150 cm). Hydraulic conductivity curves were scaled at degree of saturation (S) values corresponding to these same pressure increments. The values for these curves were calculated using the van Genuchten functions and the associated van Genuchten parameters obtained for individual samples from the inverse modeling of the multi-step outflow experiment. The optimized saturated hydraulic conductivity was used for the 70 soil samples in the “good quality” group and the measured saturated hydraulic conductivity was used for the 27 soil samples in the “poor quality” group.

4. RESULTS

4.1 Geologic Framework

The site is located on the Kings River alluvial fan, approximately 2 miles west of the current river channel. The alluvial unconsolidated sediments are derived exclusively from the hard, crystalline Sierran bedrock. They appear as intercalated, thick and thin lenses of clay, silt, sand, and gravel. The deposits contain fairly well sorted subangular to subrounded sand and gravel, and intercalated lenses of silt, sand and gravel with some lenses of clay, showing a downstream decrease in grain-size (Page and LeBlanc, 1969).

The material obtained in the borehole cores is exclusively composed of unconsolidated sediments. The top section of the core material is a recent soil (Hanford fine sandy loam). The sediments can be classified into textural groups ranging in grain-size from clay to pebble and cover a wide spectrum of silty and sandy sediments in between. The colors of the sediments range from grayish brown to yellowish brown, more randomly to strong brown (no significant reduction zones). The thickness of the beds varies from less than 1 cm for clayey material to more than 2.5 m for sandy deposits. Both, sharp and gradual vertical transitions are present between texturally different units. Five textural units are found the cores: 1) sand, 2) sandy loam, 3) silt loam/loam, 4) silt/clay loam/clayey silt/clay, 5) paleosol. The relative occurrence of each category in percent of the vertical profile length (in 5 cm sections) are 17.2% sand, 47.8% sandy loam, 13.8% silt loam/loam, 8.3% clay loam/clay and 12.9% paleosol.

The sand is quartz-rich, contains feldspar, muscovite, biotite, hornblende and lithic fragments consistent with the granitic Sierran source. Cross-bedding at the scale of few cm could be observed occasionally within fine-grained sand, showing reddish-brown layers intercalated with gray-brown ones. The dominant color of the sand is a light gray to light brown, the brown hue increasing with increasing loam content. The thickness of the sand beds is as much as 2.5 m and is dependent on the location of the core relative to the course of an ancient secondary distributary channel in which the sediments deposited. The channel appears to have a northeast-southwest orientation, diagonally through the orchard site. The mean thickness is 1.7 m. Very coarse sand and particles up to pebble grain-size (up to 1 cm) could be observed occasionally at the bottom of sand units, but were not present in all the cores. These are probably channel lag deposits and were laid down in deeper parts of the channels.

Sandy loam is the most frequent category within the profile. The color is usually light olive to yellowish brown. Some of the sandy loam sediments are considered to be weakly developed paleosols because of their stronger brownish color, root traces and presence of aggregates. Mean bed thickness is 50 cm. Individual beds can be as much as 2 m thick. The sorting is moderate to good. Clay flasers and thin (0.5-1 cm) clay layers occasionally occur in sandy loam units. Sandy loam sediments are assumed to have developed at the edge of channels, as levee or as proximal floodplain deposits near the channels.

Silt loam, loam and silty clay loam are usually slight olive brown to brownish gray in color. The bed thickness is within a scale of a few cm to dm. Fine grained sediments often show sharp contacts between the units. Changes from one unit to the next exist on small distances. Cross-bedding can more frequently be observed within silty sediments than in fine sands. Root traces and rusty brown colored spots are quite common. The depositional environment was presumably the proximal to distal floodplain of the alluvial fan, an area dissected by distributary branched braided streams.

The finest sediments are grouped in the 4th category: Silt, clay and clay loam. These are believed to have been deposited in the distal floodplain and in ponds that developed in abandoned channels. The main color is brownish gray to olive brown. Fine, less than 1 mm thick root traces and rusty brown spots are quite frequent also in the clay sediments. Statistics for the thickness of clay layers in the unit between 8 and 13 m depth show a mean thickness of 12.8 cm, but the mode is about 3 cm. A thick clay bed even extends to 50 cm and is observed in most of the cores.

Paleosols could be recognized in different stages of maturity. They show a brown to strong brown, slightly reddish color, exhibit aggregates, ferric nodules and concretions, few calcareous nodules and hard, cemented layers. They also display a sharp upper and a gradual lower boundary as is typical for paleosols (Retallack, 1990). Clay content decreases downwards in the paleosols. Another feature is fine root traces. Paleosols formed in periods of stasis marked by non-erosion and non-deposition, during the interglacials. Thickness of the paleosol horizons ranges from 50 cm to about 2 m.

Several thicker units are recognized throughout the orchard and are used to construct a large scale geologic framework for the research site (Figure 4.1.1). The deepest parts of the cores from 15.8 to 15 m display a strong brownish colored, partly clayey paleosol hardpan. This paleosol marks the top of the Turlock Lake II formation (see below). From a depth of 15 to 12 m below surface, the main textural units are sandy loam to fine sandy loam, occasionally coarse sand and gravel, and occasionally fine-grained sediments right on top of the paleosol. In the cores with fine sediment at the bottom of this unit a coarsening-upward, in the other cores a fining-upward cycle can be observed. The sediments show a remarkable wetness due to proximity to aquifer water table. The sediments are vertically and laterally quite heterogeneous with relatively thin bedding (thickness cm to dm) between about 12 and 8 m depth, consisting mainly of clayey, silty and loamy material. Another strong brownish paleosol can be distinguished at a depth of 9-10 m. Between 9 and 6 m below surface a sand layer is found with laterally varying thickness averaging 1.7 m. A weak, mostly eroded paleosol is developed on top of the sand unit. Up to about 4-3 m below surface, sandy loam with intercalated sand, clayey and silty material is found. Different trends of upward-fining and -coarsening are found on top of each other and laterally next to each other within this unit. A 0.2 m to more than 1 m thick paleosol hardpan occurs at a depth of about 4-3 m. This paleosol marks the top of the Modesto formation. Sandy loam and subordinated loamy sand and loam are present from the top of the hardpan to the surface. 2.5 m below surface a laterally continuous clay horizon with a thickness of few cm is found in most of the cores.

Stratigraphically, the Quaternary deposits in this part of the valley can be divided into four units (Marchand & Allwardt, 1981). The Turlock Lake, Riverbank and Modesto Formations are of Pleistocene age (which began 2 million years ago). The Post-Modesto Formation belongs to the Holocene (which began 10,000 years ago). Most of the stratigraphic units found at the site are believed to represent separate alluvial episodes related to Sierran glaciations. The deposits are likely related to flood events that predominantly occurred during the end of a glaciation period. Paleosols, on the other hand, are indicative of substantial time intervals (several thousands to tens of thousands of years) between periods of aggradation (Marchand & Allwardt, 1981) and represent stratigraphic sequence boundaries. Paleosols are buried soil horizons that were formed on stable upper-fan, terrace or hillslope surfaces during interglacial periods (Lettis, 1982). At the site, they consist of strongly cemented sand to sandy loam with a characteristic reddish-brown color. Cementation is primarily by Fe-oxide and Mn-oxide, but also from calcification. They result from initial stratification or drainage boundaries in soil parent material (Harden & Marchand, 1977). Soils that formed on top of the upper Turlock Lake Formation are estimated to be 600 Ka (1Ka = 1000 years) old (Harden, 1987). The estimated age of the Riverbank formation is 130-450 Ka. The Modesto Formation corresponds to the most recent glaciation period (Huntington, 1980).

4.2 Laboratory Measurements

Table 4.2.1 summarizes the Univ. of California Division of Agriculture and Natural Resources Analytical Laboratory (now UC ANR Analytical Laboratory) results which include:

- sand, silt, and clay fractions,
- saturated hydraulic conductivity (K_s),
- bulk density,
- saturated water content (θ_s),
- porosity,
- percent organic matter,
- percent organic carbon.

The USDA texture classification for each soil sample is also included in Table 4.2.1 and corresponds to the “Group 2” assignment in Table 3.3.1. The results are organized by the run and cell number associated with the multi-step outflow sets. The core ID and sample number are also included. Hard copies of the results were compiled by Jim MacIntyre and can be obtained from Thomas Harter. Additional measurements performed on the MSO and other samples (including, but not limited to, nitrate concentration, dry and wet soil weight, depth, field water content, and pH) are tabulated in a master database. The master database is too large to include in this report but may be obtained in electronic format from Thomas Harter.

Table 4.2.2 shows a summary of the basic statistics for the 118 MSO soil samples 1) as a whole (group 1 classification) and, 2) grouped according to texture (group 2 classification). Notice that any missing data, as explained in Section 3.2, are reflected in the first column

of the table (Valid N). For example, recall that 6 samples did not have measured K_s values. This can be seen in the “All” category in which there are 118 soil samples for each measurement except K_s which has 112.

Figure 4.2.1a-i shows the histograms for each of the 9 lab measurements for the soils grouped as a whole. The bulk density is fairly uniformly distributed with about 97% of the samples having a bulk density between 1.4 and 1.9 g/cm³ (Figure 4.2.1a). The organic matter and organic carbon are both nearly normally distributed with an average value of 0.094% and 0.054%, respectively (Figures 4.2.1b-c). About 91% of the samples have a saturated water content between 0.2 and 0.4 (Figure 4.2.1h). There is much more variability in the sand and silt content than in the clay content (Table 4.2.2). Overall, the soils have a surprisingly high sand content, much higher than silt or clay content. In fact, over 75% of the samples have a sand content greater than 60% (Figure 4.2.1d). Each of the grain size fractions has a skewed distribution (Figures 4.2.1d-f). About 84% of the samples have a measured saturated hydraulic conductivity less than 10 cm/hr. (Figure 4.2.1i). This is to be expected as K_s is generally log-normally distributed. The geometric mean of K_s is 0.712 cm/hr.

The box and whisker plots in Figures 4.2.1a-b to Figure 4.2.10a-b show the nine lab measurements categorized by texture (group 2 classification). Each measurement has two box and whisker plots, one showing the mean, standard deviation, and twice the standard deviation and the other showing the minimum, maximum, and lower and upper quartiles. The graphs for the silt texture show a single point and no box or whiskers because this texture consists of only one sample. The arithmetic mean is used for all measurements except for K_s for which we use the geometric mean.

The loam has the least amount of variability in bulk density, while the loamy sand and silt loam have the most variability (Figure 4.2.2a-b). Organic matter content is very low in all samples. Sand has the least amount of organic matter and organic carbon at 0.06% and 0.03%, respectively. Loam, sandy loam, and silt loam have approximately the same amount of organic matter and organic carbon at about 0.11% and 0.063%, respectively. The loamy sand has slightly less organic matter and organic carbon at 0.09% and 0.05%, respectively (Figure 4.2.3a-b and Figure 4.2.4a-b). The silt loam, some of which could be loess deposits, has the greatest porosity and saturated water content while the loam has the least amount of spread in these two parameters (Figure 4.2.5a-b and Figure 4.2.6a-b). The amount of sand, silt, and clay in each texture is straight forward as the designation of each sample to a texture is directly based upon these fractions (Figures 4.2.7a-b, 4.2.8, and 4.2.9a-b). The sand has the most variability in the saturated hydraulic conductivity while the loam has the least (Figure 4.2.10a). Loamy sand, sandy loam, and silt loam have similar geometric mean K_s at 0.636, 0.325, and 0.289 cm/hr, respectively (Table 4.2.2).

4.3 Multi-step Outflow Experiment and Parameter Estimation

The experimental data obtained from the multi-step outflow experiment for one sample (core 5-10-2 #20 /Run 4 Cell 1) are shown in Figure 4.3.1a-b. The sample shown is one with transient data and is categorized as a sand. Figure 4.3.1a displays the transient water

outflow and Figure 4.3.1b displays the transient pressure head. The measured values are shown (as blue dots) along with the optimized curves resulting from the low, medium, and high initial guesses.

Figure 4.3.2 shows the results for a sand sample (core 13-10-2 #3/Run 4 Cell 9) having only handwritten equilibrium points (pressure head vs. water content). Notice there are some data points at the same pressure with different water content values especially at the higher pressure heads. This is because the experimenter continued to make measurements until it was certain that the sample had reached equilibrium.

The van Genuchten parameters obtained either through optimization of the transient data with SF OPT or optimization of the steady-state data points with a spreadsheet function (MS Excel) are summarized in Table 4.3.1. The bold numbers are the chosen results that have been considered to be the best parameter fits and were chosen for further statistical analysis and scaling (“final parameter set”). The final parameter set was selected by comparing the mass balance error (%mbe) of the computed flow simulation and the sum of the squared residual (ssq) of measured vs. simulated data. There are blanks for some of the samples for K_s because these samples do not have transient data and therefore do not have an optimized K_s value. These samples also do not have a value for %mbe because the Excel solver does not calculate that value. In some cases, a particular guess did not converge and these are denoted with an “n/a” entry.

The basic statistics for the chosen van Genuchten parameters for the 97 soil samples grouped 1) grouped as a whole and 2) grouped according to the texture, are in Table 4.3.2. Notice that there are 70 values for K_s , because optimized K_s values exist for only 70 samples. All the texture groups will have fewer K_s samples than α , n , and θ_r samples. Notice that the number of samples in the loam category has been reduced from 4 to 2. That is because Run 6 Cell 4 and Run 10 Cell 1 (both loams) were removed because of SF-OPT convergence problems.

Figure 4.3.3a-d shows the histograms for the van Genuchten (optimized) K_s , α , n , and θ_r for the 97 samples. K_s is log-normally distributed with 84% of the samples having an optimized K_s less than 20 cm/hr. The maximum and minimum optimized K_s are 99.5 cm/hr (associated with a sand sample) and 0.0077 cm/hr (associated with a silt loam), respectively. The remaining 3 parameters (α , n , and θ_r) all appear to be log-normally distributed.

Figure 4.3.4a-h shows categorized box and whisker plots for the van Genuchten parameters. Notice there is not a K_s box and whisker plot for the loam texture since there are no optimized K_s values for the loam. Also, the box and whisker plots for the loam texture showing the minimum and maximum, interquartiles, and median have no whiskers because there are only 2 loam samples. The sand has the highest mean and greatest amount of variation in K_s , α , and n but has the least amount of variation in θ_r .

4.4 Generating Pedotransfer Functions: *NeuroMultistep*

The extensive database generated from the nearly one-hundred multi-step outflow experiments constitutes a unique opportunity to fine-tune pedotransfer functions for the type of unsaturated sediment conditions typically encountered in the eastern San Joaquin Valley. “Pedotransfer function” refers to any kind of tool that allows a user to determine the unsaturated hydraulic conductivity and water retention functions and their parameters (which are time-consuming and expensive to measure) from inexpensive, quickly measurable soil properties. Common pedotransfer function tools estimate unsaturated (soil) hydraulic properties from information about the sand, silt, and clay content of a sample. In addition, saturated water content and bulk density, which can also be measured inexpensively, are sometimes used as input. A popular pedotransfer function tool is Rosetta (Schaap et al., 2001). Rosetta can be obtained for free from the internet (<http://www.ussl.ars.usda.gov/models>). The user provides the textural analysis (% sand, % silt, % clay) and, optionally, bulk density and saturated water content. With this input (entered through a Microsoft Windows interface), the software tool estimates the unsaturated hydraulic functions. These estimates are not accurate measurements and are provided with a confidence interval.

Pedotransfer function tools are based on a sophisticated regression-like analysis of extensive soil hydraulic property databases, which contain information from hundreds of soil samples from often dozens of sites where both, textural data and hydraulic properties have been determined. The drawback of these databases is that they combine data from many different sites, measured by many different methods. Few have considered unsaturated hydraulic properties below the root zone.

Our multi-step outflow experiments completed a series of three multi-year projects in Dr. Hopmans unsaturated zone hydraulics laboratory, each of which examined extensive collections of soil samples from three different locations in the Central Valley: In addition to our Eastern San Joaquin Valley site, these projects investigated soils (limited to within the root zone) in Yolo County (fine-grained, relatively heavy soils), and in the western San Joaquin Valley (wide range of textures, well drained uniform soil profiles).

We used a regression-like technique, known as neural network analysis, to generate pedotransfer functions from these three datasets that are specifically useful for unsaturated sediments and soils in the Central Valley or locations with similar alluvial sediments and soils. Using the dataset described in the previous section, we developed a pedotransfer function tool that is based on our Central Valley specific dataset (“training dataset”) obtained under identical measurement protocols. We find that the resulting tool predicts unsaturated hydraulic properties for Central Valley soils with significantly higher accuracy than Rosetta due to the consistency of the measurement method with which the training dataset was obtained. Prediction errors for water content, for example, are approximately 3% to 4%. The pedotransfer function software, called *NeuroMultistep*, is available for free from Dr. Jan Hopmans (jwhopmans@ucdavis.edu) or at <http://www.agric.usyd.edu.au/acpa>. See Minasny et al. (2004) for detailed information on the neural network analysis and pedotransfer functions.

4.5 Scaling

Recall from Section 3.3 that the samples were assembled into 4 groups:

- Group 1.** Soils scaled all together. No a priori knowledge, such as texture, was used.
- Group 2.** Scaled within individual sub-groups, where sub-groups represent texture classes (USDA soil triangle) as determined in sieve analyses obtained by the UC ANR Analytical Laboratory, without regard to the specific facies that the samples belonged to.
- Group 3.** Scaled within individual sub-groups, where sub-groups represent field determined texture classes (visual determination), but without regard to facies location.
- Group 4.** Scaled samples within individual sub-groups, where each sub-group is associated with a specific facies location (primarily texture-driven). See Figure 4.1.1.

Also recall from Section 3.3 that for each scaling group there are two populations. The first population consists of a mixture of good and poor quality datasets (97 soil samples) and will be referred to as Population 1. The second population contains only good quality datasets (70 soil samples) and will be referred to as Population 2. Each population is scaled with two methods. Method 1 simultaneously scales soil-water pressure, h , and the natural logarithm of hydraulic conductivity, $\ln K$. Method two simultaneously scales $\ln h$ and $\ln K$. Each group, except group 1, has a series of subgroups. For each subgroup there are 5 graphs for pressure head and 5 graphs for unsaturated hydraulic conductivity:

- the original data are graphed with the Powell curve (initial guess curve),
- the scaled values and scaled mean curve using pressure head and the log of the conductivity (method 1),
- the scaled values and scaled mean curve using the log of pressure head and the log of the conductivity (method 2),
- a comparison of the original data and de-scaled data for method 1
- a comparison of the original data and de-scaled data for method 2

In the following figures the two solid curves represent the best fit through the unscaled data and the optimized scaled mean curves. The open triangles represent the unscaled data, the open diamonds represent the scaled data using Method 1, and the open squares represent the scaled data using Method 2. The closed diamonds and the closed squares on the 1:1 graphs represent Method 1 and Method 2, respectively. The correlation between the original data and the estimated or de-scaled values (1:1 graph) is an indicator of the degree of success of the scaling procedure. The estimates are calculated by multiplying the mean curve by the appropriate scale factor. The percent reduction in the sum of the squares (SS) is another indicator for the degree of success of the scaling procedure.

Figure 4.5.1a-j shows scaled and unscaled soil-water pressure and unsaturated hydraulic conductivity curves and the 1:1 curves for Group 1 Population 1 using both scaling

methods. Both the retention and conductivity curves span a large range of values making it clear that this group contains soil samples that do not have similar flow properties. As seen in the scaled and 1:1 curves for h , method 2 yields better results in scaling h while the scaled curve and 1:1 curves for $\ln k$ show that method 1 yields better results for $\ln K$. In the 1:1 curves for h some values stray significantly from the 1:1 line. These values are primarily associated with sands. The percent reductions in SS (the individual sum of squares reduction for h and $\ln K$ are not considered) for method 1 and method 2 are 93% and 66.4%, respectively, indicating that method 1 yields superior results than method 2.

Figure 4.5.2a-j shows scaled and unscaled soil-water pressure and unsaturated hydraulic conductivity curves and the 1:1 curves for Group 1 Population 2 using both scaling methods. As before, it appears that method 2 yields better results for h and method 1 yields better results for $\ln K$. The SS reduction for method 1 is 90.2% and for method it is 62.4%. Again, overall method 1 yields better results than method 2.

To evaluate groups 2-4 the percent reduction in SS for the sandy loam subgroup, appearing in all three groups, was compared. In Group 2 the sandy loam subgroup has 39 samples, in Group 2 the sandy loam subgroup has 20 samples, and in Group 3 the sandy loam subgroup has only 4 samples. Refer to Table 3.3.1 to recall the subgroup designations.

Figure 4.5.3a-j shows scaled and unscaled soil-water pressure and unsaturated hydraulic conductivity curves and the 1:1 curves for Group 2 Population 1. Figure 4.5.4a-j shows scaled and unscaled soil-water pressure and unsaturated hydraulic conductivity curves and the 1:1 curves for Group 3 Population 1. Figure 4.5.5a-j shows scaled and unscaled soil-water pressure and unsaturated hydraulic conductivity curves and the 1:1 curves for Group 4 Population 1. Table 4.5.1 summarizes the SS percent reduction using both scaling methods for the sandy loam subgroup. Method 1 appears to be the superior method for scaling these datasets. The greatest reduction in SS is in group 4 which is the group that uses facies information along with location information. This leads one to ask whether *a priori* knowledge of facies will aid us in scaling the other subgroups. To answer this question a complete statistical analysis will be performed and presented in Michelle Denton's thesis (*in progress*).

4.6 Nitrogen Field Scale Mass Balance, Nitrogen Spatial Variability, and Total Unsaturated Zone Nitrogen Storage

From an agronomic perspective, annual nitrogen losses (either to leaching below the root zone, to ammonia volatilization, or to denitrification) can be estimated using a simple mass balance model for the root zone:

$$\begin{aligned} \text{net N losses} &= \text{Fertilizer N} + \text{Irrigation water N} + \text{Atmospheric N} - \text{Harvest N} \\ \text{net N flux to groundwater} &= \text{net N loss} - \text{volatilization N} - \text{denitrification N} \end{aligned}$$

Using the climatic, crop, irrigation, and fertilization data, we computed both, the average annual water balance and nitrogen balance for the orchard (Onsoy, 2004). Losses due to volatilization and denitrification in the root zone were estimated based on available

research literature. The annual amount of N losses to below the root zone were estimated to be on the order of 51, 83, and 245 lbs/ac/yr (57, 93, and 275 kg/ha/yr) for the control, standard, and high subplot. The average annual recharge rate obtained from the water balance is 43.4 in/yr (110 cm/yr). Combining the two results and assuming uniform, homogeneous flow conditions, the vadose zone is predicted to contain 194, 233, and 426 lbs/acre (218, 261, and 478 kg/ha) of nitrate-N at the three subplots, respectively.

The core data obtained at the field site were used to estimate the actual vadose zone storage of nitrate-N for comparison to the above predictions. Due to the high degree of spatial variability in the water content and nitrate data, a detailed statistical and geostatistical analysis of the core data was implemented to quantify the spatial distribution of water content and nitrate concentration with respect to depth, fertilizer treatment, and the major stratigraphic units within the unsaturated zone. Nitrate in the vadose zone nitrate was highly variable and lognormally distributed. Of the over 800 samples, 225 samples did not contain measurable amount of nitrogen. Particularly in the coarsest-textured facies (sand), a relatively large fraction of samples did not detect nitrate. The remaining samples averaged 5.2, 3.3, and 7.4 mg NO₃-N/l for the control, standard, and high subplot, respectively. Due to the high spatial variability, only the mean of the high subplot was found to be significantly higher relative to the others.

Geostatistical analysis of the data revealed that significant spatial correlation existed between nitrate samples in close proximity to each other, despite the large spatial variability observed. The variograms (correlograms) derived from the dataset show that such correlations are measurable over distances of up to 6 m vertically, but less than 2 m horizontally (in geostatistics referred to as the “range” of the variograms). These findings are consistent with field research on the spatial variability of nitrate in the root zone. Based on the geostatistical models defined from the dataset, nitrate concentrations were estimated throughout the entire vadose zone underneath the site using a geostatistical estimation method called “kriging”, then integrated to obtain an estimate of the total mass of nitrate stored. The deep vadose nitrate-N mass (without the root zone) was 43, 32, and 78 lbs/acre (48, 36, and 87 kg N/ha) for the control, standard, and high subplot, respectively. These latter kriged (“measured”) total N masses amount to 24% (15 - 40%), 15% (9 - 27%), and 19% (12 - 34%), respectively, of those predicted from the agronomic nitrogen mass balance analysis for 1997 when assuming uniform flow conditions (values in parentheses account for estimation errors in the mass balance analysis). A more detailed presentation of the methods and results is presented in Onsoy et al. (2004).

5. DISCUSSION AND CONCLUSIONS

The results about the nitrogen storage in the deep vadose zone raise several issues: 1) What are the potential measurement and estimation errors contributing to the difference between predicted and measured vadose zone N? 2) How representative and significant is the amount of observed spatial variability of water content and nitrate? 3) What is the potential role of spatial variability of water content and nitrate with respect to the spatial distribution of water flux and the expected fate of transport? Can that role explain why the deep vadose

zone nitrogen mass estimated by kriging measured data totaled only one-sixth to one-third of the mass predicted by the nitrogen and uniform water flux mass balance approach? Or does deep vadose zone denitrification account for this discrepancy?

In Onsoy et al. (2004), we quantify measurement and estimation errors and determine that these cannot explain the significant difference between measured vadose zone nitrogen storage and that predicted by using the agronomic nitrogen mass balance and assuming uniform flow conditions in the deep vadose zone. Denitrification, inferred from ^{15}N isotope data measured on select samples, may account for relatively limited nitrogen losses. However, the lack of a significant vertical trend in ^{15}N indicates that denitrification is not a function of depth or specific textural facies and that a significant amount of water in the deeper portion of the unsaturated zone had in fact not experienced denitrification (Harter et al., 2004). In the remainder of the discussion, we therefore focus on the interpretation of the geologic and hydraulic data with respect to nitrate transport and occurrence. Is it possible to explain the relatively low amount of N storage in the vadose zone consistent with the results from the agronomic nitrogen mass balance?

The geologic analysis reveals a significant amount of textural and structural variability throughout the thick unsaturated zone at the site. In the cores, sub-facies structures have been identified at the millimeter, centimeter, and decimeter scale, particularly in the finer-grained sedimentary facies units. More uniformity is observed in the thicker coarse grained sand facies. Several major geologic units (facies) have been identified at the site, some with significant textural contrasts to their neighboring facies, some with gradual transition into the adjacent facies. Within all of the major facies, the smaller scale variability has been thought to contribute significantly to the overall geologic and hydrologic variability within the unsaturated zone.

Hence, when analyzing the observed hydraulic characteristics of the sediments at the site, we must distinguish between two major scales of variability: the variability between the major sedimentologic facies, and the much smaller-scale variability within individual sedimentologic facies identified at the site.

We note that the major sedimentologic facies are horizontally continuous layers throughout the field site, albeit of somewhat variable thickness. As Weissmann et al. points out, these facies themselves are variable, but at a scale that is much larger than our site. For example, if we repeated the same investigation several thousand feet away from the site, we would encounter a similar range of facies types, but their vertical assemblage or sequence, and their thickness would be significantly different.

On the other hand, we find little lateral continuity in the sub-facies structures observed in the continuous cores. These small scale geologic patterns vary not only over short vertical distances, but appear to also vary rapidly in the lateral direction. The lateral spacing of our cores (4 feet minimum distance) is mostly too large to map identifiable sub-facies units across two or more boreholes. Their lateral continuity is therefore limited to generally less than 2 m.

Are the two scales evident in the spatial variability of the hydraulic properties? The significance of this question relates to our ability to appropriately model the spatial heterogeneity of the unsaturated flow and transport processes. Indeed, the extensive database of soil hydraulic properties, with more than ten samples from each major textural unit, strongly indicates that much hydraulic variability exists at the smaller, sub-facies scale. In fact, much of the overall variability of most soil properties (Table 4.2.2) and estimated hydraulic parameters (Table 4.3.2) and even of the scaling factor occurs at the sub-facies scale. The variance of the sub-facies grouped samples are not much smaller than the overall variance of soil properties found at the site (Table 4.2.2, 4.3.2). However, the difference in within-facies variability and total variability is significant, supporting the hypothesis that an identification of the major sedimentologic facies at a site may help identify a significant part of the hydraulic variability acting at the site. In particular, the grain size distribution, as expected, is significantly less variable within facies than in the total sample population.

We expect that similar properties and similar variability exists in facies with comparable textural classification. The statistical data shown in Table 4.2.2 and 4.3.2 are therefore transferable to other sites in the eastern San Joaquin Valley with similar facies textures, even if the facies assemblage or sequence is different.

The amount of spatial variability of the hydraulic properties (within facies and between facies) is tremendous: the variance of $\ln K_s$ exceeds 5, the coefficient of variation of α is greater than 1, that of n is approximately 50% (Table 4.2.2, 4.3.2). Theoretical work on the effects of such strong spatial variability for water and solute transport (Harter et al., 1996, 1998, 1999) suggests, that highly heterogeneous flow conditions are prevalent at the site with strong fingering or preferential flow paths channeling much of the water flow and solute transport through a relatively small portion of the unsaturated domain. This theoretical work suggests that infiltration and downward displacement velocities are log-normally distributed with high variance, which leads to highly variable distribution of nitrate. This is indeed consistent with the site conditions, where nitrate is found to vary over several orders of magnitude. On the other hand, we have found relatively uniform distribution of chloride and bromide (when compared to the variability of nitrate) in a few selected samples from the upper 15 feet (not reported above). The variability of chloride and bromide is comparable to that of the organic matter content, which varies within less than two orders of magnitude. The discrepancy in variability between nitrate and chloride (or bromide) should be explored further in future work.

Highly heterogeneous flow-paths, suggested by the variability of hydraulic properties and nitrate, are further enhanced by the strong fingering created by the infiltration and redistribution of water in the sandy loamy root zone at the site, as described in Wang et al., 2003. On the other hand, low permeability layers such as the hardpans and the fine grained facies below the channel deposits may counteract some of the flux variability; however those effects can only be quantified using explicit computer modeling based on the parameter distributions defined above (we are currently investigating these effects in a follow-up project).

The highly heterogeneous, log-normally distributed flow conditions that apparently dominate unsaturated flow at the site should be considered to be representative for the flow patterns in most unsaturated zones in the Eastern San Joaquin Valley. Extrapolating the field data based on our theoretical understanding of flow in such systems, we expect water flux to be as variable as or more variable than hydraulic conductivity. With that degree of heterogeneity in the flow pattern, flow in the unsaturated zone is essentially divided into two phases: much of the unsaturated zone is moist with almost stagnant water; a small fraction of the unsaturated zone – possibly less than one-fifth of its volume, is part of narrow, tortuous flow paths that are relatively wet and transmit the bulk of the recharge water and consequently, the bulk of nitrate.

From the analysis of the long-term annual water balance and assuming homogeneous, uniform water flow, we predicted that nitrate and water would need 3.2 years to travel from the land surface to the water table at 52 feet. However, given the large variance in geologic, textural, and hydraulic properties, it can be shown with computer models that water flow is not uniform under the geologic and hydraulic conditions described above. Instead, nitrate is leached in preferential flow paths resulting in quick transport throughout the unsaturated zone, possibly within one to two years or even less. This could explain the relatively low amounts of total nitrogen found in the deep unsaturated zone.

These findings, if confirmed with our ongoing stochastic modeling project, have major implications for the interpretation of nitrate or other chemical distributions in the unsaturated zone: In estimating the net annual losses from core samples, one of the standard practices is to collect composite soil samples from the bottom of the root zone (usually 120 cm – 180 cm). Composite samples provide an arithmetic average nitrate concentration. They are interpreted using uniform flow conditions as the underlying conceptual model for estimating nitrogen losses. Based on the findings reported here, which suggest that preferential flow conditions may prevail in the root zone, but also throughout a thick unsaturated zone, we hypothesize that such a uniform flow based interpretation may significantly underestimate the nitrogen leaching rate.

Overcoming Site-Specificity:

How can results from this particular research orchard be extrapolated to other sites? The particular conditions at the Kearney site are typical for the tree fruit orchard areas in much of Fresno and Tulare County east of Highway 41. The field research component helps built a much improved understanding of the general relationship between characteristics of geologic and soil heterogeneity in alluvial unsaturated sediments (horizontal and vertical variability, range of layer thickness, contrast of soil textures encountered, degree of interbedding with clays, silty clays, and hardpan) and the overall characteristics of the fate and transport of nitrate in such sediments. With these data, we are able to develop and validate a new approach to model nitrate leaching in deep vadose zones, which is the second (and ongoing) research component of this project. It is the detailed site geologic and hydrologic characterization, combined with the improved understanding and nitrate transport modeling capability that will most benefit the assessment of nitrate leaching at other sites with thick vadose zones of alluvial sediments. To overcome site-specificity, we developed pedotransfer functions that allow users to compute unsaturated hydraulic

properties from soil texture data. We also characterized the spatial variability found in typical alluvial fan deposits of the eastern San Joaquin Valley. The statistical properties of unsaturated hydraulic properties and their scale factors are tabulated as a function of typical facies groups. We believe that these are representative for such facies at other locations in the eastern San Joaquin Valley as well. Together, the pedotransfer functions and the scaling factor analysis provide a unique, site-independent database for soil physicists and others needing to characterize the hydraulic properties of the unsaturated zone from texture data or facies description of soil or sediment cores.

Publications and New Products Generated by Project:

PUBLICATIONS

- Publication 1. Tuli, A., M.A. Denton, J.W. Hopmans, T. Harter, and J.L. Mac Intyre. 2001. Multi-step outflow experiment: From soil preparation to parameter estimation. Hydrology program, Dept of Land, Air, and Water Resources, University of California, Davis, CA, Paper number 100037.
- Publication 2. Minasny, B., J. W. Hopmans, T. Harter, S. O. Eching, A. Tuli, M. A. Denton, 2004. Neural networks prediction of soil hydraulic functions for alluvial soils using multistep outflow data, Soil Science Soc. Of Am. Journal 68:417-429.
- Publication 3. Onsoy, Y. S., T. Harter, T. R. Ginn, W. R. Horwath, 2004. Spatial variability and transport of nitrate in a deep alluvial vadose zone. Vadose Zone J., (in print).
- Publication 4. Harter, T., Y. S. Onsoy, K. Heeren, M. Denton, G. Weissmann, J. W. Hopmans, W. R. Horwath, 2004. Deep Vadose Zone Hydrology and the Fate of Nitrate in the Eastern San Joaquin Valley. California Agriculture (in review).

PUBLICATIONS RESULTING FROM ESTABLISHMENT OF THIS FIELD SITE

- Publication 6. Wang, Z., L. Wu, T. Harter, J. Lu, W. A. Jury, 2003. A field study of unstable preferential flow during soil water redistribution, Water Resour. Res. 39(4), 10.1029/2001WR000903, 01 April 2003.
- Publication 7. Wang, Z., Lu, L. Wu, T. Harter, W. A. Jury, 2002. Visualizing preferential flow paths using ammonium carbonate and a pH-Indicator, Soil Sci. Soc. Of America J. 66:347-351.

PRODUCTS

- Large database of texture and facies specific geologic, texture, and hydrologic data;
- *NeuroMultistep*, a simple hands-on computer tool to predict hydraulic properties of soils from simple texture data;

Extension Activities Related to This Project:

- Harter, T., "Drilling in a tree orchard to assess nitrate leaching", 2 field tours to researchers, water district personnel, farmers, tree fruit industry, fertilizer industry representatives, 7/22/97; 7/25/97; 8/6/97; 9/17/97; 9/19/97; 9/30/98.

- Harter, T., "Understanding nitrate and pesticide contamination when locating water supply wells: spatial variability and long-term trends", California/Nevada American Water Works Association, Fall Conference, Los Angeles, 10/22/97.
- Harter, T., "Nitrate management and groundwater contamination: Walking on the razor's edge?", California Fertilizer Association Nutrient Seminar, Fresno, 10/8/98.
- Harter, T., "Groundwater resources management in the vineyard", UC Coop. Ext. San Luis Obispo County, Vineyard Water Management Shortcourse, Paso Robles, 5/11-13/99.
- Harter, T., "Drinking water source protection through nutrient management", FREP/SAREP Joint Annual Conference, Modesto, 11/30/99.
- Harter, T., "Nitrate distribution in a deep, alluvial unsaturated zone: Geologic control vs. fertilizer management", California chapter of the American Society of Agronomy (CASA) Annual Meeting, Fresno, 2/6/02.
- Harter, T., "Nitrate in the deep alluvial unsaturated zone: Linking agriculture with groundwater quality?", Monterey County Water Resources Management Agency, Nitrate Technical Advisory Committee Meeting, 6/27/02.
- Harter, T., *Member*, Monterey County Nitrate Technical Advisory Committee, 1997-current.
- Harter, T., *Member*, Subcommittee on denitrification, USDA-NRCS Technical Committee for developing the Comprehensive Nutrient Management Plans for confined animal farming operations, 2002-current.
- Harter, T., *Member*, CALFED Panel on Appropriate Water Measurement in Agriculture, 2001-2003.

Technical/Scientific Conference Presentations:

- Harter, T., "Flow and transport processes in the non-shallow vadose zone: Heterogeneity and uncertainty", Dept. of Geological and Environmental Sciences, Stanford University, 2/25/98.
- Harter, T., "Field-scale transport of reactive contaminants in the vadose zone", American Geophysical Union Fall Meeting, San Francisco, 12/7/98.
- Denton, M., T. Harter, J. W. Hopmans, W. R. Horwath, "Spatial variability of hydraulic properties in unsaturated alluvial sediments", American Geophysical Union Fall Meeting, San Francisco, 12/19/00.
- Harter, T., "Nonpoint source pollution from animal farming in Semi-arid regions: Spatio-temporal variability and groundwater monitoring strategies", UNESCO Conference on Future Groundwater Resources at Risk, Lisbon, Portugal, 6/25/01
- Harter, T., "Stratigraphic control of nonpoint source pollution in alluvial aquifer systems", Dept. of Civil Engineering, Universidad Polytechnica Barcelona, Spain, 7/3/01.
- Harter, T., "Stratigraphic control of nonpoint source pollution in alluvial aquifer systems", Dept. of Environmental & Applied Geology, Tuebingen University, Germany, 7/10/01.

- Denton, M., T. Harter, J. W. Hopmans, W. R. Horwath, “Nitrogen transport in thick, unsaturated, spatially variable alluvial sediments”, American Geophysical Union, Fall Meeting, San Francisco, 12/15/01.
- Onsoy, Y. S., T. Harter, T. Ginn, “Assessing Impacts of Agricultural Management Practices on Groundwater Quality: Modeling Nitrate Reactive Transport in Deep Unsaturated Alluvial Sediments”, Nitrate In Groundwater: Sources, Impacts, and Solutions, Fresno, California, The Sixth Symposium in Groundwater Resources Association’s Series on Groundwater Contaminants in California; November 12-13, 2002.
- Onsoy, Y. S., T. Harter, T. R. Ginn “Estimating N Budget in a Deep Alluvial Unsaturated Zone: Potential for Nitrate Leaching to Groundwater”, December 6-10, 2002, American Geophysical Union 2002 Fall Meeting, San Francisco, California.
- Onsoy, Y. S., Harter, T., Ginn, T., Hopmans, J. W., Horwath, W. “Geostatistical Interpolation of Field Data in Three Dimensions to Assess Nitrate Leaching to Groundwater”, April 7-11, 2003, 2003 EGS - AGU – EGU Joint Assembly Meeting, Nice France;

6. REFERENCES

- ASTM, Standard test method for particle-size analysis of soils, D 422-63, *1985 Annual Book of ASTM Standards, 04.08*, 117-127, American Society for Testing and Materials, Philadelphia, 1985.
- Brooks, R.H., and A.T. Corey, 1964. Hydraulic properties of porous media. Fort Collins, Colorado State University Hydrology Paper no. 3, 27 p.
- Chow, Ven Te, D.R. Maidment, and L.W. Mays, 1988. *Applied Hydrology*, McGraw-Hill, New York.
- Clausnitzer, V., J.W. Hopmans and D.R. Nielsen, 1992. Simultaneous scaling of soil water retention and hydraulic conductivity curves, *Water Resources Research*, 28: 19-31.
- Clausnitzer, V., J.W. Hopmans and D.R. Nielsen, 1990. A comprehensive algorithm for simultaneous scaling of soil water retention and hydraulic conductivity data. Dept of Land, Air, and Water Resources, University of California, Davis, CA, Paper number 100018.
- Eching, S. O., and J. W. Hopmans, 1993. Optimization of hydraulic functions from transient outflow and soil water pressure head data *Soil Sci. Soc. Amer. J.*, 57: 1167-1175.
- Eching, S. O., J. W. Hopmans, and O. Wendroth, 1994. Unsaturated hydraulic conductivity from transient multi-step outflow and soil water pressure data, *Soil Sci. Soc. Amer. J.*, 58: 687-695.
- Fogg, G.E., D.E. Rolston, E.M. LaBolle, K.R. Burow, L.A. Maserjian, D. Decker, and S.F. Carle, 1995. Matrix diffusion and contaminant transport in granular geologic materials, with case study of nitrate contamination in Salinas Valley, California: Final Technical Report submitted to Monterey County Water Resources Agency and U.S. Geological Survey in fulfillment of Water Resources Research Award No. 14-08-0001-G1909, 65 p.

- Gardner, W.R., 1958. Some steady-state solutions of the unsaturated moisture flow equation with application to evaporation from a water table. *Soil Science*, vol. 85, no. 1, p. 228-232.
- Gilliam, J. W., S. Dasberg, L. J. Lund, and D. D. Focht, 1978. Denitrification in four California soils: Effect of soil profile characteristics, *J. Soil Sci. Soc. of Amer.*, 42, 61-66.
- Harden, J.W., 1987. Soils developed in granitic alluvium near Merced, California. U.S Geological Survey Bulletin 1590-A, 65p.
- Harden, J.W., and Marchand, D.E., 1977. The soil chronosequence of the Merced River area. In: Singer, M.J. (ed.). Soil development, geomorphology, and Cenozoic history of the northeastern San Joaquin Valley and adjacent areas, California. Soil Science Society of America-Geological Society of America joint field session, 1977, guidebook, p. 22-38.
- Harter, T., and T.-C. J. Yeh, 1996. Stochastic analysis of solute transport in heterogeneous, variably saturated soils. *Water Resour. Res.*, 32(6): 1585-1595.
- Harter, T., and T. C. J. Yeh. 1998, Flow in unsaturated random porous media nonlinear numerical analysis and comparison to analytical stochastic models. *Advances in Water Resources*. 22 (2): 257-272.
- Harter, T., and D. Zhang. 1999. Water flow and solute spreading in heterogeneous soils with spatially variable water content. *Water Resour. Res.* 35(2), 415-426.
- Hartz, T. K., and F. Costa, 1995. Nitrogen movement through intensive on-farm monitoring, in: Walsh Cady, C. and R. Coppock (eds.), *Proceedings of the Third Annual Fertilizer Research and Education Program Conference*, California D.F.A., 1220 N Str. Sacramento, CA 95814, p. 20-22.
- Haverkamp, R. et al, 1977. A comparison of numerical simulation models for one-dimensional infiltration. *Soil Science Society of America Proceedings*, vol. 41, p. 285-294.
- Hopmans, J.W., J.C. van Dam, S.O. Eching, and J.N.M. Stricker. 1994. Parameter estimation of soil hydraulic functions using inverse modeling of transient outflow experiments. *Trends in Hydrology*, 1:217-242.
- Hopmans, J.W., J. Simunek, N. Romano and W. Durner. 2002. Simultaneous determination of water transmission and retention properties-inverse methods. In J. Dane, D.E. Elrick, D. Reynolds and B Clothier (eds). *Methods of Soil Analysis*. Part I. Third Edition American Society of Agronomy, Monograph No. 9, Madison, WI.
- Horwath, W. R. and E. A. Paul. 1994. Microbial Biomass. *In Methods of Soil Analysis-Part2-Microbiological and Biochemical Properties*. Weaver, R. W., J. S. Angle, and P. S. Bottomley, eds., Soil Science Society of America, Madison, WI, pp. 753-773.
- Huntington, G.L., 1980. Soil-land form relationships of portions of the San Joaquin River and Kings River alluvial depositional systems in the Great Valley of California. Ph.D. dissertation, University of California, Davis, 147p.
- Johnson, R.S., F.G. Mitchell, and C.H. Crisosto, 1995. Nitrogen fertilization of Fantasia nectarine – A 12 year study. *UC Kearney Tree Fruit Review* Vol 1, 14-19.
- Kellogg, R.L., M.S. Maizel, and D.W. Goss, 1992. *Agricultural chemical use and groundwater quality: Where are the potential problem areas?* USDA-SCS National Center for Resource Innovations, Washington, D.C.

- Klein, J.M., and W.L. Bradford, 1979. Distribution of nitrate and related nitrogen species in the unsaturated zone, Redlands and vicinity, San Bernardino County, California, *United States Geological Survey Water Resources Investigations Report 79-60*, 81 p.
- Klute, A (ed.), 1986. *Methods of Soil Analysis, Part 1: Physical and Mineralogical Methods*, 2nd Edition, American Society of Agronomy, Soil Science Society of America, Madison, WI, 1188p.
- Kosugi, K., 1994. Three parameter lognormal distribution model for soil water retention. *Water Resources Research*, 30: 891-901.
- Lettis, W.R., 1982. Late Cenozoic stratigraphy and structure of the western margin of the central San Joaquin Valley, California. U.S. Geological Survey Open-File Report, 82-526, 203 p.
- Lovatt C. J., 1995. Avocado growers can reduce nitrate groundwater pollution and increase yield and profit, in: Walsh Cady, C. and R. Coppock (eds.), *Proceedings of the Third Annual Fertilizer Research and Education Program Conference*, California D.F.A., 1220 N Str. Sacramento, CA 95814, p. 32-33.
- Lovatt, C.J., and J.G. Morse, 1995. Citrus growers can reduce nitrate groundwater pollution and increase profits by using foliar urea fertilization, in: Walsh Cady, C. and R. Coppock (eds.), *Proceedings of the Third Annual Fertilizer Research and Education Program Conference*, California D.F.A., 1220 N Str. Sacramento, CA 95814, p. 45-47.
- Lund, L. J., D. C. Adriano, and P. F. Pratt, 1974. Nitrate concentrations in deep soil cores as related to soil profile characteristics, *J. Environ. Qual.*, 3, 78-82.
- Marchand, D.E. and Allwardt, A., 1981. Late Cenozoic Stratigraphic Units, Northeastern San Joaquin Valley, California: US Geological Survey Bulletin 1470.
- Metropolitan Water District of Southern California, 1987. Groundwater quality and its impact on water supply in the Metropolitan Water District service area, *Report No. 969, Los Angeles, Metropolitan Water District of Southern California*, 45 p.
- Meyer, R. D., 1995. Potential nitrate movement below the root zone in drip irrigated almonds, in: Walsh Cady, C. and R. Coppock (eds.), *Proceedings of the Third Annual Fertilizer Research and Education Program Conference*, California D.F.A., 1220 N Str. Sacramento, CA 95814, p. 50-51.
- Miller, R. O., and R. Friedman, 1995. Use of ion exchange resin bags to monitor soil nitrate in tomato cropping systems of Yolo County, in: Walsh Cady, C. and R. Coppock (eds.), *Proceedings of the Third Annual Fertilizer Research and Education Program Conference*, California D.F.A., 1220 N Str. Sacramento, CA 95814, p. 35.
- Miller, E.E. and R.D. Miller, 1956. Physical theory for capillary flow phenomena, *J. Applied Physics*, 27(4), 324-332.
- Minasny, B., J. W. Hopmans, T. Harter, S. O. Eching, A. Tuli, M. A. Denton, 2004. Neural networks prediction of soil hydraulic functions for alluvial soils using multistep outflow data, *Soil Science Soc. Of Am. Journal* 68:417-429.
- Mualem, Y. 1976. A new model for predicting the hydraulic conductivity of unsaturated porous media. *Water Resour. Res.* 12:513-522.
- Onsoy, Y. S., T. Harter, T. R. Ginn, W. R. Horwath, 2004. Spatial variability and transport of nitrate in a deep alluvial vadose zone. *Vadose Zone J.* (in print)

- Page, R.W. and LeBlanc, R.A., 1969. Geology, hydrology and water quality in the Fresno area, California. USGS Open-File Report, 70p.
- Powell, M.J.D., 1964. An efficient method for finding the minimum of a function of several variables without calculating derivatives. *The Computer Journal* 7:155-162.
- Pratt, P. F., W. W. Jones, and V. E. Hunsaker, 1972. Nitrate in deep soil profiles in relation to fertilizer rates and leaching volume, *J. Environ. Qual.*, 1, 97-102.
- Rees, T. F., D. J. Bright, R. G. Fay, A. H. Christensen, R. Anders, B. S. Baharie, and M. T. Land, 1995. Geohydrology, water quality, and nitrogen geochemistry in the saturated and unsaturated zones beneath various land uses, Riverside and San Bernardino Counties, California, 1991-93, *United States Geological Survey Water Resources Investigations Report 94-4127*, 267p.
- Retallack, G.J., 1990. Soils of the Past – An introduction to paleopedology. Unwin Hyman (Ed.), Winchester/Mass., 520p.
- Schaap, M.G., F.L. Leij, and M.Th. van Genuchten, 2001. Rosetta: a computer program for estimating soil hydraulic parameters with hierarchical pedotransfer functions. *J. Hydrol.* 251:163-176
- Tanji, K. K., M. Fried, and R. M. Van De Pol, 1977. A steady-state conceptual nitrogen model for estimating nitrogen emissions from cropped lands, *J. Environ. Qual.*, 6, 155-159.
- Tanji, K. K., F. E. Broadbent, M. Mehran, and M. Fried, 1979. An extended version of a conceptual model for evaluating annual nitrogen leaching losses from croplands, *J. Environ. Qual.*, 8, 114-120.
- Tuli, A., M.A. Denton, J.W. Hopmans, T. Harter, and J.L. Mac Intyre. 2001. Multi-step outflow experiment: From soil preparation to parameter estimation . Hydrology program, Dept of Land, Air, and Water Resources, University of California, Davis, CA, Paper number 100037.
- van Genuchten, M.TH., 1980. A closed form equation for predicting the hydraulic conductivity of unsaturated soils. *Soil Sci. Soc. Am. J.* 44:892-898.
- Wang Z., A. Tuli, and W.A. Jury. 2003. Unstable flow during a redistribution period in homogeneous soil. *Vadose Zone Journal*, 2:52-60.
- Weinbaum, S. A., and D. A. Goldhamer, 1995. Nitrogen fertilizer management to reduce groundwater degradation, in: Walsh Cady, C. and R. Coppock (eds.), *Proceedings of the Third Annual Fertilizer Research and Education Program Conference*, California D.F.A., 1220 N Str. Sacramento, CA 95814, p. 38-40.
- Weissmann, G.S., S.F. Carle, and G.E. Fogg, 1999. Three-dimensional hydrofacies modeling based on soil surveys and transition probability geostatistics. *Water Resources Research*, 35: 1761-1170.

TABLES

Key
AS = Ammonium Sulfate (21% N)
CN = Calcium Nitrate (15.5% N)
AN = Ammonium Nitrate (34% N)

Table 2.2.1. Fertilizer amounts and application dates.

DATE	TREATMENT PLOTS			
	100 lbs/acre N	175 lbs/acre N	250 lbs/acre N	325 lbs/acre N
9/14/1982	5 lbs Ammonium Sulfate per tree to all trees			
2/24/1983			5# AS	5# AS
4/22/1983			2.5# AS	2.5# AS
5/26/1983		4.9# CN		4.9# CN
9/15/1983	2.6 lbs Ammonium Nitrate per tree to all trees			
3/13/1984			3# AN	3# AN
4/26/1984			1.5# AN	1.5# AN
5/23/1984		4.9# CN		4.9# CN
9/11/1984	2.1 lbs Ammonium Nitrate per tree to all trees			
3/20/1985			3# AN	3# AN
5/1/1985			1.5# AN	1.5# AN
5/29/1985		4.9# CN		4.9# CN
9/4/1985	3.2 lbs Ammonium Nitrate per tree to all trees			
3/7/1986			3# AN	3# AN
4/17/1986			1.5# AN	1.5# AN
5/29/1986		5# CN		5# CN
9/9/1986	3.3 lbs Ammonium Nitrate per tree to all trees			
Mid-March 1987			3# AN	3# AN
Mid-April 1987			1.5# AN	1.5# AN
6/1/1987		5# CN		5# CN
9/18/1987	~3 lbs Ammonium Nitrate per tree to all trees			
4/5/1988			3# AN	3# AN
5/5/1988			1.5# AN	1.5# AN
6/6/1988		5# CN		5# CN
9/7/1988	3.0 lbs Ammonium Nitrate per tree to all trees			
3/29/1989			3# AN	3# AN
5/1/1989			1.5# AN	1.5# AN
June 1989		5# CN		5# CN
9/27/1989	2.6 lbs Ammonium Nitrate per tree to all trees			
3/28/1990			3# AN	3# AN
5/7/1990			1.5# AN	1.5# AN
6/4/1990		5# CN		5# CN
9/17/1990	3.6 lbs Ammonium Nitrate per tree to all trees			
3/22/1991			3# AN	3# AN
5/2/1991			1.5# AN	1.5# AN
6/3/1991		5# CN		5# CN
9/5/1991	3.6 lbs Ammonium Nitrate per tree to all trees			
3/20/1992			3# AN	3# AN
4/29/1992			1.5# AN	1.5# AN
5/28/1992		5# CN		5# CN
9/9/1992	3.1 lbs Ammonium Nitrate per tree to all trees			
3/17/1993			3# AN	3# AN
5/3/1993			1.5# AN	1.5# AN
6/1/1993		5# CN		5# CN
9/13/1993	3.1 lbs Ammonium Nitrate per tree to all trees			
3/21/1994			3# AN	3# AN
5/10/1994			1.5# AN	1.5# AN
6/1/1994		5# CN		5# CN
9/16/1994	3.3 lbs Ammonium Nitrate per tree to all trees			

Table 2.3.1. Irrigation dates for the orchard. The date shown is the afternoon start date.

1983	1990	1991	1992	1993	1994	1995	1996	1997
28-Apr	29-Mar	7-Feb	22-Apr	19-Mar	21-Mar	1-May	1-May	25-Mar
19-May	17-Apr	3-May	29-Apr	16-Apr	14-Apr	10-May	9-May	10-Apr
31-May	8-May	22-May	7-May	3-May	10-May	22-May	21-May	21-Apr
14-Jun	4-Jun	3-Jun	18-May	18-May	23-May	31-May	3-Jun	5-May
24-Jun	14-Jun	20-Jun	28-May	1-Jun	1-Jun	8-Jun	25-Jun	15-May
30-Jun	21-Jun	1-Jul	3-Jun	9-Jun	9-Jun	20-Jun	2-Jul	27-May
11-Jul	27-Jun	15-Jul	9-Jun	18-Jun	16-Jun	3-Jul	30-Jul	9-Jun
21-Jul	3-Jul	30-Jul	18-Jun	24-Jun	23-Jun	10-Jul	11-Sep	19-Jun
1-Aug	10-Jul	8-Aug	25-Jun	1-Jul	30-Jun	25-Jul	3-Oct	30-Jun
9-Aug	24-Jul	6-Sep	1-Jul	9-Jul	16-Jul	7-Aug		10-Jul
22-Aug	9-Aug		8-Jul	16-Jul	28-Jul	23-Aug		21-Jul
29-Aug	5-Sep		23-Jul	30-Jul	8-Aug	6-Sep		1-Aug
19-Sep	18-Sep		6-Aug	9-Aug	16-Sep	4-Oct		13-Aug
			20-Aug	24-Aug				21-Aug
			31-Aug	2-Sep				2-Sep
			10-Sep	14-Sep				16-Sep
			28-Sep					

Table 2.4.1. Explanation of CIMIS report contents.

CIMIS Report Types	
Standard Daily report	<p>This report will provide average daily data for the stations and date range provided.</p> <p>Consists of 14 pre-determined sensors: ETo; precipitation; solar radiation; average vapor pressure; maximum, minimum, and average air temperature; maximum, minimum, and average relative humidity; dew point; wind speed; wind run; and average soil temperature.</p>
Standard Hourly report	<p>This report will provide average hourly data for the stations and date range provided.</p> <p>Consists of 10 pre-determined sensors: ETo; precipitation; solar radiation; vapor pressure; air temperature; relative humidity; dew point; wind speed; wind direction; and soil temperature.</p>
Standard Monthly report	<p>Allows you to select weather stations for which you will receive monthly summaries for a variety of sensors.</p>

Table 2.4.2. Summary statistics for weather averages from 1983 to 1999. All values are monthly with exceptions noted.

	Min	Max	Mean	Standard deviation
Total Precipitation (in.) annual	3.9	22.6	13.0	4.7
Total Precipitation (in.) monthly	0	8.7	1.1	1.5
Evapotranspiration (in.) annual	46.8	56.4	53.3	2.7
Evapotranspiration (in.) monthly	0.4	8.8	4.5	2.6
Average Solar Radiation (W/m ²)	51	355	206.02	91.5
Vapor Pressure (kPa)	0.4	2	1.23	0.35
Maximum Air Temperature (°C)	8.4	37.2	24.6	7.9
Minimum Air Temperature (°C)	-2.6	18.9	9.1	5.3
Average Air Temperature (°C)	3.3	27.5	16.5	6.7
Maximum Relative Humidity (%)	40	100	88.9	11.2
Minimum Relative Humidity (%)	17	84	41.9	16.7
Average Relative Humidity (%)	27	95	64.8	14.6
Average Dew Point (°C)	-6.1	17.7	9.2	4.5
Average Wind Speed (m/s)	1	2.5	1.7	0.36
Average Soil Temperature (°C)	6.2	29.6	17.8	6.3

Table 2.4.3. Department of Water Resources CIMIS Sensor Specifications

The following sensor specifications, except sensor heights, are provided by the particular manufacturer.

Precipitation

Sensor:	Tipping-bucket rain gauge with magnetic reed switch
Model:	TE525MM
Maker:	Texas Electronics
Height:	1.0 meters
Specifications Orifice:	24.5 cm (9.644 in)
Resolution:	0.1 mm
Accuracy:	± 1% at 5 cm/hour or less

Air temperature/ Relative humidity

Sensor:	Fenwal Thermistor/ HUMICAP H-sensor
Model:	HMP35C
Maker:	Vaisala/ modified by Campbell Scientific, Inc.
Height:	1.5 meters
Specifications Range:	0 to 100% RH, -35 to 50 °C
Accuracy:	± 2% RH (0-90% RH), ±5% RH (90-100% RH), ±0.1 °C over -24 to 48 °C range.
Note:	Both sensors are enclosed in a 12-plate naturally aspirated radiation shield made by R.M. Young.

Total solar radiation

Sensor:	Pyranometer—high stability silicon photovoltaic detector (blue enhanced)
Model:	LI200S
Maker:	Li-Cor
Height:	2.0 meters
Specifications	
Sensitivity:	±5% error under natural sunlight conditions. Typically 80 micro Ampere per 1000 watts per square meter.
Linearity:	Maximum deviation of 1% up to 3000 watts per square meter.
Response time:	10 micro seconds
Correction:	Cosine corrected up to 80 degrees angle of incidence
Azimuth:	±1% error over 360 degrees at 45 degrees elevation

Table 2.4.3 cont. Department of Water Resources CIMIS Sensor Specifications

Wind speed

Sensor: Three-cup anemometer utilizing a magnet activated reed switch whose frequency is proportional to wind speed
Model: 014A
Maker: Met-One
Height: 2.0 meters
Specifications Range: 0-45 m/s (0-100 mph)
Threshold: 0.45 m/s (1 mph)
Gust Survival: 0-53 m/s (0-120 mph)
Accuracy: 1.5% or 0.11 m/s (0.25 mph)

Soil temperature

Sensor: Soil Thermistor—Fenwal Electronic UUT51J1 thermistor in water resistant coating.
Model: 107B
Maker: Fenwal/modified by Campbell Scientific, Inc.
Height: 15 cm (6 in) below soil surface under irrigated grass
Specifications Accuracy: Worst case ± 0.4 °C over -33 to 48 °C, ± 0.5 °C at -40 °C

Table 2.5.1. Fruit yield, load and weight summary, including the 7 year average.

Yield (kg fruit/tree)		YEAR							<u>7 yr.</u> <u>Ave.</u>
		<u>1983</u>	<u>1984</u>	<u>1985</u>	<u>1991</u>	<u>1992</u>	<u>1993</u>	<u>1994</u>	
Treatment (lbs N/acre)									
0		191.0	155.9	126.1	132.2	126.3	100.2	103.3	133.6
100		202.4	194.9	202.8	207.2	203.1	160.4	155.9	189.5
175		198.9	187.2	171.1	193.6	214.5	143.4	165.5	182.0
250		201.4	205.5	186.9	222.1	209.8	160.2	177.9	194.8
325		203.5	190.4	170.7	197.9	187.7	134.0	159.4	177.7

Fruit Load (# fruit/tree)		YEAR						
		<u>1983</u>	<u>1984</u>	<u>1985</u>	<u>1991</u>	<u>1992</u>	<u>1993</u>	<u>1994</u>
Treatment (lbs N/acre)								
0		1130	945	856	906	868	641	657
100		1199	1130	1352	1313	1267	917	827
175		1118	1074	1100	1134	1418	754	933
250		1128	1191	1217	1393	1342	912	949
325		1150	1087	1135	1200	1214	745	911

Fruit Weight (grams/ fruit)		YEAR						
		<u>1983</u>	<u>1984</u>	<u>1985</u>	<u>1991</u>	<u>1992</u>	<u>1993</u>	<u>1994</u>
Treatment (lbs N/acre)								
0		168.6	152.3	139.1	130.5	137.8	149.9	145.5
100		172.8	173.8	154.4	165.8	160.3	179.2	184.7
175		176.4	172.0	153.2	167.9	153.8	187.3	181.3
250		179.3	177.9	154.0	169.4	157.1	179.9	189.8
325		177.1	172.9	150.8	166.8	152.5	176.8	175.5

Table 2.5.2. Percent nitrogen in fruit on a dry mass basis (1983).

Treatment (lbs N/acre)	Flesh	Pit	Seed	Total
100	1.57	0.60	5.71	7.88
175	1.66	0.47	5.63	7.76
250	1.78	0.78	5.92	8.48
325	2.05	0.50	5.76	8.31

Table 2.5.3. Leaf nutrients.

<u>%N</u>		Year						
		<u>1983</u>	<u>1984</u>	<u>1985</u>	<u>1991</u>	<u>1992</u>	<u>1993</u>	<u>1994</u>
Treatment (lbs N/acre)								
	0	2.82	2.51	2.44	2.69	2.59	2.52	2.66
	100	2.69	2.7	2.77	2.95	2.78	2.76	3.16
	175	3.03	3.12	3.07	3.13	2.95	2.82	3.21
	250	3.28	3.28	3.36	3.49	3.09	3.28	3.53
	325	3.19	3.4	3.37	3.48	3.16	3.17	3.54

<u>%P</u>		Year						
		<u>1983</u>	<u>1984</u>	<u>1985</u>	<u>1991</u>	<u>1992</u>	<u>1993</u>	<u>1994</u>
Treatment (lbs N/acre)								
	0	-	0.23	0.27	0.29	0.34	-	0.28
	100	-	0.22	0.18	0.19	0.21	-	0.19
	175	-	0.21	0.18	0.18	0.21	-	0.19
	250	-	0.22	0.18	0.18	0.19	-	0.19
	325	-	0.18	0.18	0.18	0.20	-	0.19

<u>%K</u>		Year						
		<u>1983</u>	<u>1984</u>	<u>1985</u>	<u>1991</u>	<u>1992</u>	<u>1993</u>	<u>1994</u>
Treatment (lbs N/acre)								
	0	2.58	2.11	2.81	2.00	2.25	3.34	3.13
	100	2.58	1.92	2.31	1.72	1.64	2.46	2.55
	175	2.52	1.76	2.18	1.47	1.36	2.39	2.57
	250	2.52	1.84	2.12	1.41	1.23	1.95	2.09
	325	2.38	1.73	2.13	1.31	1.33	2.14	2.09

Table 2.5.4. Soil nitrate concentration, in ppm, and pH in October, 1991.

Depth (ft)	Treatments (lbs N/acre/year)				
	0	100	175	250	325
	<u>Nitrate (ppm)</u>				
0 – 0.5	6.4	23.1	46.0	23.6	14.4
0.5 – 1	3.4	13.4	20.6	12.5	7.4
1 – 2	1.9	8.2	10.0	9.4	5.3
2 – 3	1.5	6.3	10.9	10.3	8.3
3 – 4	1.9	5.2	12.8	9.3	3.4
4 – 5	2.1	4.2	18.0	6.5	6.8
5 – 6	2.4	4.6	8.3	8.6	4.7
6 – 7	3.2	4.3	4.4	6.4	4.7
7 – 8	1.7	3.9	5.9	9.0	6.5
8 – 9	1.8	4.1	11.5	11.9	9.0
9 – 10	1.6	4.2	7.3	9.1	10.8
	<u>pH</u>				
0 – 0.5	7.8	6.7	6.2	6.3	7.0
0.5 – 1	7.9	7.2	6.6	6.9	7.2

Table 2.5.5. Soil nitrate concentration, in ppm, in January, 1995.

Depth (ft)	Treatments (lbs N/acre/year)				
	0	100	175	250	325
	<u>Nitrate (ppm)</u>				
0 – 0.5	4.4	6.6	6.2	6.0	6.6
0.5 – 1	3.7	5.1	5.2	4.6	5.2
1 – 2	2.8	4.4	3.7	6.3	7.6
2 – 3	2.9	13.3	10.7	10.6	15.1
3 – 4	2.9	17.8	17.0	16.5	17.6
4 – 5	3.3	9.8	14.1	9.1	15.3
5 – 6	3.1	6.3	20.4	12.7	17.5
6 – 7	3.6	4.0	7.4	5.1	22.4
7 – 8	2.7	3.8	3.9	4.4	16.6
8 – 9	3.4	4.1	4.4	4.3	11.5
9 – 10	3.0	3.4	4.6	4.2	7.2

Table 3.3.1. Comparison of scaling subgroup assignments and data quality for each soil sample.

MSO run #	MSO cell #	Core #	Sample #	Group 2	Group 3	Group 4	Data quality
3	1	3-10-1	6	sand	sand	var1	1
3	2	3-10-2	3	sand	sand	var1	1
3	3	5-10-2	9	sand	sand	sand	1
3	4	5-10-2	10	sand	sand	sand	1
3	5	10-8-2	6	sand	sand	sand	1
3	6	10-8-2	8	sand	sand	CSiL	1
3	7	10-8-5	3	sand	sand	var1	1
3	8	10-8-5	7	sand	sand	sand	1
3	9	10-10-2	8	sand	sand	sand	1
3	10	10-10-2	9	loamy sand	sand	sand	1
4	1	5-10-2	20	sand	loamy sand	sandy loam	1
4	2	10-8-5	17	sand	loamy sand	sandy loam	1
4	3	10-10-5	3	sand	sand	var1	0
4	4	11-8-2	8	sand	sandy loam	sand	0
4	5	11-8-2	16	loamy sand	loamy sand	sandy loam	1
4	6	11-10-5	3	sand	sand	var1	0
4	7	12-10-2	3	sand	sand	var1	0
4	9	13-10-2	3	sand	loamy sand	var1	0
4	10	13-10-5	2	sand	loamy sand	var1	0
4	8	13-8-2	4	sand	sand	var1	0
5	1	4-10-5	10	sandy loam	sandy loam	CSiL	1
5	2	4-10-5	16	loamy sand	sandy loam	sandy loam	1
5	3	10-8-2	5	sandy loam	sandy loam	var2	1
5	4	10-8-2	13	loamy sand	sandy loam	sL	1
5	5	10-8-5	12	silt loam	sandy loam	CSiL	1
5	6	10-8-5	16	loamy sand	sandy loam	sL	1
5	7	11-8-2	7	sandy loam	sandy loam	var2	1
5	8	11-8-2	14	sandy loam	sandy loam	sL	1
5	9	13-8-5	7	silt loam	sandy loam	var2	1
5	10	13-8-5	11	sandy loam	sandy loam	CSiL	1
6	1	3-10-5	14	sandy loam	sandy loam	CSiL	1
6	2	3-10-5	17	loamy sand	sandy loam	CSiL	1
6	3	5-10-2	17	loamy sand	sandy loam	CSiL	1
6	5	10-10-2	6	loamy sand	sandy loam	var2	1
6	6	10-10-2	14	sandy loam	sandy loam	CSiL	1
6	8	12-10-2	13	loamy sand	sandy loam	sL	1
6	9	13-10-2	12	sandy loam	sandy loam	CSiL	1
6	10	13-10-5	11	loamy sand	sandy loam	CSiL	1
7	1	3-10-1	2	loamy sand	sL-Han	sL	0
7	2	3-10-1	5	loamy sand	sL-Han	sL	0
7	3	3-10-4	3	sandy loam	sL-Han	sL	0
7	4	3-10-4	4	loamy sand	sL-Han	sL	0
7	5	4-10-5	2	sandy loam	sL-Han	var1	0
7	6	10-8-5	2	loamy sand	sL-Han	clay	0
7	7	10-10-2	2	loamy sand	sL-Han	sL-Han	0
7	8	11-10-5	2	loamy sand	sL-Han	sL-Han	0
7	9	12-10-2	2	loamy sand	sL-Han	sL-Han	0
7	10	13-10-5	1	loamy sand	sL-Han	sL-Han	0

Table 3.3.1. continued

MSO run #	MSO cell #	Core #	Sample #	Group 2	Group 3	Group 4	Data quality
3	1	3-10-1	6	sand	sand	var1	1
3	2	3-10-2	3	sand	sand	var1	1
3	3	5-10-2	9	sand	sand	sand	1
3	4	5-10-2	10	sand	sand	sand	1
3	5	10-8-2	6	sand	sand	sand	1
3	6	10-8-2	8	sand	sand	CSiL	1
3	7	10-8-5	3	sand	sand	var1	1
3	8	10-8-5	7	sand	sand	sand	1
3	9	10-10-2	8	sand	sand	sand	1
3	10	10-10-2	9	loamy sand	sand	sand	1
4	1	5-10-2	20	sand	loamy sand	sandy loam	1
4	2	10-8-5	17	sand	loamy sand	sandy loam	1
4	3	10-10-5	3	sand	sand	var1	0
4	4	11-8-2	8	sand	sandy loam	sand	0
4	5	11-8-2	16	loamy sand	loamy sand	sandy loam	1
4	6	11-10-5	3	sand	sand	var1	0
4	7	12-10-2	3	sand	sand	var1	0
4	9	13-10-2	3	sand	loamy sand	var1	0
4	10	13-10-5	2	sand	loamy sand	var1	0
4	8	13-8-2	4	sand	sand	var1	0
5	1	4-10-5	10	sandy loam	sandy loam	CSiL	1
5	2	4-10-5	16	loamy sand	sandy loam	sandy loam	1
5	3	10-8-2	5	sandy loam	sandy loam	var2	1
5	4	10-8-2	13	loamy sand	sandy loam	sL	1
5	5	10-8-5	12	silt loam	sandy loam	CSiL	1
5	6	10-8-5	16	loamy sand	sandy loam	sL	1
5	7	11-8-2	7	sandy loam	sandy loam	var2	1
5	8	11-8-2	14	sandy loam	sandy loam	sL	1
5	9	13-8-5	7	silt loam	sandy loam	var2	1
5	10	13-8-5	11	sandy loam	sandy loam	CSiL	1
6	1	3-10-5	14	sandy loam	sandy loam	CSiL	1
6	2	3-10-5	17	loamy sand	sandy loam	CSiL	1
6	3	5-10-2	17	loamy sand	sandy loam	CSiL	1
6	5	10-10-2	6	loamy sand	sandy loam	var2	1
6	6	10-10-2	14	sandy loam	sandy loam	CSiL	1
6	8	12-10-2	13	loamy sand	sandy loam	sL	1
6	9	13-10-2	12	sandy loam	sandy loam	CSiL	1
6	10	13-10-5	11	loamy sand	sandy loam	CSiL	1
7	1	3-10-1	2	loamy sand	sL-Han	sL	0
7	2	3-10-1	5	loamy sand	sL-Han	sL	0
7	3	3-10-4	3	sandy loam	sL-Han	sL	0
7	4	3-10-4	4	loamy sand	sL-Han	sL	0
7	5	4-10-5	2	sandy loam	sL-Han	var1	0
7	6	10-8-5	2	loamy sand	sL-Han	clay	0
7	7	10-10-2	2	loamy sand	sL-Han	sL-Han	0
7	8	11-10-5	2	loamy sand	sL-Han	sL-Han	0
7	9	12-10-2	2	loamy sand	sL-Han	sL-Han	0
7	10	13-10-5	1	loamy sand	sL-Han	sL-Han	0
8	1	10-10-5	11	loam	loam	CSiL	0

Table 4.2.1. Summary of DANR laboratory measurements.

MSO run #	MSO cell #	Core #	Sample #	BD (g/cm3)	OM (%)	C-org (%)	Sand (%)	Silt (%)	Clay (%)	Ksatm (cm/hr)	Porosity	Θ_s^m (cm ³ /cm ³)	texture
1	1	6-10-5	12	1.41	0.09	0.05	17	76	7	0.074	0.466	0.423	silt loam
1	2	6-10-5	13	1.48	0.09	0.05	15	81	4	0.071	0.441	0.389	silt
1	3	6-10-5	14	1.8	0.06	0.03	84	15	1	0.874	0.322	0.223	loamy sand
1	4	6-10-5	15	1.74	0.03	0.02	70	27	3	0.409	0.345	0.335	sandy loam
1	5	6-10-5	16	1.74	0.1	0.06	62	28	10	0.087	0.342	0.253	sandy loam
1	6	6-10-2	7	1.52	0.03	0.02	74	25	1	1.53	0.425	0.293	loamy sand
1	7	6-10-2	6	1.48	0.04	0.02	82	17	1	2.61	0.44	0.302	loamy sand
1	9	6-10-2	8	1.48	0.02	0.01	99	1	<1	67.32	0.443	0.327	sand
1	10	6-10-2	9	1.46	0.01	<.01	97	2	1	50.27	0.445	0.298	sand
2	1	6-10-2	2	1.72	0.17	0.1	67	28	5	<i>no data</i>	0.353	0.243	sandy loam
2	2	6-10-2	3	1.76	0.13	0.08	58	30	15	<i>no data</i>	0.336	0.31	sandy loam
2	3	6-10-2	4	1.73	0.09	0.05	71	22	7	<i>no data</i>	0.346	0.313	sandy loam
2	5	6-10-2	11	1.78	0.1	0.06	68	25	7	<i>no data</i>	0.327	0.254	sandy loam
2	6	6-10-2	15	1.58	0.09	0.05	53	41	6	<i>no data</i>	0.405	0.359	sandy loam
2	7	6-10-2	17	1.75	0.09	0.05	82	12	6	<i>no data</i>	0.341	0.289	loamy sand
2	8	6-10-5	8	1.51	0.12	0.07	95	2	3	65.22	0.429	0.372	sand
2	9	6-10-5	9	1.48	0.08	0.05	94	3	3	24.39	0.443	0.34	sand
2	10	6-10-5	10	1.47	0.07	0.04	94	2	4	20.63	0.445	0.306	sand
3	1	3-10-1	6	1.54	0.06	0.04	98	<1	2	1.702	0.421	0.322	sand
3	2	3-10-2	3	1.58	0.08	0.05	97	<1	3	2.018	0.405	0.307	sand
3	3	5-10-2	9	1.49	0.06	0.03	98	<1	3	0.407	0.439	0.339	sand
3	4	5-10-2	10	1.5	0.06	0.03	99	<1	1	51.148	0.434	0.331	sand
3	5	10-8-2	6	1.5	0.06	0.04	97	<1	3	54.902	0.436	0.369	sand
3	6	10-8-2	8	1.47	0.06	0.03	98	<1	2	72.471	0.447	0.354	sand
3	7	10-8-5	3	1.57	0.06	0.04	97	<1	3	0.718	0.407	0.3	sand
3	8	10-8-5	7	1.46	0.06	0.03	98	<1	2	61.271	0.45	0.367	sand
3	9	10-10-2	8	1.46	0.07	0.04	94	<1	7	1.976	0.45	0.399	sand
3	10	10-10-2	9	1.54	0.08	0.05	89	<1	12	4.195	0.418	0.341	loamy sand
4	1	5-10-2	20	1.81	0.09	0.05	87	11	2	0.699	0.317	0.222	sand
4	2	10-8-5	17	1.85	0.06	0.03	91	7	2	12.1	0.302	0.229	sand
4	3	10-10-5	3	1.53	0.04	0.03	98	1	1	7.67	0.422	0.267	sand
4	4	11-8-2	8	1.51	0.04	0.02	97	2	1	12.4	0.431	0.284	sand

Table 4.2.1. continued

MSO run #	MSO cell #	Core #	Sample #	BD (g/cm ³)	OM (%)	C-org (%)	Sand (%)	Silt (%)	Clay (%)	Ksatm (cm/hr)	Porosity	Θ _s ^m (cm ³ /cm ³)	texture
4	5	11-8-2	16	1.87	0.04	0.03	84	15	1	0.644	0.293	0.237	loamy sand
4	6	11-10-5	3	1.6	0.07	0.04	96	3	1	18.5	0.398	0.237	sand
4	7	12-10-2	3	1.55	0.03	0.02	98	1	1	4.29	0.415	0.319	sand
4	8	13-8-2	4	1.56	0.04	0.02	99	<1	1	16.5	0.411	0.272	sand
4	9	13-10-2	3	1.55	0.03	0.02	99	<1	1	33.9	0.414	0.281	sand
4	10	13-10-5	2	1.54	0.04	0.02	97	2	1	10.6	0.419	0.283	sand
5	1	4-10-5	10	1.72	0.09	0.05	61	35	4	0.098	0.349	0.309	sandy loam
5	2	4-10-5	16	1.85	0.07	0.04	78	18	4	1.791	0.302	0.275	loamy sand
5	3	10-8-2	5	1.55	0.09	0.05	67	29	4	0.437	0.415	0.302	sandy loam
5	4	10-8-2	13	1.83	0.07	0.04	74	21	5	0.341	0.309	0.252	loamy sand
5	5	10-8-5	12	1.5	0.09	0.05	37	59	4	2.264	0.434	0.395	silt loam
5	6	10-8-5	16	1.81	0.06	0.03	78	17	5	0.772	0.317	0.269	loamy sand
5	7	11-8-2	7	1.51	0.06	0.03	63	32	5	1.552	0.43	0.329	sandy loam
5	8	11-8-2	14	1.75	0.08	0.05	87	8	5	1.922	0.34	0.263	sandy loam
5	9	13-8-5	7	1.62	0.08	0.05	42	54	4	0.308	0.389	0.329	silt loam
5	10	13-8-5	11	1.53	0.07	0.04	71	25	4	2.649	0.423	0.346	sandy loam
6	1	3-10-5	14	1.75	0.12	0.07	69	23	8	0.089	0.338	0.248	sandy loam
6	2	3-10-5	17	1.81	0.09	0.05	81	15	4	0.027	0.318	0.256	loamy sand
6	3	5-10-2	17	1.48	0.08	0.05	83	13	4	0.887	0.442	0.309	loamy sand
6	4	5-10-2	19	1.57	0.09	0.05	49	43	8	0.024	0.409	0.301	loam
6	5	10-10-2	6	1.71	0.07	0.04	82	13	5	0.208	0.354	0.248	loamy sand
6	6	10-10-2	14	1.51	0.07	0.04	71	24	5	0.812	0.43	0.345	sandy loam
6	7	12-10-2	10	1.6	0.09	0.05	77	16	7	0.316	0.396	0.133	loamy sand
6	8	12-10-2	13	1.7	0.07	0.04	86	10	4	0.555	0.36	0.278	loamy sand
6	9	13-10-2	12	1.71	0.07	0.04	66	30	4	0.276	0.355	0.285	sandy loam
6	10	13-10-5	11	1.66	0.06	0.03	75	21	4	0.43	0.375	0.267	loamy sand
7	1	3-10-1	2	1.65	0.17	0.1	74	23	3	0.0454	0.378	0.257	loamy sand
7	2	3-10-1	5	1.69	0.15	0.09	76	23	1	0.222	0.361	0.262	loamy sand
7	3	3-10-4	3	1.66	0.17	0.1	72	25	3	0.0192	0.373	0.245	sandy loam
7	4	3-10-4	4	1.69	0.14	0.08	74	23	3	0.247	0.361	0.265	loamy sand
7	5	4-10-5	2	1.56	0.16	0.09	72	26	2	0.946	0.41	0.287	sandy loam
7	6	10-8-5	2	1.59	0.16	0.09	82	17	1	0.593	0.399	0.254	loamy sand

Table 4.2.1. continued

MSO run #	MSO cell #	Core #	Sample #	BD (g/cm ³)	OM (%)	C-org (%)	Sand (%)	Silt (%)	Clay (%)	Ksatm (cm/hr)	Porosity	Θ _s ^m (cm ³ /cm ³)	texture
7	7	10-10-2	2	1.63	0.13	0.07	76	21	3	0.386	0.386	0.27	loamy sand
7	8	11-10-5	2	1.63	0.12	0.07	83	16	1	0.842	0.384	0.229	loamy sand
7	9	12-10-2	2	1.65	0.1	0.06	83	15	2	4.27	0.376	0.288	loamy sand
7	10	13-10-5	1	1.64	0.12	0.07	82	16	2	1.07	0.383	0.245	loamy sand
8	1	10-10-5	11	1.57	0.13	0.07	43	50	7	0.0989	0.408	0.333	loam
8	2	10-10-5	12	1.8	0.13	0.08	69	22	9	0.121	0.321	0.245	sandy loam
8	3	11-10-5	5	1.77	0.13	0.08	74	18	8	0.0496	0.332	0.238	sandy loam
8	4	11-10-5	6	1.77	0.2	0.12	71	20	9	5.61	0.332	0.229	sandy loam
8	5	11-10-5	7	1.71	0.1	0.06	68	20	12	2.83	0.355	0.278	sandy loam
8	6	11-10-5	11	1.61	0.13	0.07	27	63	10	2.88	0.392	0.366	silt loam
8	7	11-10-5	13	1.64	0.18	0.1	57	36	7	3.56	0.381	0.328	sandy loam
8	8	12-10-2	12	1.71	0.1	0.06	68	22	10	24.6	0.355	0.325	sandy loam
8	9	13-8-2	11	1.26	0.17	0.1	40	53	7	15.4	0.525	0.471	silt loam
8	10	13-8-2	12	1.57	0.14	0.08	49	44	7	0.0169	0.408	0.307	loam
9	1	3-10-4	14	1.55	0.08	0.05	57	37	6	0.664	0.414	0.362	sandy loam
9	2	3-10-4	19	1.48	0.13	0.07	44	50	6	1.217	0.442	0.408	silt loam
9	3	3-10-5	13	1.49	0.06	0.03	34	63	3	0.327	0.437	0.385	silt loam
9	4	4-10-5	5	1.53	0.13	0.07	72	24	4	1.444	0.423	0.296	sandy loam
9	5	4-10-5	8	1.58	0.07	0.04	38	58	4	0.382	0.402	0.354	silt loam
9	6	10-8-5	14	1.55	0.13	0.08	25	71	4	0.799	0.415	0.426	silt loam
9	7	11-10-5	10	1.43	0.08	0.05	74	22	4	6.166	0.46	0.389	loamy sand
9	8	12-10-2	6	1.54	0.07	0.04	74	22	4	1.48	0.419	0.333	loamy sand
9	9	13-8-5	15	1.63	0.06	0.03	34	62	4	0.268	0.385	0.348	silt loam
9	10	13-10-2	13	1.59	0.1	0.06	40	54	6	0.092	0.402	0.386	silt loam
10	1	4-10-5	13	1.59	0.1	0.06	44	49	7	0.206	0.4	0.339	loam
10	2	4-10-5	14	1.52	0.1	0.06	51	43	6	0.188	0.427	0.397	sandy loam
10	3	5-10-2	18	1.31	0.18	0.1	13	70	17	0.00262	0.507	0.433	silt loam
10	4	10-8-2	10	1.37	0.12	0.07	29	67	4	0.199	0.484	0.458	silt loam
10	5	10-8-2	12	1.68	0.07	0.04	74	21	5	0.578	0.364	0.276	sandy loam
10	6	10-8-5	9	1.69	0.11	0.06	60	33	7	0.334	0.361	0.3	sandy loam
10	7	10-8-5	15	1.46	0.13	0.08	40	54	6	0.143	0.412	0.348	silt loam
10	8	10-10-5	13	1.32	0.14	0.08	15	76	9	0.0713	0.501	0.443	silt loam

Table 4.2.1. continued

MSO run #	MSO cell #	Core #	Sample #	BD (g/cm3)	OM (%)	C-org (%)	Sand (%)	Silt (%)	Clay (%)	Ksatm (cm/hr)	Porosity	Θ_s^m (cm³/cm³)	texture
10	9	11-8-2	10	1.41	0.12	0.07	27	70	3	0.18	0.469	0.408	silt loam
10	10	13-10-5	10	1.48	0.1	0.06	20	76	4	0.106	0.443	0.426	silt loam
11	1	3-10-1	8	1.85	0.07	0.04	76	17	7	0.0447	0.302	0.251	sandy loam
11	2	3-10-5	5	1.87	0.16	0.09	67	24	9	0.00447	0.294	0.23	sandy loam
11	3	5-10-2	3	1.64	0.2	0.12	57	34	9	0.0175	0.381	0.344	sandy loam
11	4	5-10-2	4	1.61	0.07	0.04	79	14	7	0.591	0.392	0.328	loamy sand
11	5	10-10-2	3	1.74	0.13	0.07	62	25	13	0.0132	0.343	0.303	sandy loam
11	6	10-10-2	4	1.87	0.07	0.04	69	20	11	0.00201	0.294	0.244	sandy loam
11	7	11-8-2	4	1.75	0.11	0.06	63	22	15	0.0831	0.34	0.297	sandy loam
11	8	11-10-5	4	1.79	0.15	0.09	64	24	12	0.0893	0.325	0.279	sandy loam
11	9	13-8-2	6	1.66	0.11	0.06	65	28	7	0.141	0.374	0.27	sandy loam
11	10	13-8-5	3	1.79	0.06	0.03	70	21	9	0.0505	0.325	0.283	sandy loam
12	1	10-8-2	14	1.67	0.07	0.04	74	18	8	1.149	0.37	0.279	sandy loam
12	2	10-8-2	15	1.8	0.12	0.07	69	21	10	0.137	0.321	0.281	sandy loam
12	3	10-8-5	18	1.8	0.11	0.06	68	23	9	1.523	0.321	0.239	sandy loam
12	4	10-10-5	19	1.69	0.09	0.05	72	21	7	0.188	0.362	0.255	sandy loam
12	5	11-8-2	17	1.78	0.14	0.08	70	20	10	5.247	0.328	0.237	sandy loam
12	6	11-10-5	17	1.6	0.09	0.05	77	16	7	2.667	0.396	0.315	sandy loam
12	7	12-10-2	15	1.59	0.09	0.05	76	16	8	0.505	0.4	0.275	sandy loam
12	8	13-8-2	16	1.69	0.14	0.08	74	18	8	14.841	0.362	0.293	sandy loam
12	9	13-8-5	17	1.77	0.07	0.04	78	15	7	0.39	0.332	0.238	loamy sand
12	10	13-10-2	15	1.74	0.04	0.02	66	28	6	0.333	0.343	0.263	sandy loam

Table 4.2.2. Summary statistics of DANR laboratory measurements

	Valid N	Mean	Median	Mode	Mode Frequency	Minimum	Maximum	Lower Quartile	Upper Quartile	Std. Deviation
<u>ALL</u>										
Bulk Density (g/cm ³)	118	1.621	1.605	1.48	7	1.26	1.87	1.52	1.74	0.134
Organic Matter (%)	118	0.094	0.09	0.07	18	0.01	0.20	0.07	0.12	0.040
Organic Carbon(%)	118	0.054	0.05	0.05	23	0.01	0.12	0.04	0.07	0.024
Sand (%)	118	69.415	72	74	10	13	99	61	83	21.59
Silt (%)	118	25.398	22	1	15	1	81	14	32	20.24
Clay(%)	118	5.347	5	4	21	1	17	3	7	3.41
K _s (cm/hr)	112	0.712*	0.619	0.19	2	0.002	72.471	0.162	2.749	15.257
Porosity	118	0.388	0.394	Multiple		0.293	0.525	0.345	0.425	0.050
Saturated Water Content	118	0.307	0.299	Multiple		0.133	0.471	0.263	0.341	0.059
<u>DANR - loam</u>										
Bulk Density (g/cm ³)	4	1.575	1.57	1.57	3	1.570	1.590	1.570	1.580	0.010
Organic Matter (%)	4	0.115	0.115	Multiple		0.090	0.140	0.095	0.135	0.024
Organic Carbon(%)	4	0.065	0.065	Multiple		0.050	0.080	0.055	0.075	0.013
Sand (%)	4	46.250	46.5	49	2	43	49	43.5	49.0	3.202
Silt (%)	4	46.500	46.5	Multiple		43	50	43.5	49.5	3.512
Clay(%)	4	7.250	7.0	7	3	7	8	7	7.5	0.5
K _s (cm/hr)	4	0.054*	0.062	Multiple		0.017	0.206	0.020	0.152	0.088
Porosity	4	0.406	0.408	0.408	2	0.400	0.409	0.404	0.409	0.004
Saturated Water Content	4	0.320	0.32	Multiple		0.301	0.339	0.304	0.336	0.019
<u>DANR - loamy sand</u>										
Bulk Density (g/cm ³)	27	1.664	1.65	Multiple		1.430	1.870	1.590	1.770	0.121
Organic Matter (%)	27	0.088	0.08	0.07	7	0.030	0.170	0.070	0.120	0.037
Organic Carbon(%)	27	0.051	0.05	0.04	7	0.020	0.100	0.040	0.070	0.021
Sand (%)	27	79.407	79	74	6	74	89	75	83	4.308
Silt (%)	27	16.889	16	15	5	1	25	15	21	5.056
Clay(%)	27	3.778	4	Multiple		1	12	1	5	2.562
K _s (cm/hr)	26	0.636*	0.619	Multiple		0.027	6.166	0.341	1.480	1.504
Porosity	27	0.372	0.376	0.361	2	0.293	0.460	0.332	0.399	0.045
Saturated Water Content	27	0.271	0.267	Multiple		0.133	0.389	0.248	0.293	0.047
<u>DANR - sand</u>										
Bulk Density (g/cm ³)	23	1.542	1.510	1	3	1.460	1.850	1.480	1.560	0.100
Organic Matter (%)	23	0.057	0.060	0	8	0.010	0.120	0.040	0.070	0.024
Organic Carbon(%)	23	0.033	0.030	Multiple		0.010	0.070	0.020	0.040	0.014
Sand (%)	23	96.391	97	Multiple		87	99	95	98	2.872
Silt (%)	23	2.087	1	1	14	1	11	1	2	2.353
Clay(%)	23	2.130	2	1	10	1	7	1	3	1.424
K _s (cm/hr)	23	11.072*	16.500	Multiple		0.407	72.471	2.018	51.148	25.266
Porosity	23	0.418	0.429	Multiple		0.302	0.450	0.411	0.443	0.038
Saturated Water Content	23	0.310	0.307	Multiple		0.222	0.399	0.281	0.340	0.047
<u>DANR - sandy loam</u>										
Bulk Density (g/cm ³)	46	1.695	1.715	1.74	4	1.510	1.870	1.640	1.770	0.099
Organic Matter (%)	46	0.108	0.100	Multiple		0.030	0.200	0.080	0.130	0.040
Organic Carbon(%)	46	0.062	0.060	Multiple		0.020	0.120	0.050	0.080	0.024
Sand (%)	46	67.565	68.500	Multiple		51	87	63	72	6.781
Silt (%)	46	25.000	24	Multiple		8	43	21	28	6.864
Clay(%)	46	7.500	7	7.0	8	2	15	5	9	3.017
K _s (cm/hr)	41	0.325*	0.334	0.188	2	0.002	24.600	0.089	1.523	4.451
Porosity	46	0.360	0.354	Multiple		0.294	0.430	0.332	0.381	0.037
Saturated Water Content	46	0.288	0.282	Multiple		0.229	0.397	0.253	0.313	0.040

Table 4.2.2. continued

	Valid N	Mean	Median	Mode	Mode Frequency	Minimum	Maximum	Lower Quartile	Upper Quartile	Std. Deviation
<u>DANR - silt loam</u>										
Bulk Density (g/cm ³)	17	1.475	1.48	Multiple		1.26	1.63	1.41	1.58	0.1149
Organic Matter (%)	17	0.112	0.12	0.13	4	0.06	0.18	0.09	0.13	0.03504
Organic Carbon(%)	17	0.064	0.07	0.07	4	0.03	0.1	0.05	0.08	0.02093
Sand (%)	17	30.706	34	40	3	13	44	25	40	10.01102
Silt (%)	17	63.294	63	Multiple		50	76	54	70	8.79463
Clay(%)	17	6.000	4	4	7	3	17	4	7	3.4821
K _s (cm/hr)	17	0.289*	0.268	Multiple		0.00262	15.4	0.106	0.799	3.68542
Porosity	17	0.441	0.437	0.402	2	0.385	0.525	0.402	0.469	0.04411
Saturated Water Content	17	0.400	0.408	Multiple		0.329	0.471	0.366	0.426	0.04147

* geometric mean used for K_s

Table 4.3.1. Summary of the optimized van Genuchten parameters.

				LOW GUESS						MEDIUM GUESS						HIGH GUESS						
MSO run #	MSO cell #	core #	sample #	α (cm ⁻¹)	n	Θ_r (cm ³ /cm ³)	K_s (cm/hr)	% mbe	ssq	α (cm ⁻¹)	n	Θ_r (cm ³ /cm ³)	K_s (cm/hr)	% mbe	ssq	α (cm ⁻¹)	n	Θ_r (cm ³ /cm ³)	K_s (cm/hr)	% mbe	ssq	
3	1	3-10-1	6	0.035	5.367	0.000	0.045	0.125	4.351	0.031	7.469	0.069	3.057	0.746	0.492	n/a						
3	2	3-10-2	3	0.046	5.002	0.079	14.57	0.042	0.682	0.046	5.013	0.080	14.862	0.141	0.689	n/a						
3	3	5-10-2	9	n/a						0.046	4.611	0.055	37.793	0.392	2.568	n/a						
3	4	5-10-2	10	0.031	3.520	0.000	0.092	0.734	7.949	0.043	4.898	0.054	22.611	0.346	1.999	n/a						
3	5	10-8-2	6	0.027	4.133	0.000	0.078	0.254	1.672	0.037	5.018	0.093	99.534	0.279	1.819	0.022	2.576	0.0001	0.0302	0.7425	10.730	
3	6	10-8-2	8	0.044	5.046	0.060	60.49	0.420	3.653	0.044	5.130	0.062	69.624	0.122	3.656	0.034	4.421	0.0001	0.0611	0.8987	10.01	
3	7	10-8-5	3	0.037	3.605	0.000	0.133	0.559	5.171	0.052	5.246	0.122	24.237	0.848	1.575	0.053	5.243	0.1218	24.502	0.8630	1.575	
3	8	10-8-5	7	0.036	4.674	0.045	23.97	0.069	1.451	0.036	4.679	0.045	24.134	0.081	1.451	0.042	6.027	0.0001	0.0243	2.5369	13.65	
3	9	10-10-2	8	0.026	4.998	0.155	22.73	0.235	1.219	0.026	5.003	0.155	22.972	1.217	1.220	0.019	4.789	0.0001	0.0351	0.1066	6.043	
3	10	10-10-2	9	0.027	3.558	0.166	1.44	0.105	0.517	0.027	3.563	0.166	1.451	0.165	0.516	0.019	4.789	0.0001	0.0351	0.1066	6.043	
4	1	5-10-2	20	0.005	2.734	0.000	0.12	1.208	0.309	0.005	3.081	0.032	0.152	4.112	0.302	n/a						
4	2	10-8-5	17	0.009	1.711	0.000	0.036	0.892	0.655	0.019	2.424	0.097	26.632	0.002	0.296	0.192	8.861	0.1570	0.0001	NaN	2.015	
4	3	10-10-5	3	0.055	4.970	0.050			0.004	0.055	4.970	0.050			0.004	0.055	4.970	0.0500			0.0040	
4	4	11-8-2	8	0.034	3.833	0.074			0.000	0.034	3.833	0.074			0.000	0.034	3.833	0.0738			0.0002	
4	5	11-8-2	16	0.003	3.063	0.000	0.178	0.104	0.138	0.003	3.433	0.046	0.232	0.378	0.141	n/a						
4	6	11-10-5	3	0.048	3.933	0.079			0.000	0.048	3.933	0.079			0.000	0.048	3.933	0.0786			0.0002	
4	7	12-10-2	3	0.077	3.597	0.063			0.000	0.077	3.597	0.063			0.000	0.077	3.597	0.0629			0.0004	
4	8	13-8-2	4	0.078	3.551	0.050			0.000	0.078	3.551	0.050			0.000	0.078	3.549	0.0500			0.0005	
4	9	13-10-2	3	0.061	3.910	0.060			0.001	0.061	3.910	0.060			0.001	0.061	3.910	0.0603			0.0012	
4	10	13-10-5	2	0.060	3.911	0.066			0.000	0.060	3.911	0.066			0.000	0.060	3.911	0.0664			0.0005	
5	1	4-10-5	10	0.007	2.700	0.258	0.029	0.212	0.201	0.007	2.760	0.258	0.028	0.199	0.201	n/a						
5	2	4-10-5	16	0.004	1.404	0.003	0.085	0.234	0.476	0.004	2.225	0.150	0.214	0.174	0.254	n/a						
5	3	10-8-2	5	0.009	3.290	0.143	0.811	0.023	1.264	0.008	3.933	0.148	1.203	0.307	1.090	n/a						
5	4	10-8-2	13	0.005	1.658	0.000	0.056	0.360	0.626	0.005	1.663	0.001	0.055	0.354	0.626	n/a						
5	5	10-8-5	12	0.004	1.237	0.008	0.602	0.181	0.497	0.004	1.547	0.210	0.356	0.248	0.465	0.002	1.6939	0.0001	0.0047	0.1669	1.311	
5	6	10-8-5	16	0.009	1.893	0.000	0.228	0.471	0.768	0.008	2.346	0.042	0.416	0.169	0.692	n/a						
5	7	11-8-2	7	0.006	2.003	0.000	0.072	0.391	0.883	0.006	1.983	0.000	0.074	0.398	0.883	n/a						
5	8	11-8-2	14	0.015	2.686	0.030	1.267	0.285	0.735	0.015	2.720	0.032	1.375	0.269	0.735	n/a						
5	9	13-8-5	7	0.003	1.271	0.075	0.017	0.249	0.412	0.002	1.400	0.064	0.018	0.219	0.348	n/a						
5	10	13-8-5	11	0.005	1.759	0.000	0.011	0.475	2.662	0.013	1.479	0.001	0.241	0.409	1.363	0.013	1.4771	0.0001	0.2420	0.4087	1.363	
																6				0		
6	1	3-10-5	14	0.008	4.557	0.211	0.630	0.221	0.296	0.008	4.586	0.211	0.652	0.162	0.295	0.090	1.0826	0.0001	30.0	0.1465	0.573	
6	2	3-10-5	17	0.005	1.384	0.000	0.310	0.225	0.334	0.006	1.932	0.131	0.260	0.231	0.319	0.005	1.3873	0.0002	0.3068	0.2098	0.3334	
6	3	5-10-2	17	0.007	1.046	0.033	0.739	0.216	0.770	0.015	2.667	0.279	2.230	0.600	0.305	n/a						
6	4	5-10-2	19							NO MSO DATA AVAILABLE FOR THIS SAMPLE												
6	5	10-10-2	6	0.011	2.721	0.154	0.223	0.610	0.385	0.011	2.717	0.155	0.254	0.211	0.363	0.005	1.7478	0.0001	0.0068	0.2299	1.545	
6	6	10-10-2	14	0.012	1.337	0.001	2.345	0.196	0.566	0.011	1.724	0.138	1.439	0.209	0.515	n/a						
6	7	12-10-2	10							NO MSO DATA AVAILABLE FOR THIS SAMPLE												
6	8	12-10-2	13	0.006	2.459	0.028	0.197	0.552	0.469	0.006	2.680	0.050	0.253	0.158	0.409	0.006	2.2187	0.0001	0.1887	0.1622	0.49	
6	9	13-10-2	12	0.002	2.066	0.000	0.057	0.251	0.231	0.003	2.599	0.130	0.126	0.138	0.222	0.002	2.0004	0.0002	0.0769	0.1039	0.226	

Table 4.3.1. continued

				LOW GUESS						MEDIUM GUESS						HIGH GUESS					
MSO run #	MSO cell #	core #	sample #	α (cm ⁻¹)	n	Θ_r (cm ³ /cm ³)	K_s (cm/hr)	% mbe	ssq	α (cm ⁻¹)	n	Θ_r (cm ³ /cm ³)	K_s (cm/hr)	% mbe	ssq	α (cm ⁻¹)	n	Θ_r (cm ³ /cm ³)	K_s (cm/hr)	% mbe	ssq
6	10	13-10-5	11	0.042	1.319	0.000	5.11	0.058	1.663	0.007	4.569	0.151	0.370	0.046	0.580	0.007	4.5638	0.1514	0.3685	0.0265	0.58
7	1	3-10-1	2	0.028	1.217	0.000			0.000	0.028	1.217	0.000			0.000	0.028	1.2315	0.0124			0.001
7	2	3-10-1	5	0.005	1.673	0.000			0.000	0.005	1.673	0.000			0.000	n/a					
7	3	3-10-4	3	0.017	1.435	0.090			0.000	0.017	1.435	0.090			0.000	n/a					
7	4	3-10-4	4	0.015	1.536	0.090			0.000	0.015	1.536	0.090			0.000	0.015	1.5364	0.0900			0.0003
7	5	4-10-5	2	0.007	1.657	0.019			0.000	0.007	1.691	0.031			0.000	0.007	1.7115	0.0368			0.0001
7	6	10-8-5	2	0.010	2.036	0.090			0.000	0.010	2.036	0.090			0.000	0.010	2.0360	0.0900			0.0001
7	7	10-10-2	2	0.027	1.300	0.000			0.000	0.027	1.300	0.000			0.000	0.027	1.2996	0.0001			0.0001
7	8	11-10-5	2	0.011	2.407	0.084			0.000	0.011	2.407	0.084			0.000	0.011	2.4069	0.0841			0.0001
7	9	12-10-2	2	0.022	2.197	0.090			0.001	0.022	2.197	0.090			0.001	0.022	2.1973	0.0900			0.0011
7	10	13-10-5	1	0.018	2.078	0.090			0.000	0.018	2.078	0.090			0.000	0.018	2.0781	0.0900			0.0004
8	1	10-10-5	11	0.007	1.183	0.000			0.000	0.008	1.237	0.084			0.000	0.008	1.2362	0.0809			0.0002
8	2	10-10-5	12	0.006	1.784	0.090			0.000	0.006	1.784	0.090			0.000	n/a					
8	3	11-10-5	5	0.017	1.474	0.090			0.000	0.017	1.474	0.090			0.000	n/a					
8	4	11-10-5	6	0.012	1.450	0.090			0.000	0.012	1.450	0.090			0.000	n/a					
8	5	11-10-5	7	0.016	1.342	0.090			0.000	0.016	1.342	0.090			0.000	0.016	1.3421	0.0900			0.0003
8	6	11-10-5	11	0.022	1.137	0.090			0.000	0.022	1.137	0.090			0.000	0.022	1.1368	0.0900			0.0003
8	7	11-10-5	13	0.019	1.114	0.000			0.000	0.021	1.136	0.061			0.000	0.020	1.1646	0.0896			0.0002
8	8	12-10-2	12	0.023	1.193	0.090			0.000	0.023	1.193	0.090			0.000	0.023	1.1927	0.0900			0.0004
8	9	13-8-2	11	0.016	1.128	0.058			0.000	0.016	1.141	0.090			0.000	0.016	1.1414	0.0900			0.0004
8	10	13-8-2	12	0.003	1.367	0.090			0.000	0.003	1.367	0.090			0.000	0.003	1.3669	0.0900			0.0001
9	1	3-10-4	14	n/a						0.005	2.407	0.172	0.212	0.109	0.832	0.004	1.6226	0.0187	0.1360	0.1202	0.8477
9	2	3-10-4	19	0.005	1.259	0.000	1.275	0.237	0.541	0.007	1.870	0.268	1.616	0.063	0.521	0.007	1.9569	0.2890	2.5175	1.2160	4.5040
9	3	3-10-5	13	n/a						0.003	2.511	0.075	0.391	0.575	0.526	0.003	2.1784	0.0001	0.3320	0.1854	0.5339
9	4	4-10-5	5	0.007	3.136	0.122	0.793	0.203	0.476	0.007	3.139	0.122	0.794	0.283	0.476	n/a					
9	5	4-10-5	8	n/a						0.007	1.161	0.155	2.286	0.166	2.347	0.002	5.0424	0.0002	0.0139	0.7388	0.2154
9	6	10-8-5	14	0.011	1.451	0.241	13.443	0.074	0.110	0.012	2.054	0.318	30.000	0.631	0.098	0.013	1.1522	0.0017	30.0	0.0459	0.1266
9	7	11-10-5	10	0.011	2.854	0.169	1.941	0.338	0.850	0.010	2.901	0.170	1.914	0.235	0.852	0.010	2.8949	0.1696	1.9394	0.1609	0.8512
9	8	12-10-2	6	0.009	5.298	0.164	9.554	1.424	0.223	0.009	5.355	0.164	10.285	2.302	0.225	n/a					
9	9	13-8-5	15	0.001	2.153	0.000	0.204	0.301	0.024	0.001	2.146	0.000	0.204	0.188	0.024	n/a					
9	10	13-10-2	13	0.004	1.247	0.000	1.184	0.191	0.211	0.009	2.638	0.311	12.246	1.118	0.112	0.002	1.8108	0.0001	0.0782	0.1539	0.2083
10	1	4-10-5	13	n/a						n/a						n/a					
10	2	4-10-5	14	0.004	1.616	0.003	0.357	0.236	1.004	0.004	1.695	0.054	0.393	0.222	1.013	0.003	2.6438	0.0001	0.0081	0.1442	2.9090
10	3	5-10-2	18	0.011	1.866	0.364	0.201	0.237	0.234	0.011	1.868	0.364	0.201	0.205	0.234	0.011	1.7259	0.3571	0.2027	0.2090	0.2364
10	4	10-8-2	10	0.002	1.735	0.000	0.296	0.394	0.992	0.008	1.487	0.255	12.783	0.583	0.545	0.007	1.1823	0.0002	30.0	0.5387	0.5534
10	5	10-8-2	12	0.005	1.986	0.000	0.126	0.373	1.268	0.005	2.067	0.017	0.150	0.201	1.256	n/a					
10	6	10-8-5	9	0.002	1.665	0.000	0.023	0.195	0.782	0.011	1.422	0.166	1.069	0.178	0.456	n/a					
10	7	10-8-5	15	0.004	3.143	0.245	2.115	0.838	0.003	0.004	3.132	0.245	2.055	1.821	0.003	0.002	2.8172	0.0001	0.0142	0.4233	0.3447
10	8	10-10-5	13	0.011	2.534	0.363	4.960	0.987	0.592	0.011	2.908	0.369	30.000	5.500	0.545	0.005	1.6936	0.2258	0.0510	0.3631	1.1270

Table 4.3.1. continued

LOW GUESS										MEDIUM GUESS						HIGH GUESS					
MSO run #	MSO cell #	core #	sample #	α (cm ⁻¹)	n	Θ_r (cm ³ /cm ³)	K_s (cm/hr)	% mbe	ssq	α (cm ⁻¹)	n	Θ_r (cm ³ /cm ³)	K_s (cm/hr)	% mbe	ssq	α (cm ⁻¹)	n	Θ_r (cm ³ /cm ³)	K_s (cm/hr)	% mbe	ssq
10	9	11-8-2	10	0.001	1.233	0.022	0.937	0.522	0.034	0.003	2.533	0.339	0.565	0.888	0.026	0.001	1.6657	0.0001	19.6319	28.788	0.0587
10	10	13-10-5	10	n/a						0.013	1.624	0.396	0.202	0.347	0.252	0.007	1.7093	0.3960	0.0077	0.3941	0.2282
11	1	3-10-1	8	0.005	1.433	0.000	0.254	0.201	0.150	0.012	1.976	0.158	2.732	0.287	0.113	0.008	1.3055	0.0001	0.6544	0.1842	0.1574
11	2	3-10-5	5	0.005	2.810	0.165	0.251	0.152	0.170	0.005	2.995	0.169	0.318	0.482	0.170	0.377	10.0	0.2000	0.0001	NaN	1.9860
11	3	5-10-2	3	n/a						0.003	1.206	0.008	0.338	0.164	0.416	n/a					
11	4	5-10-2	4	0.007	1.501	0.138	0.179	0.265	0.243	0.007	1.502	0.138	0.179	0.266	0.243	n/a					
11	5	10-10-2	3	n/a						0.010	1.872	0.110	2.829	0.335	1.232	0.011	2.7195	0.1677	24.1866	0.8611	1.0820
11	6	10-10-2	4	n/a						0.002	1.290	0.000	0.027	0.162	0.348	0.006	1.1215	0.0001	0.4808	0.1702	0.3451
11	7	11-8-2	4	n/a						0.012	2.474	0.143	2.557	0.310	1.367	0.012	2.4707	0.1426	2.5282	0.3611	1.3670
11	8	11-10-5	4	n/a						0.011	2.859	0.234	0.319	0.437	0.337	n/a					
11	9	13-8-2	6	n/a						0.004	1.359	0.005	0.358	0.183	0.428	0.004	1.3551	0.0021	0.3578	0.1753	0.4281
11	10	13-8-5	3	0.006	2.138	0.139	0.141	0.209	0.359	0.006	2.125	0.138	0.141	0.166	0.361	0.004	1.787	0.0001	0.0177	0.1685	0.9009
12	1	10-8-2	14	0.011	2.460	0.144	1.283	0.350	0.551	0.011	2.463	0.144	1.289	0.367	0.551	n/a					
12	2	10-8-2	15	n/a						0.003	1.415	0.139	0.020	0.155	0.121	0.002	1.2562	0.0169	0.0246	0.1583	0.1196
12	3	10-8-5	18	0.008	1.840	0.151	0.221	0.249	0.196	0.008	1.837	0.152	0.227	0.204	0.196	n/a					
12	4	10-10-5	19	0.006	1.662	0.000	0.276	0.529	0.345	0.007	2.027	0.072	0.370	0.766	0.291	0.007	2.0264	0.0723	0.3696	0.7720	0.2905
12	5	11-8-2	17	0.007	1.564	0.115	0.129	0.299	0.246	0.008	1.954	0.153	0.157	0.284	0.236	n/a					
12	6	11-10-5	17	0.017	1.715	0.117	3.111	0.305	0.628	0.016	1.718	0.117	3.095	0.349	0.628	0.016	1.7187	0.1172	3.0966	0.0034	0.6276
12	7	12-10-2	15	0.033	1.274	0.000	3.627	0.108	0.979	0.008	2.466	0.133	0.163	0.163	0.400	0.008	2.4598	0.1325	0.1623	0.0016	0.3997
12	8	13-8-2	16	0.009	2.359	0.120	0.751	0.176	0.921	0.009	2.360	0.120	0.751	0.173	0.921	n/a					
12	9	13-8-5	17	0.007	2.575	0.074	1.040	1.608	0.808	0.007	2.579	0.075	1.040	1.601	0.808	0.007	2.573	0.0743	1.0341	1.5724	0.8078
12	10	13-10-2	15	0.007	3.316	0.172	0.690	0.204	0.686	0.007	3.321	0.172	0.687	0.171	0.686	n/a					

Table 4.3.2. Summary statistics of the van Genuchten parameters.

	Valid N	Mean	Median	Mode	Mode Frequency	Minimum	Maximum	Lower Quartile	Upper Quartile	Std. Deviation
<u>ALL</u>										
α	97	0.016	0.010	.0074700	2	0.001	0.078	0.006	0.018	0.017
n	97	2.619	2.359	Multiple		1.122	7.469	1.658	3.136	1.280
θ_r	97	0.114	0.090	0.090	12	0.000	0.396	0.054	0.155	0.092
K_s	70	0.863*	0.523	30.000	2	0.008	99.534	0.212	2.732	15.940
<u>DANR - loam</u>										
α	2	0.005	0.005	Multiple		0.003	0.007	0.003	0.007	0.003
n	2	1.275	1.275	Multiple		1.183	1.367	1.183	1.367	0.130
θ_r	2	0.045	0.045	Multiple		0.000	0.090	0.000	0.090	0.064
K_s	0	n/a		Multiple						
<u>DANR - loamy sand</u>										
α	22	0.012	0.010	Multiple		0.003	0.028	0.006	0.015	0.008
n	22	2.459	2.286	Multiple		1.217	5.298	1.673	2.717	1.002
θ_p	22	0.096	0.090	0.090	4	0.000	0.279	0.042	0.151	0.073
K_s	14	0.5*	0.315	Multiple		0.056	9.554	0.214	1.451	2.475
<u>DANR - sand</u>										
α	18	0.044	0.045	Multiple		0.005	0.078	0.034	0.055	0.019
n	18	4.454	4.642	Multiple		2.424	7.469	3.833	5.002	1.093
θ_r	18	0.072	0.065	.0500000	2	0.032	0.155	0.054	0.079	0.029
K_s	11	15.496*	23.974	Multiple		0.152	99.534	14.566	37.793	28.041
<u>DANR - sandy loam</u>										
α	39	0.009	0.008	Multiple		0.002	0.023	0.006	0.012	0.005
n	39	2.104	1.976	Multiple		1.122	4.586	1.450	2.599	0.787
θ_r	39	0.106	0.120	.0900000	6	0.000	0.258	0.032	0.153	0.069
K_s	31	0.447*	0.358	Multiple		0.025	24.187	0.163	1.203	4.290

Table 4.3.2. continued

	Valid N	Mean	Median	Mode	Mode Frequency	Minimum	Maximum	Lower Quartile	Upper Quartile	Std. Deviation
DANR - silt loam										
α	16	0.008	0.007	Multiple		0.001	0.022	0.003	0.011	0.006
n	16	2.195	1.962	Multiple		1.128	5.042	1.517	2.586	0.973
θ_r	16	0.210	0.250	Multiple		0.000	0.396	0.069	0.329	0.140
K_s	14	0.66*	0.478	30.000	2	0.008	30.000	0.201	12.246	10.869

* geometric mean used for K_s

Table 4.5.1. Summary of percent reduction in sum of squares (SS) for subgroup "sandy loam" in groups 2, 3, and 4 using two scaling methods.

Group	Reduction in SS (%)	
	Method 1	Method 2
Group 2	83.6	57.9
Group 3	85.3	60.0
Group 4	86.7	54.0

FIGURES

Figure 2.1.1. Fantasia Nectarine Orchard Plot Map

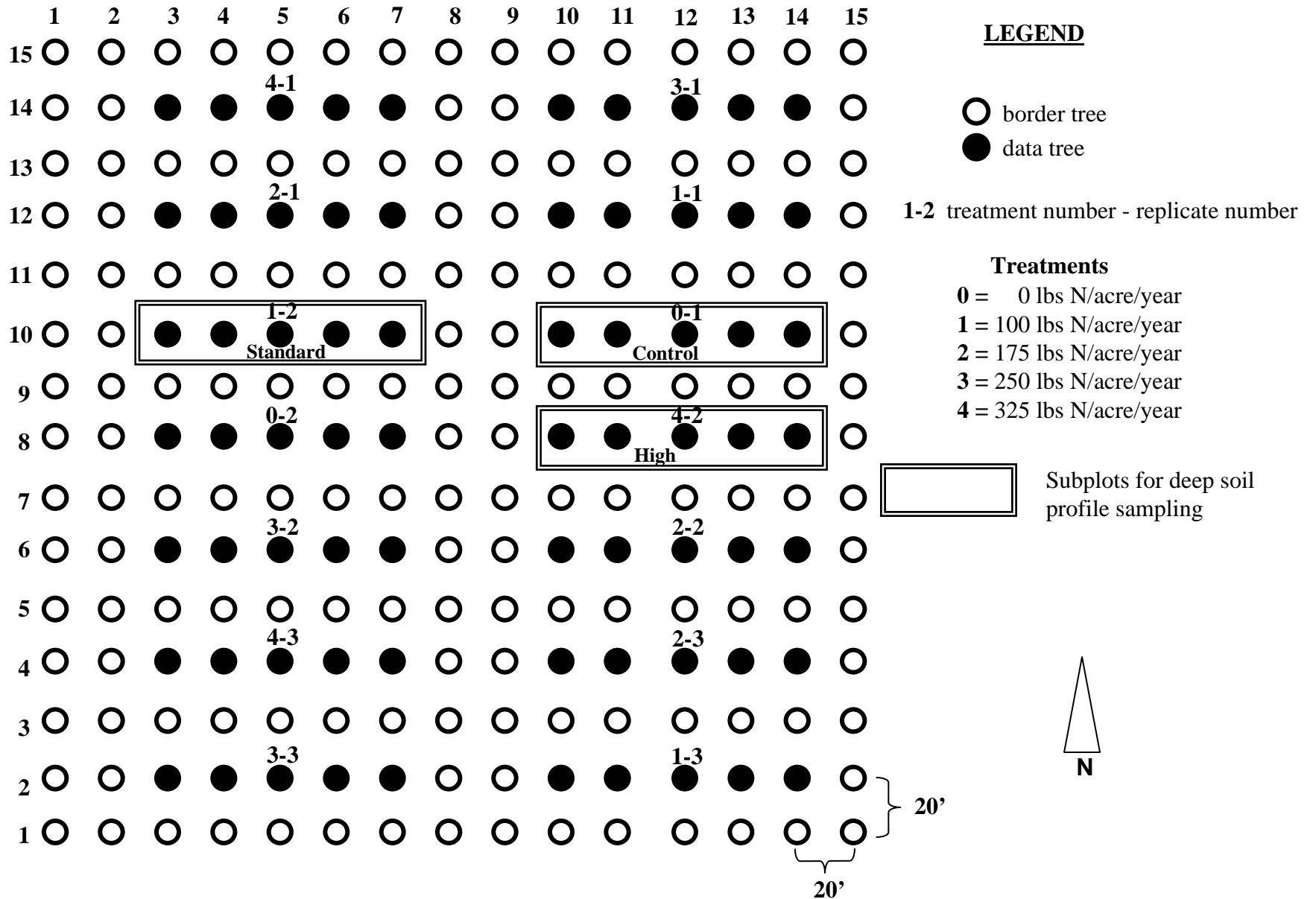
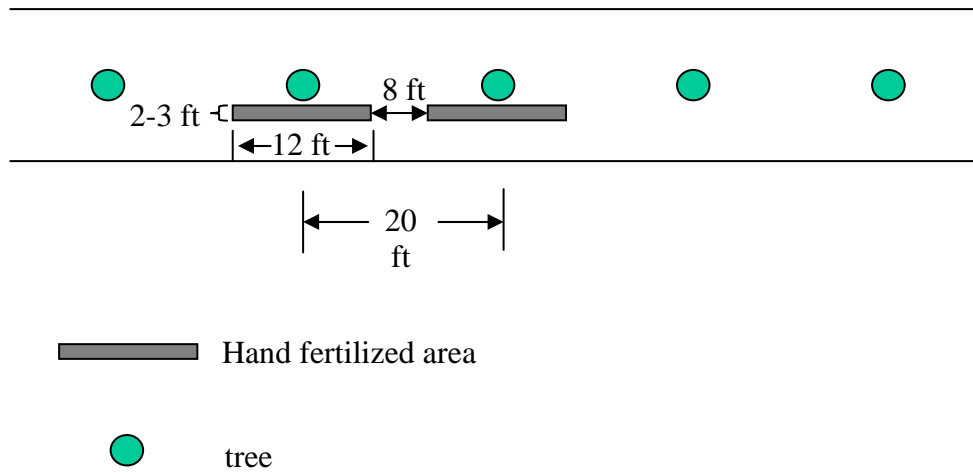


Figure 2.2.1. Hand Application of Fertilizer



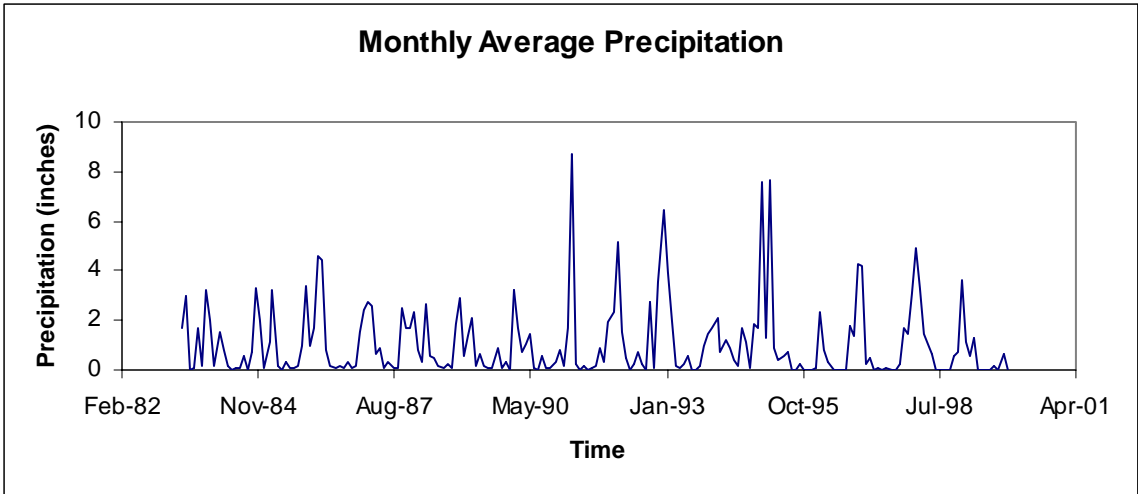


Figure 2.4.1. Average monthly precipitation from 1983 to 1999.

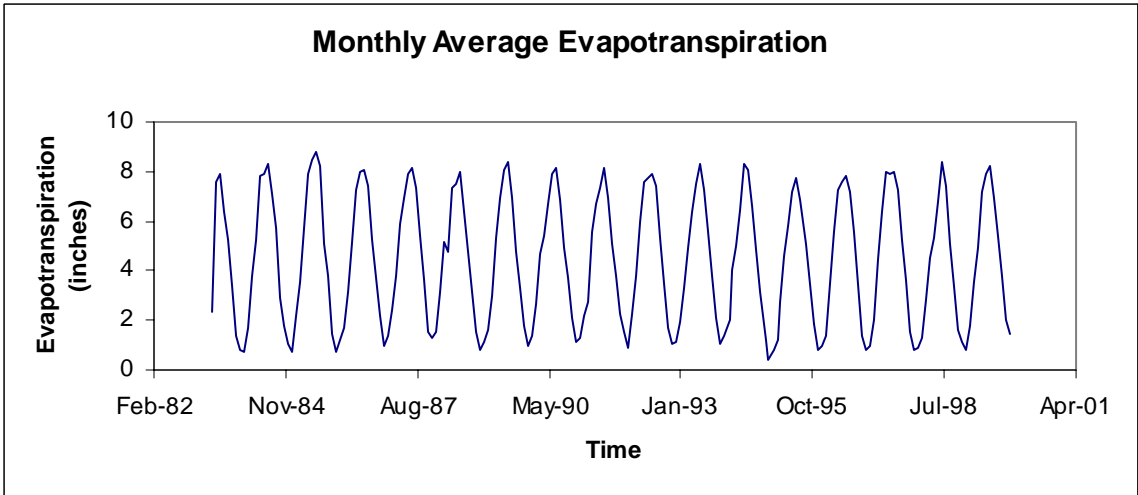


Figure 2.4.2. Average monthly ETo from 1983 to 1999.

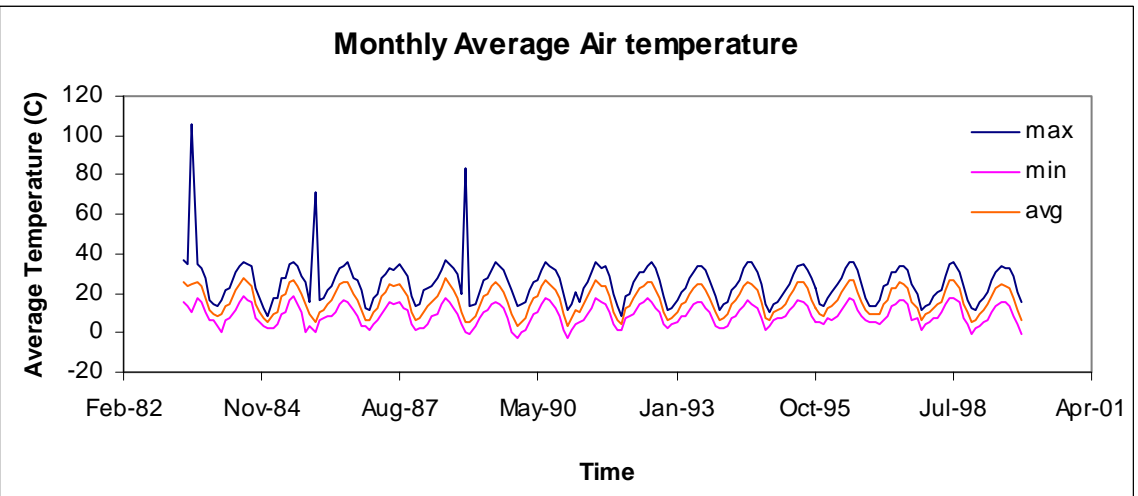


Figure 2.4.3. Average monthly air temperature from 1983 to 1999.

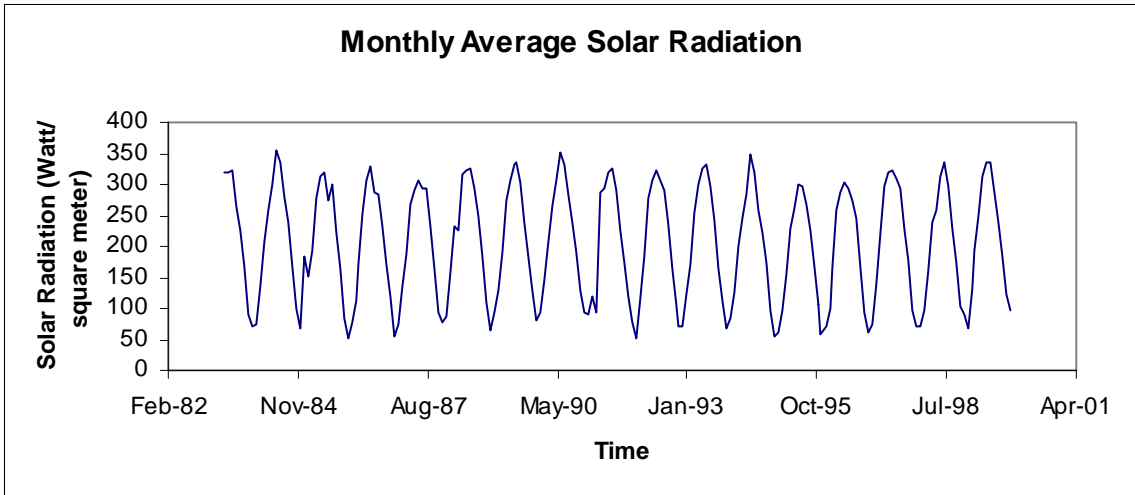


Figure 2.4.4. Average monthly solar radiation from 1983 to 1999.

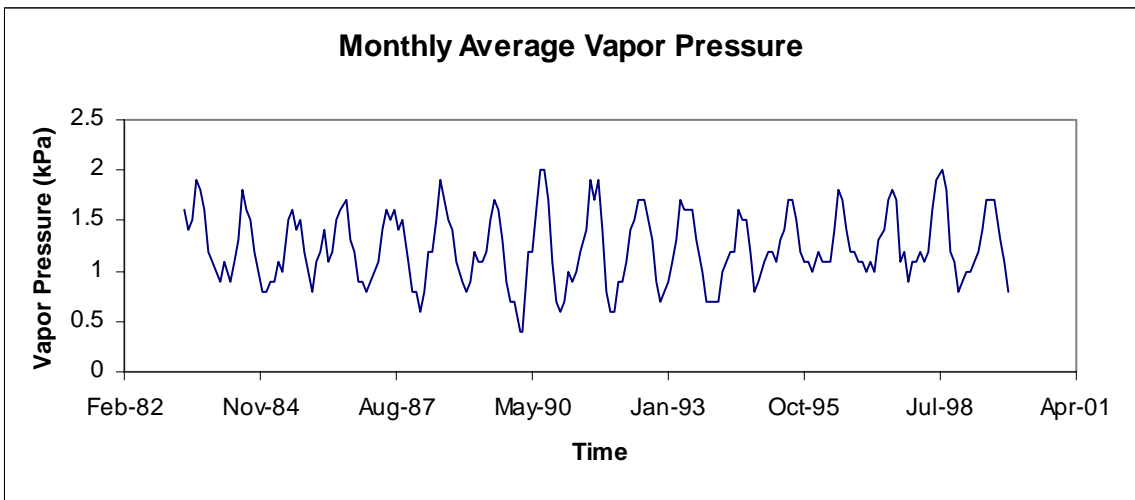


Figure 2.4.5. Average monthly vapor pressure from 1983 to 1999.

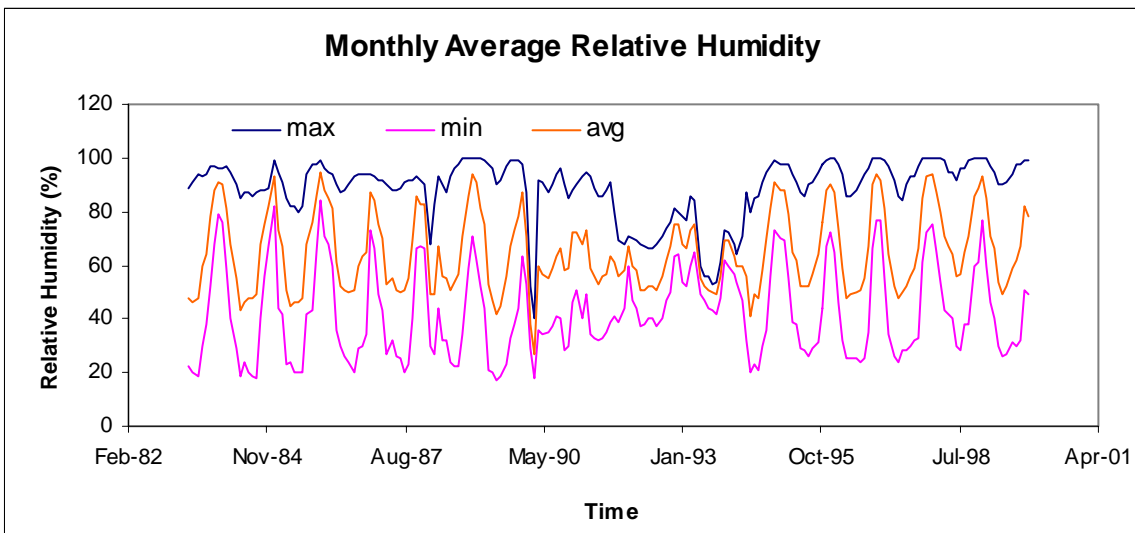


Figure 2.4.6. Average monthly relative humidity from 1983 to 1999.

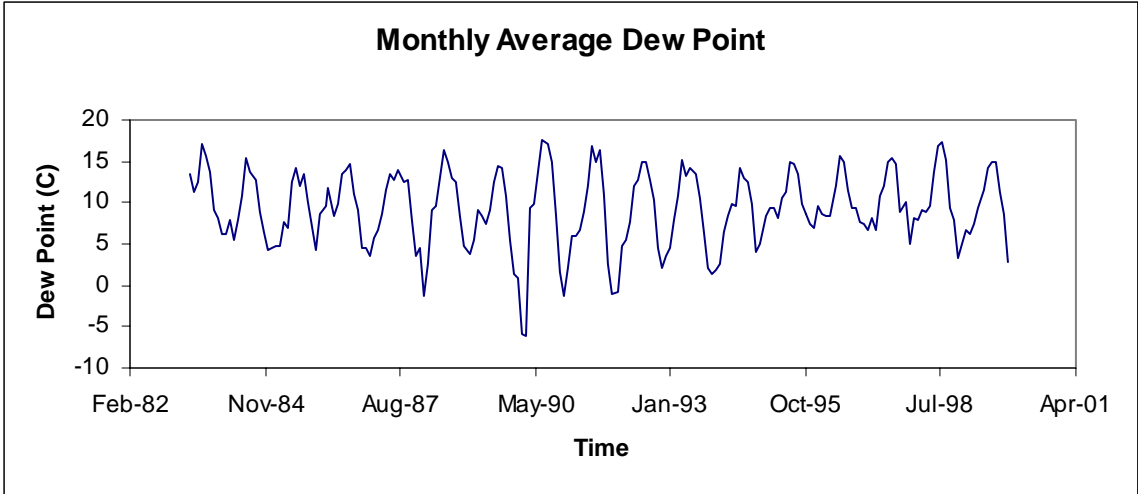


Figure 2.4.7. Average monthly dew point from 1983 to 1999.

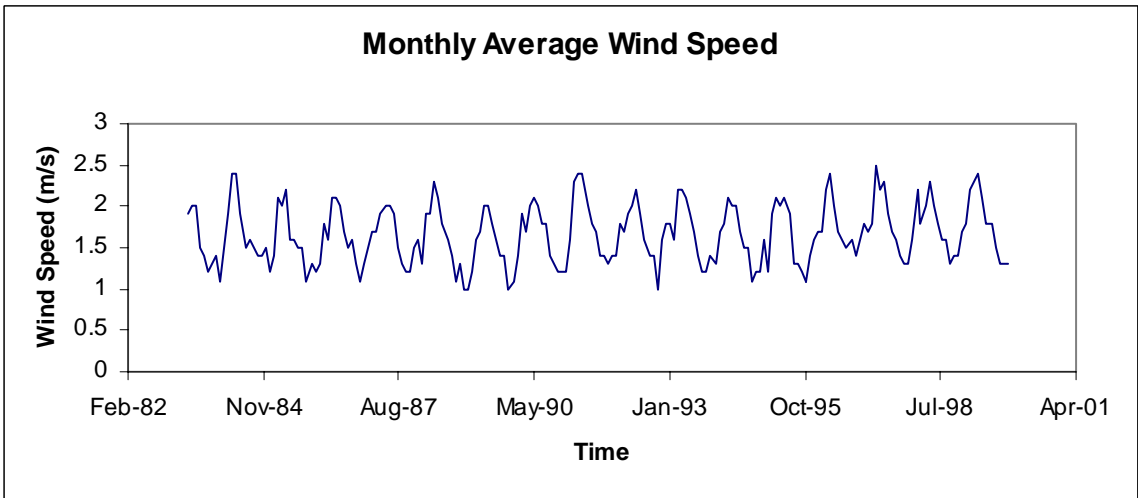


Figure 2.4.8. Average monthly wind speed from 1983 to 1999.

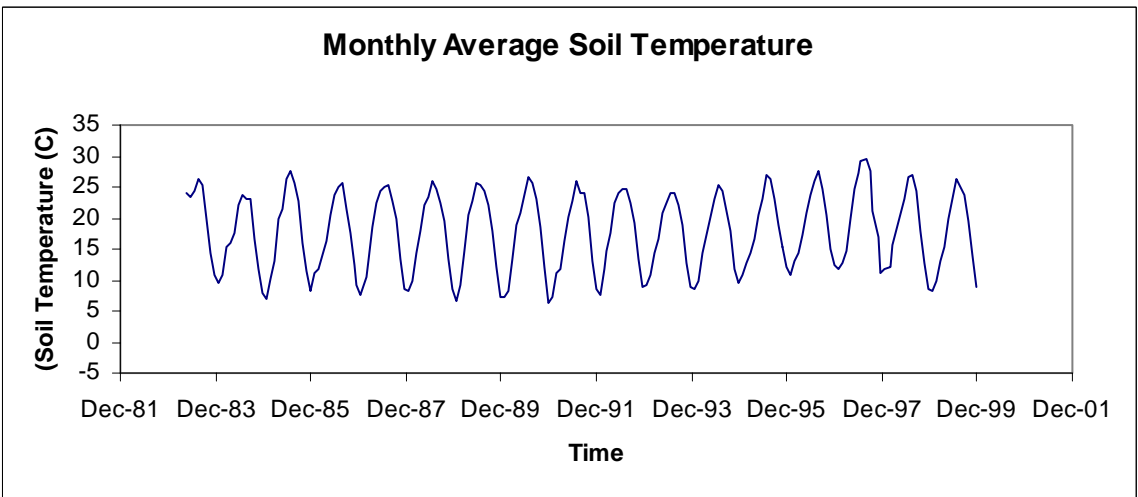


Figure 2.4.9. Average soil temperature from 1983 to 1999.

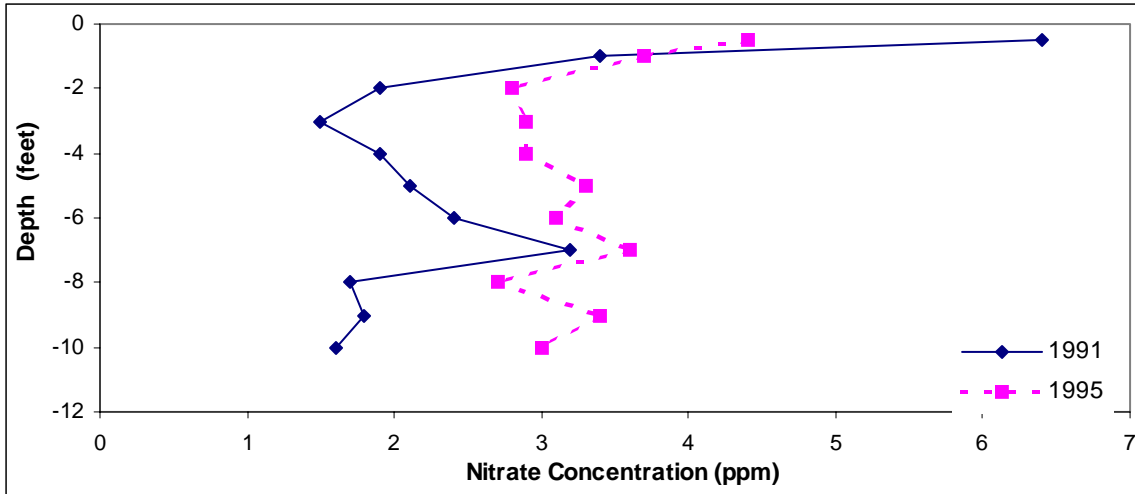


Figure 2.5.1a. Soil nitrate concentration measured in 1991 and 1995 for the 0 treatment subplot.

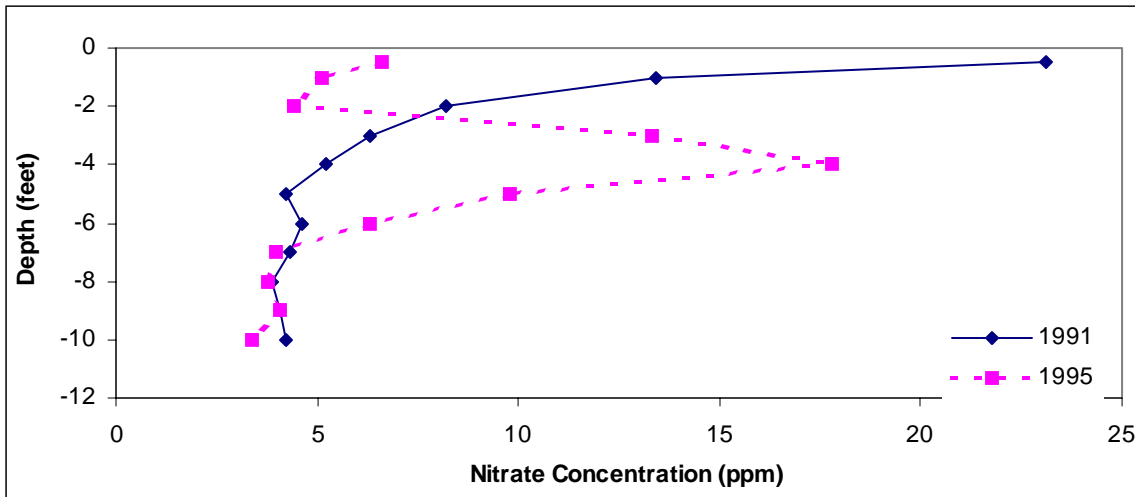


Figure 2.5.1b. Soil nitrate concentration for the 100 lbs N/acre subplot.

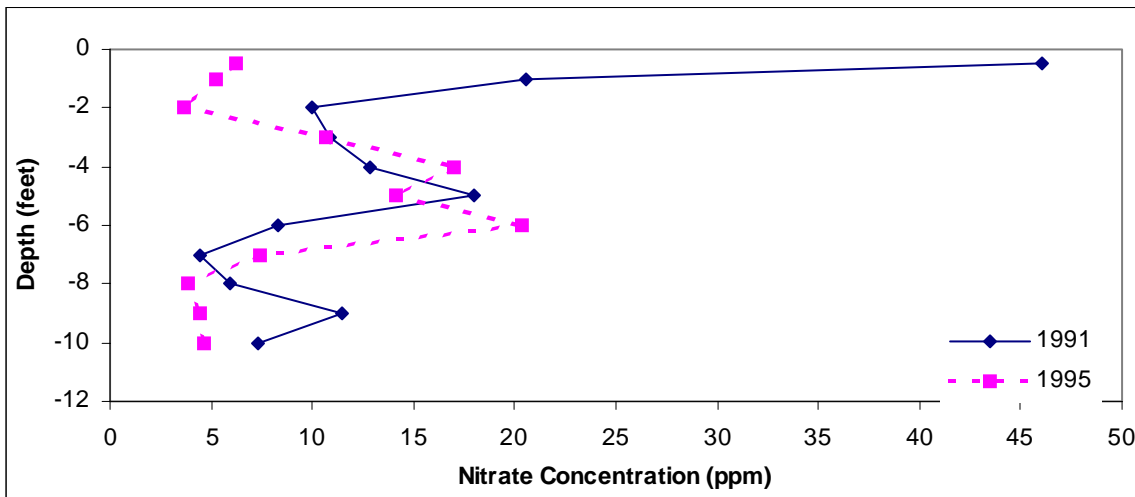


Figure 2.5.1c. Soil nitrate concentration for the 175 lbs N/acre subplot.

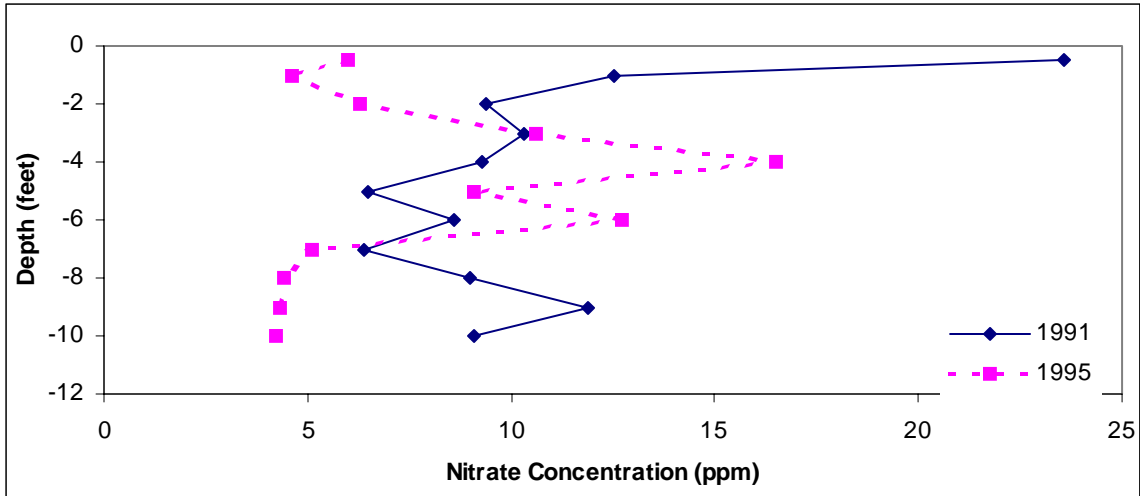


Figure 2.5.1d. Soil nitrate concentration for the 250 lbs N/acre subplot.

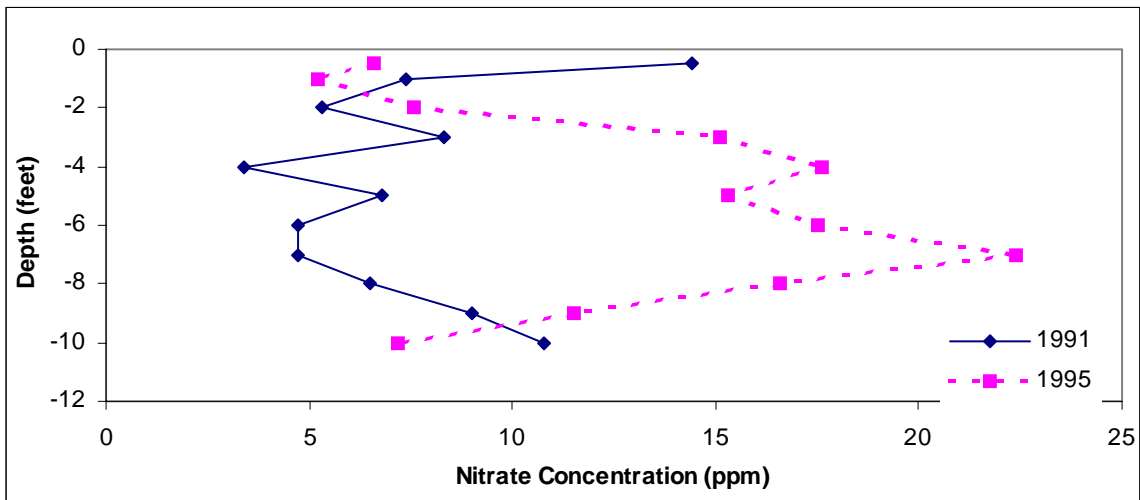
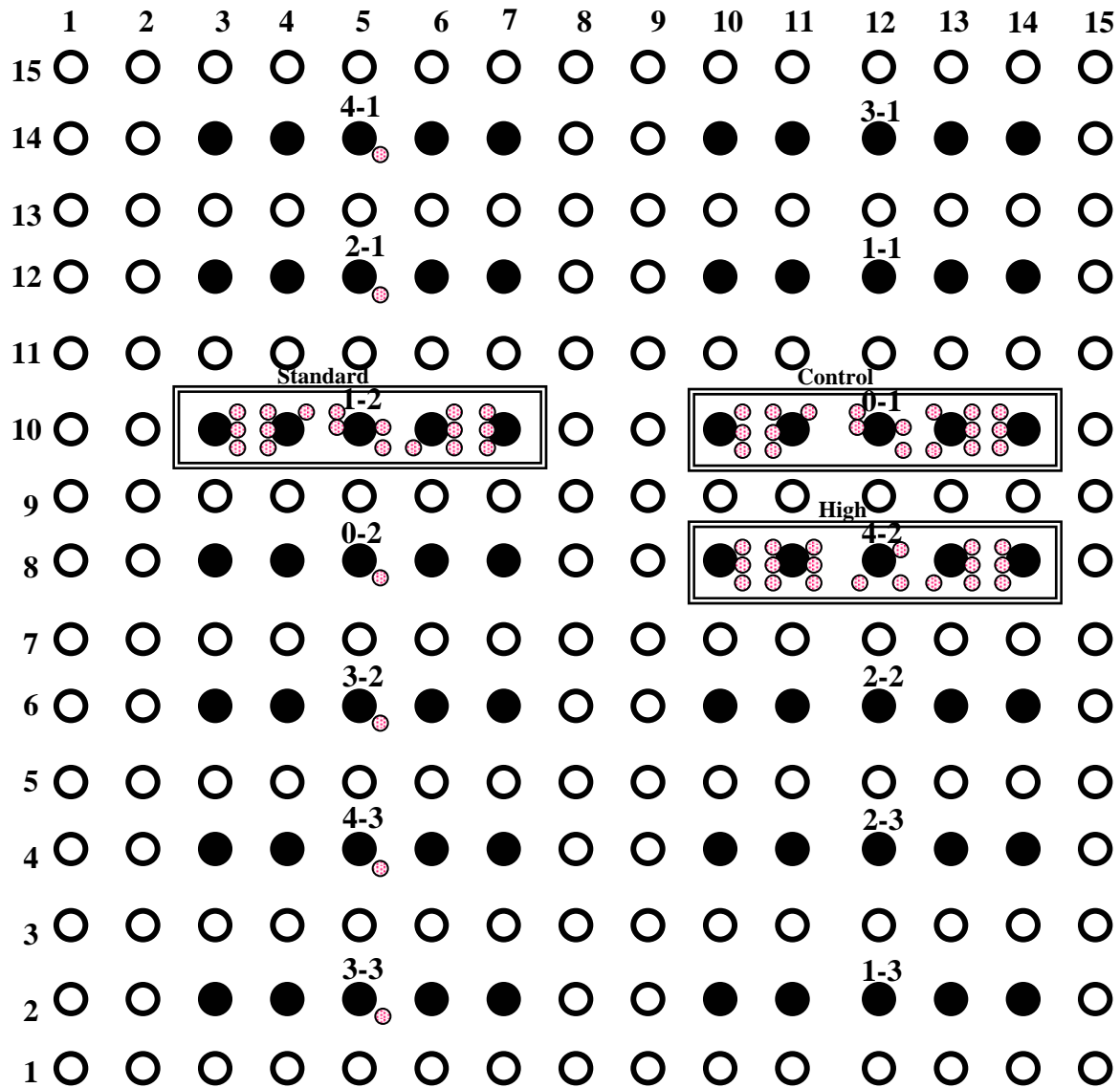


Figure 2.5.1e. Soil nitrate concentration for the 325 lbs N/acre subplot.

Figure 2.7.1. Fantasia Nectarine Soil Core Map



LEGEND

- border tree
- data tree
- ⊙ soil coring location

1-2 treatment number - replicate number

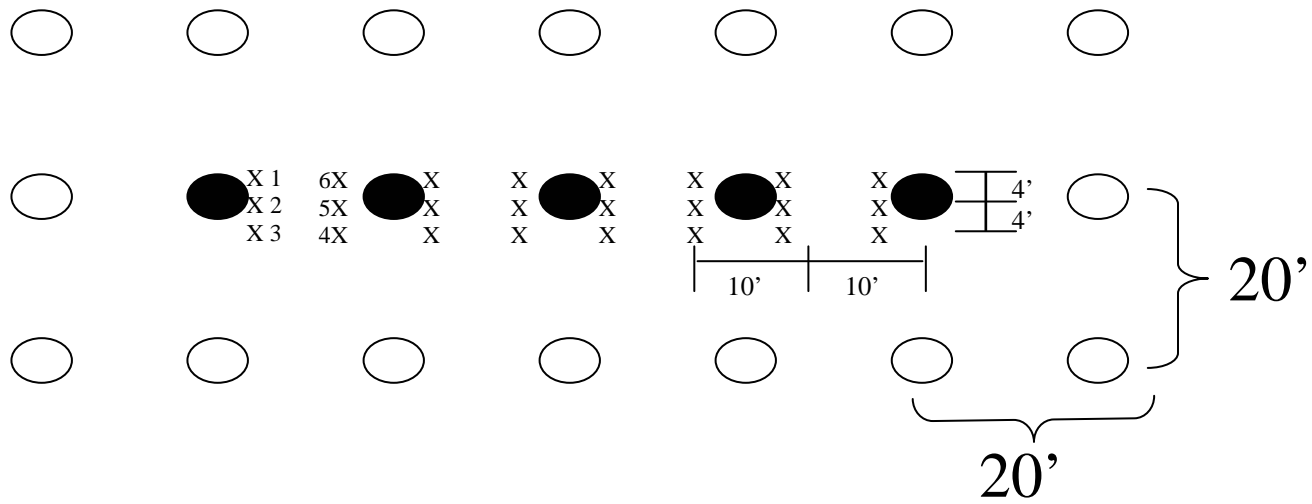
Treatments

- 0 = 0 lbs N/acre/year
- 1 = 100 lbs N/acre/year
- 2 = 175 lbs N/acre/year
- 3 = 250 lbs N/acre/year
- 4 = 325 lbs N/acre/year

Subplots for deep soil profile sampling

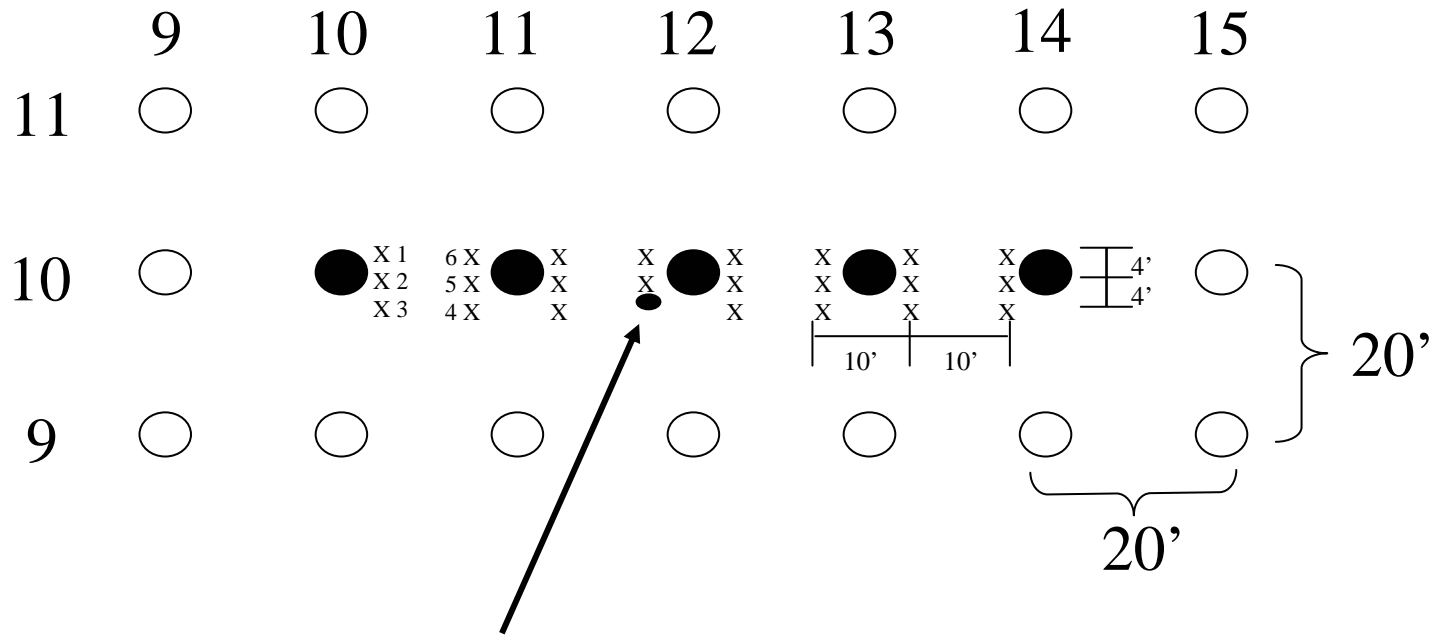


Figure 2.7.2. Deep Soil Profile Sampling Strategy



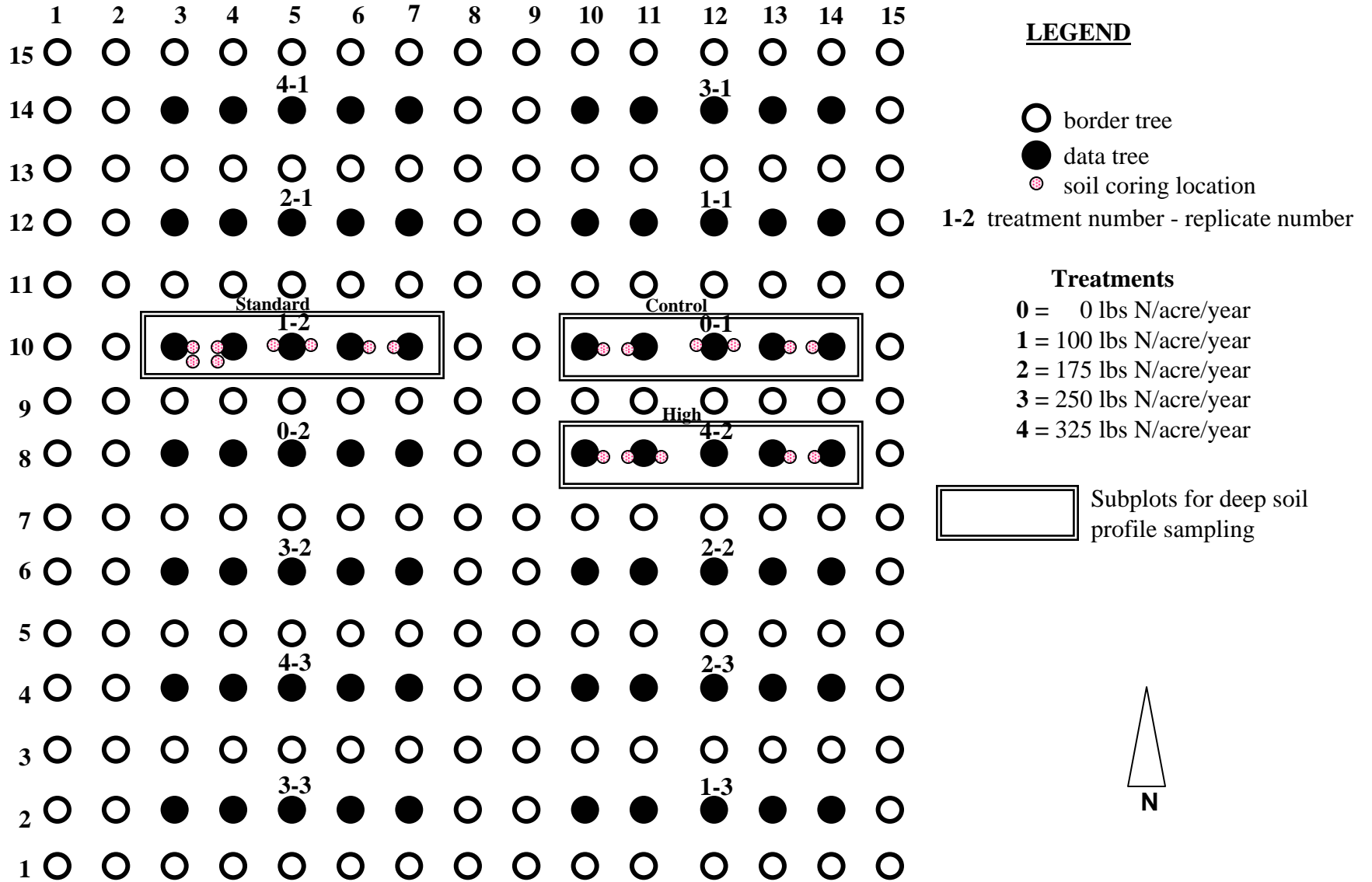
- border tree
- data tree
- X soil core location

Figure 2.7.3. Soil Sample Numbering



Core number 11-10-4

Figure 3.1.1. Fantasia Nectarine Hydraulic Soil Core Map



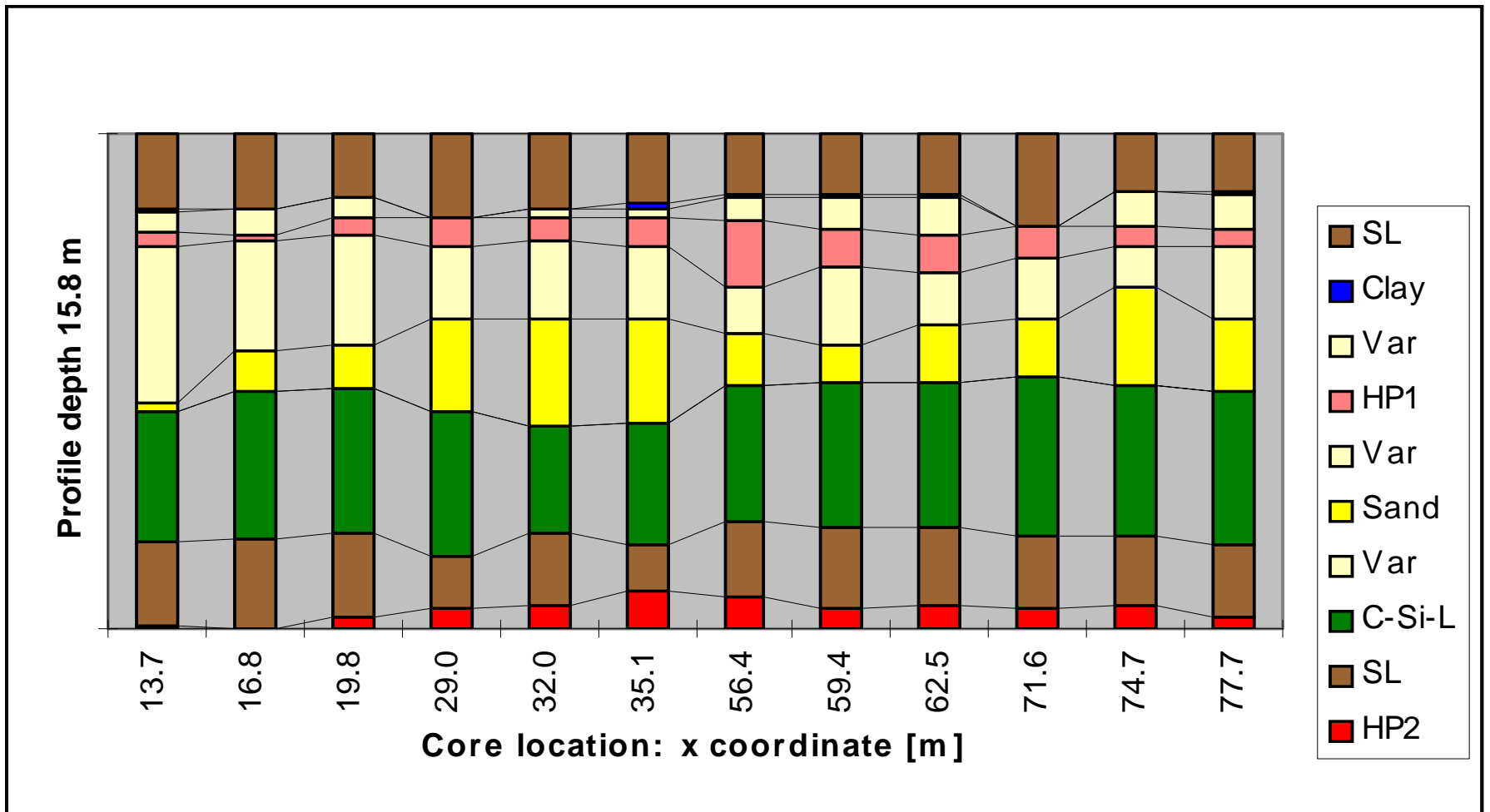
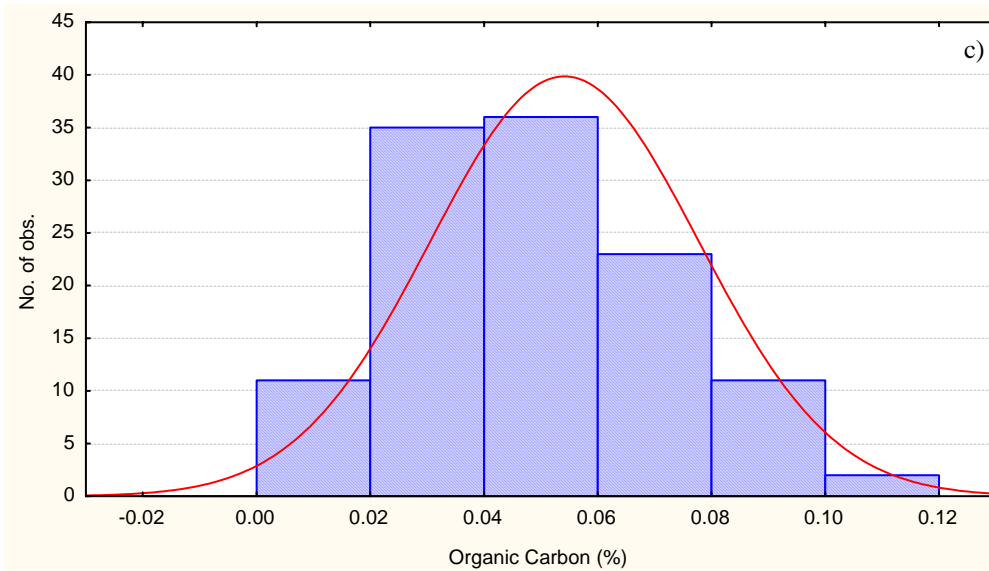
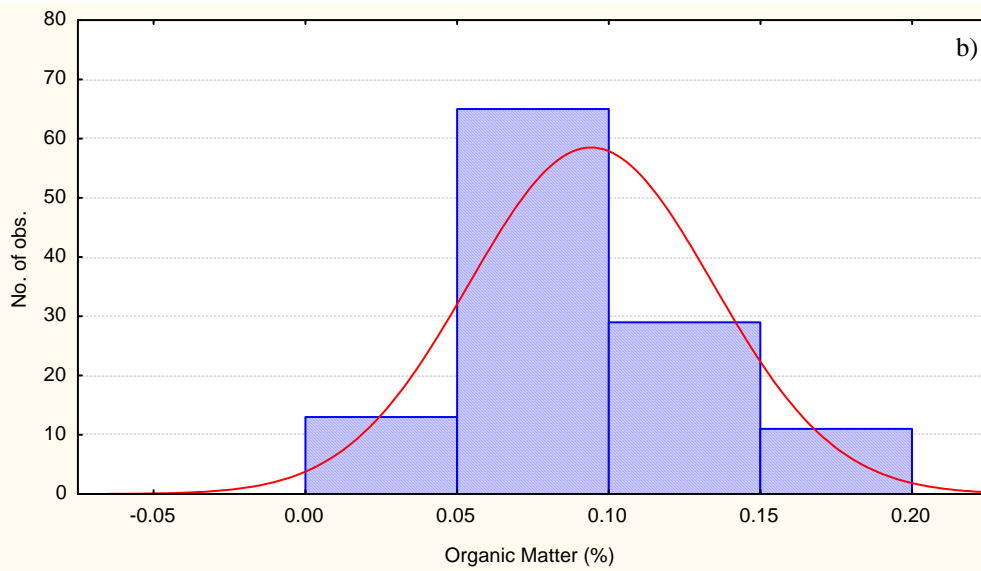
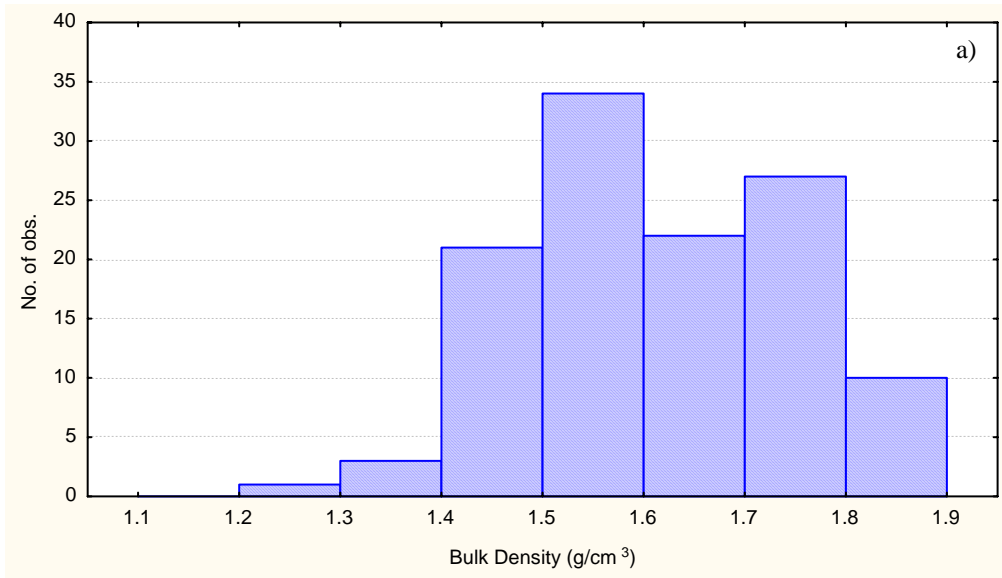
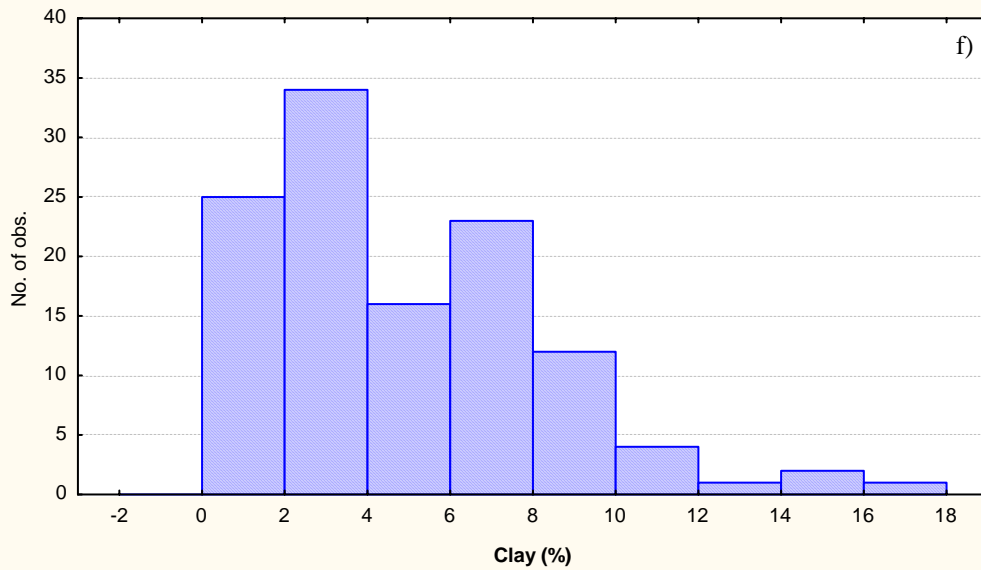
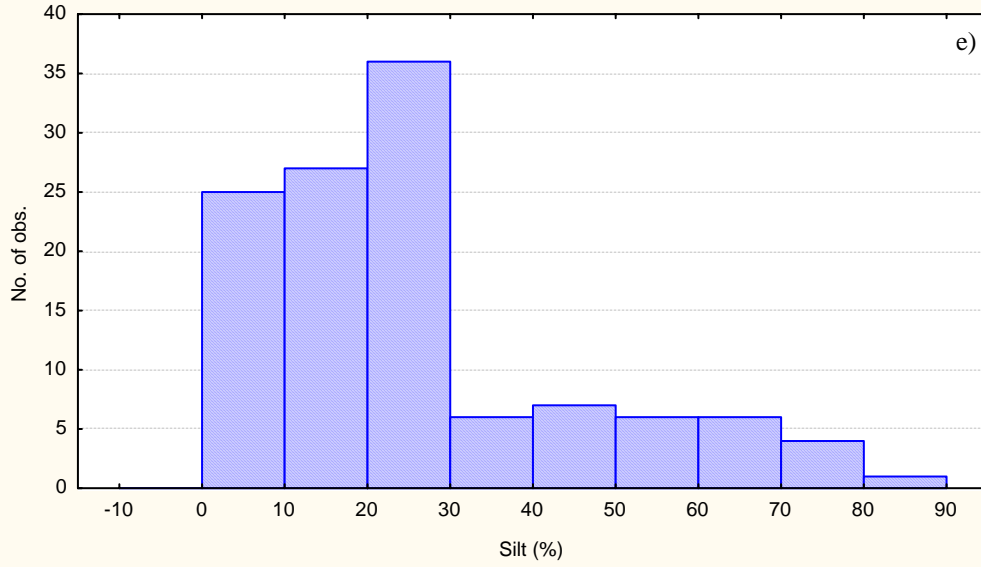
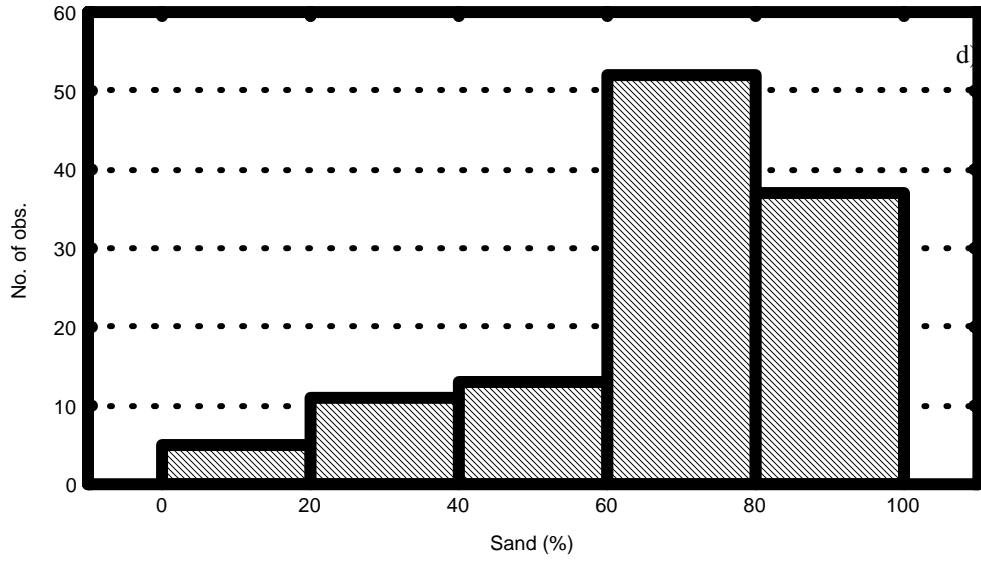


Figure 4.1.1. Stratigraphic cross-section along a tree-row showing the major stratigraphic units.





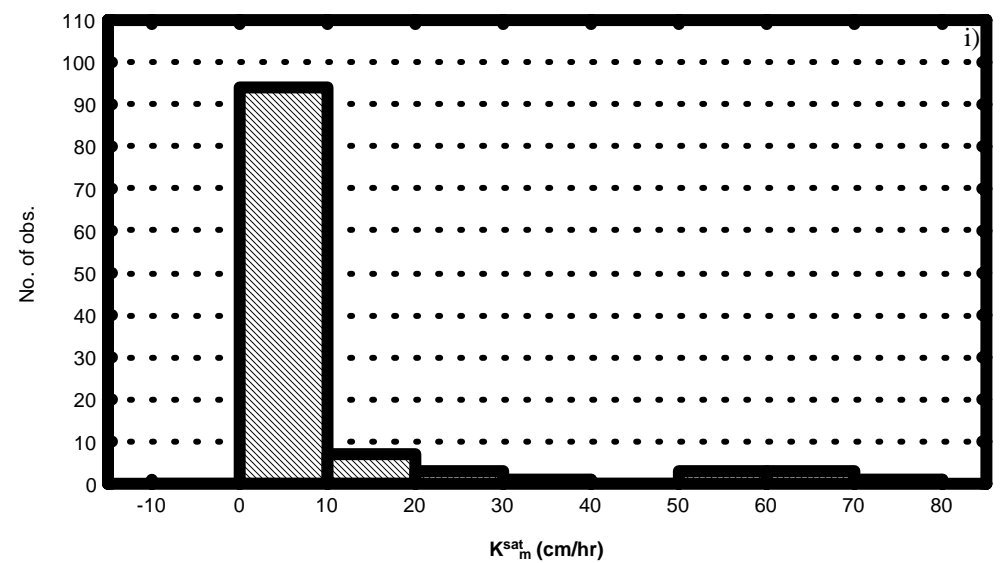
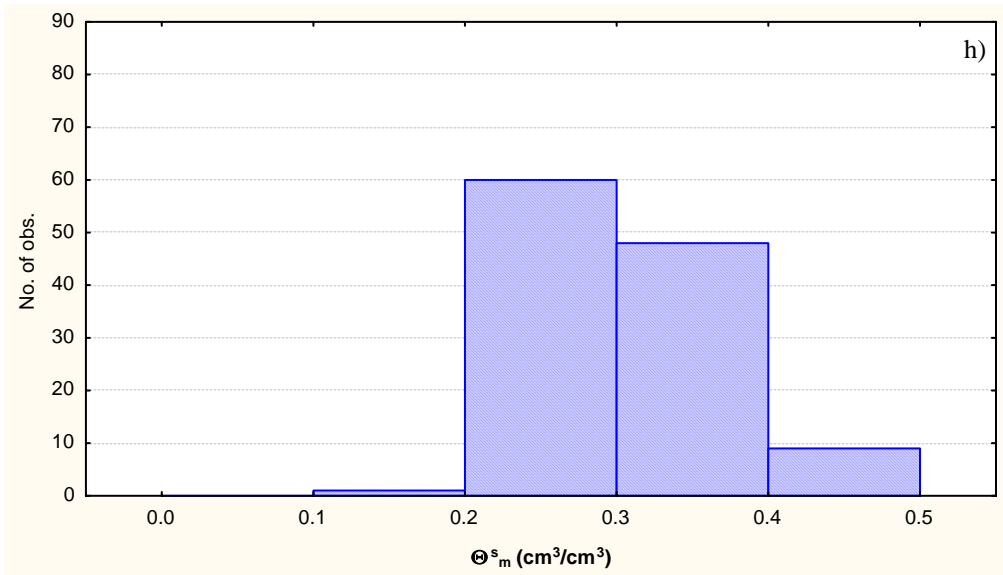
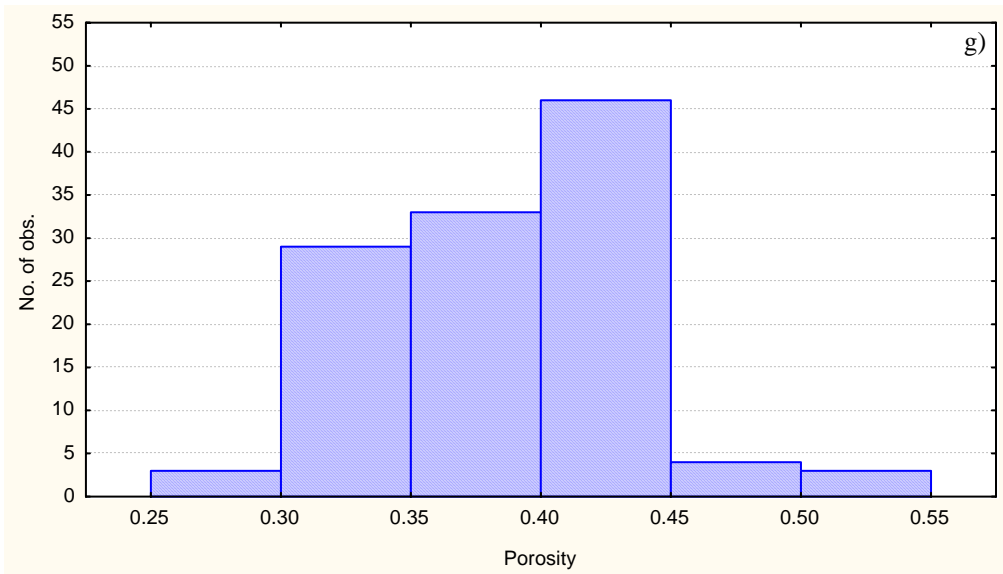


Figure 4.2.1 a-i. Histograms for the nine laboratory measurements for 118 soil samples.

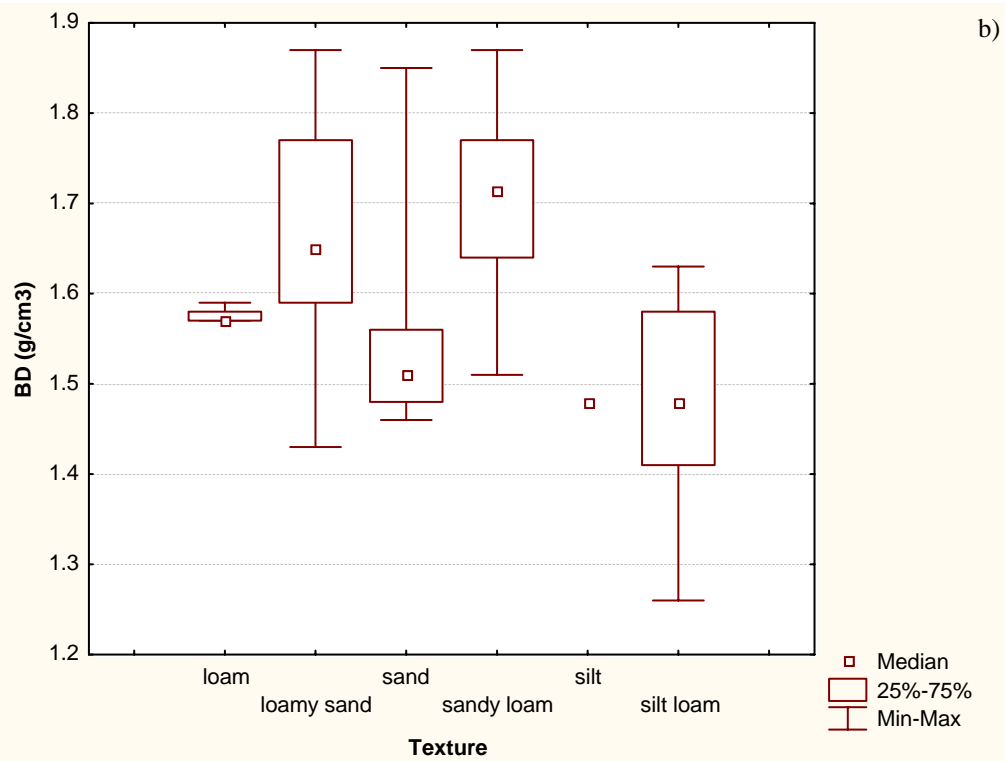
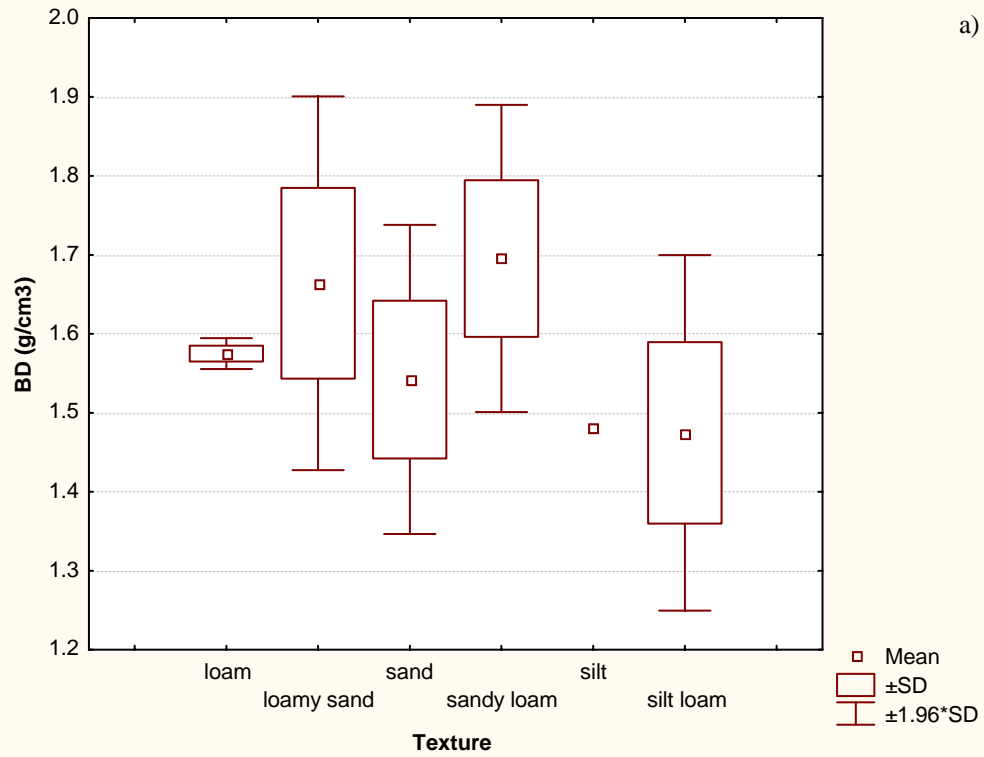


Figure 4.2.2a-b. Categorized box and whisker plots for bulk density.

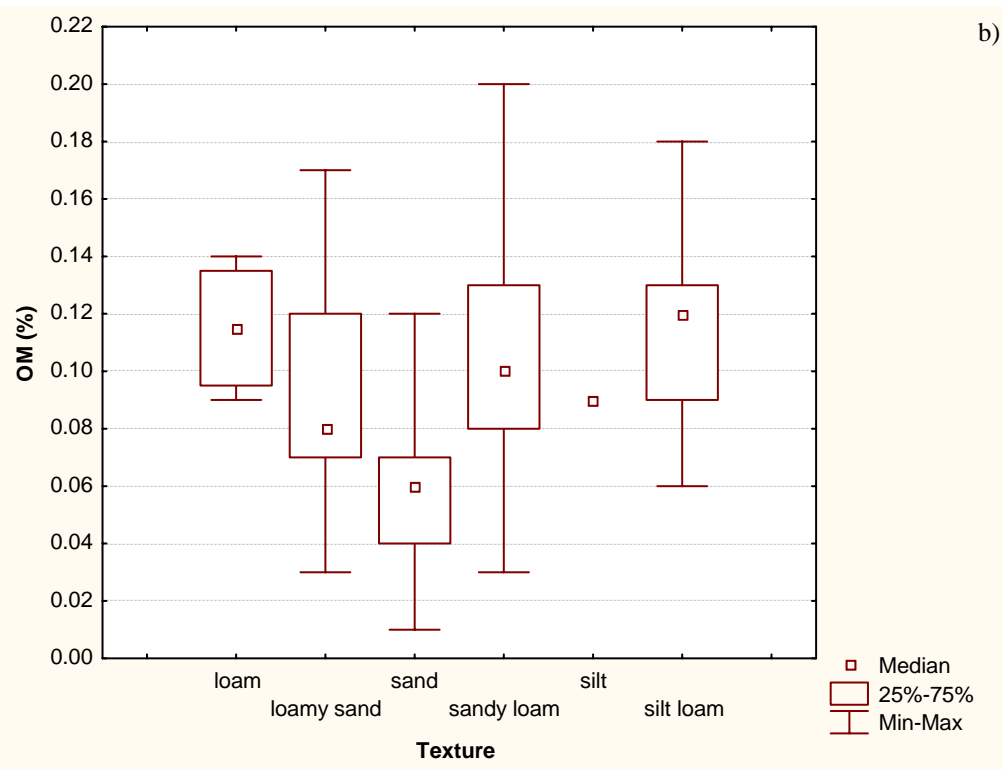
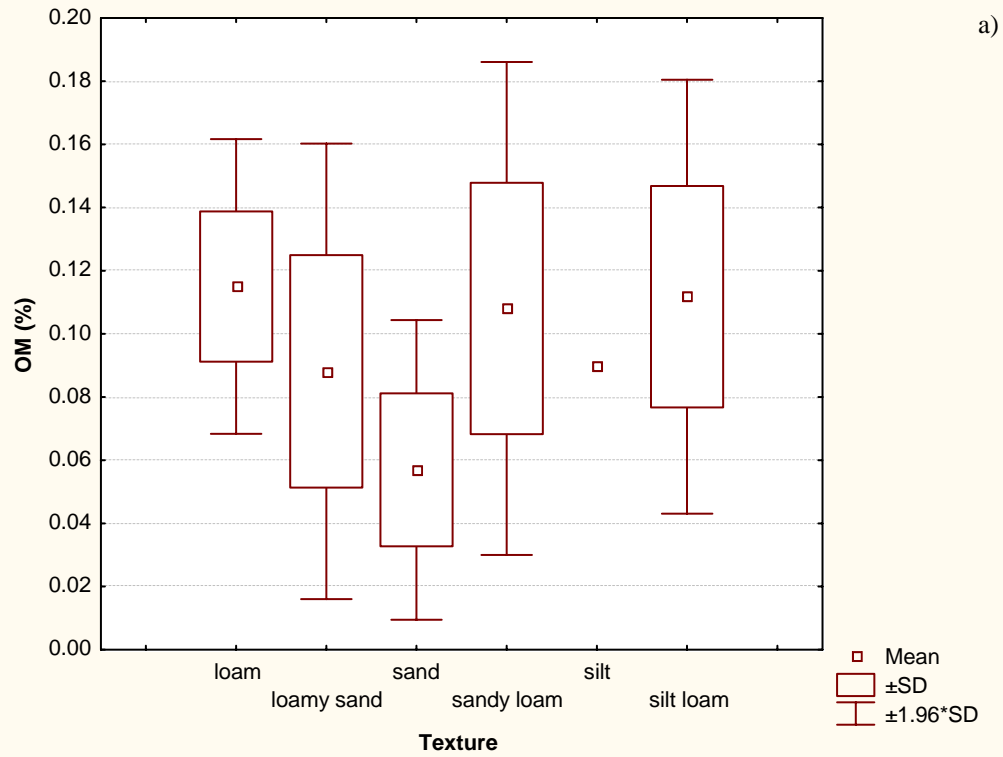


Figure 4.2.3a-b. Categorized box and whisker plots for organic matter content.

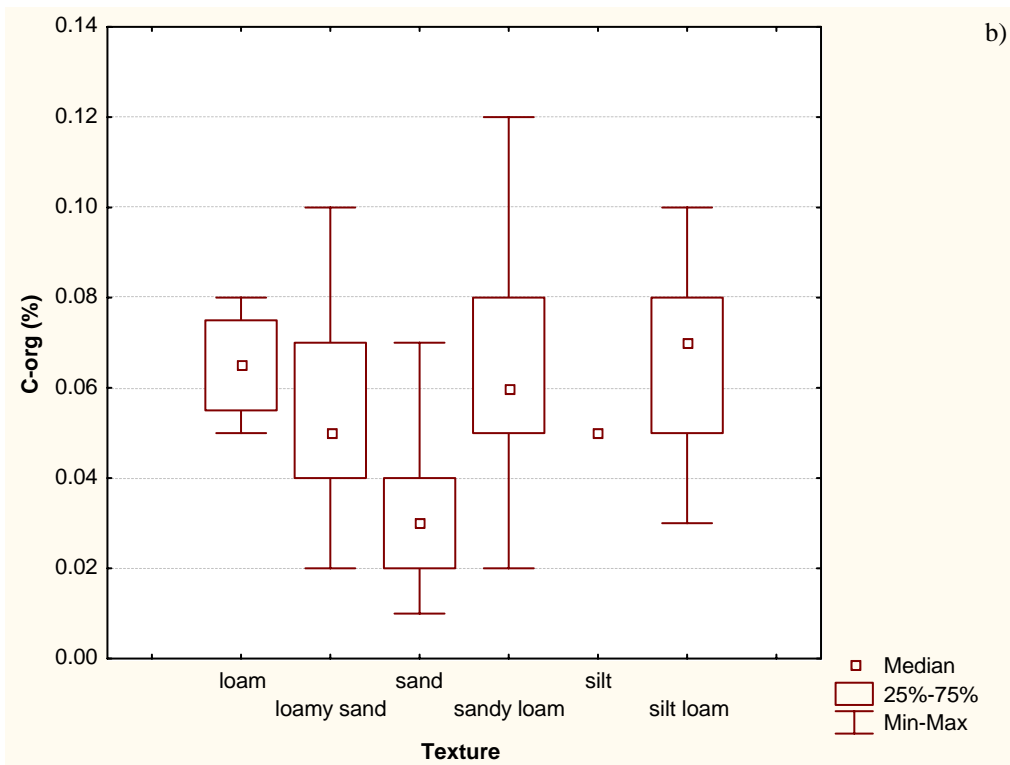
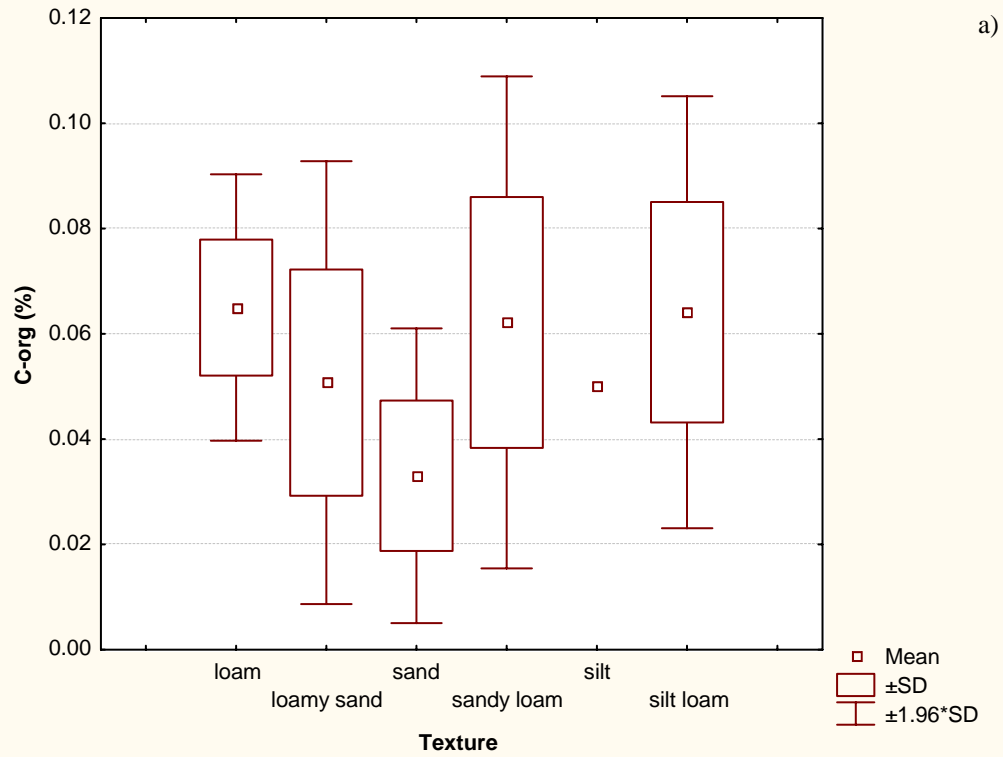


Figure 4.2.4a-b. Categorized box and whisker plots for organic carbon content.

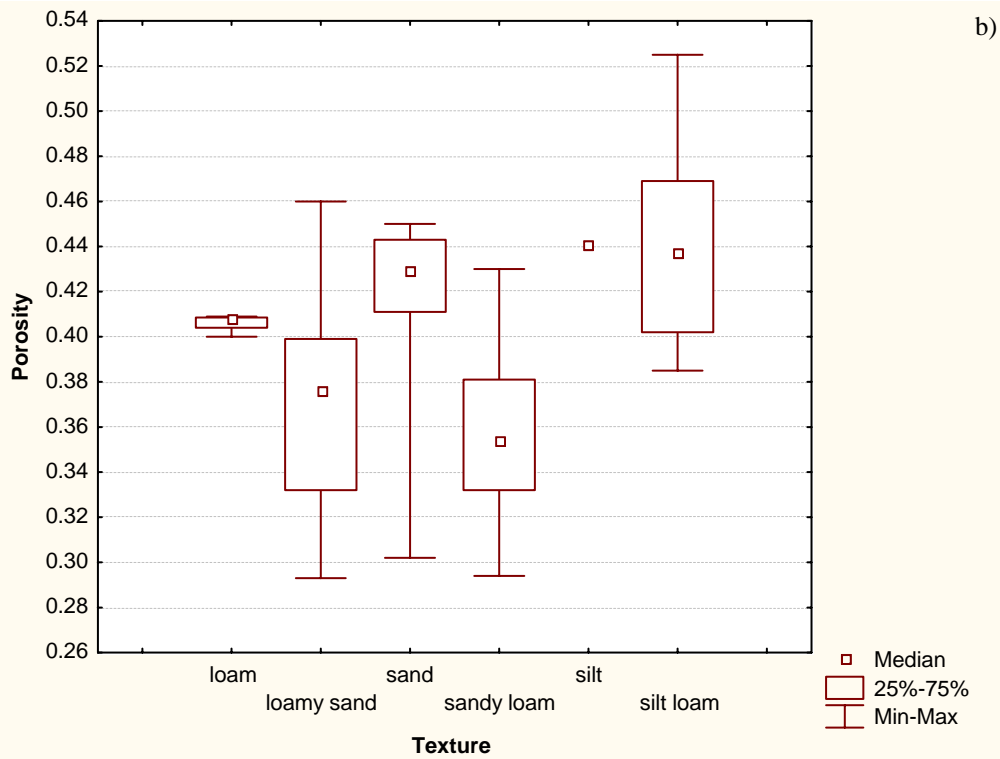
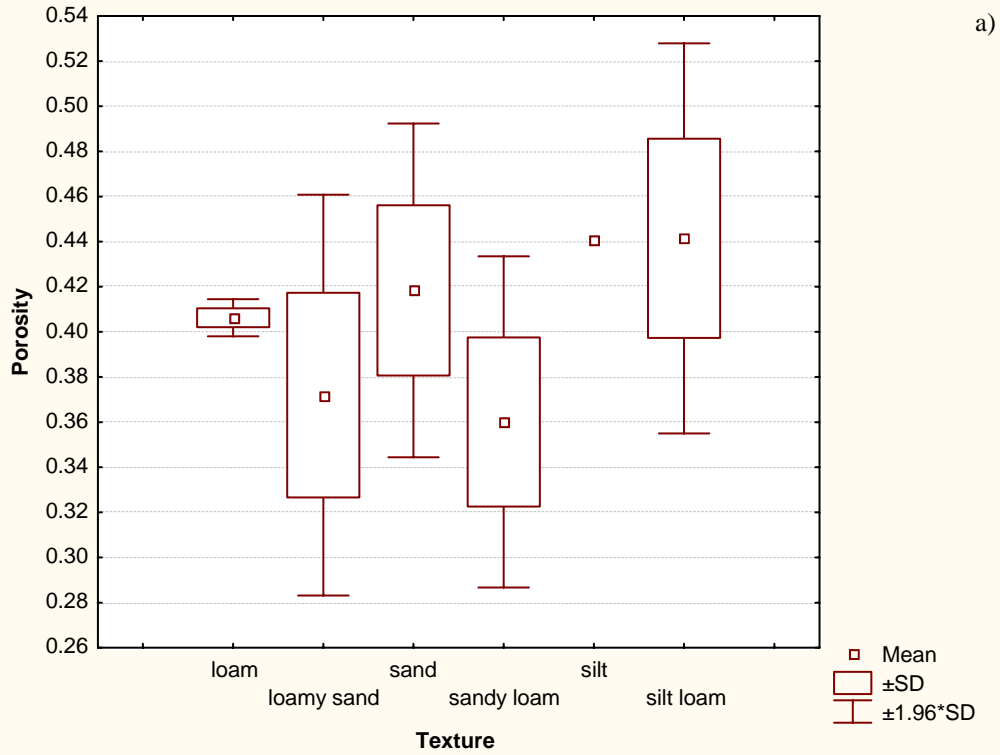


Figure 4.2.5a-b. Categorized box and whisker plots for porosity.

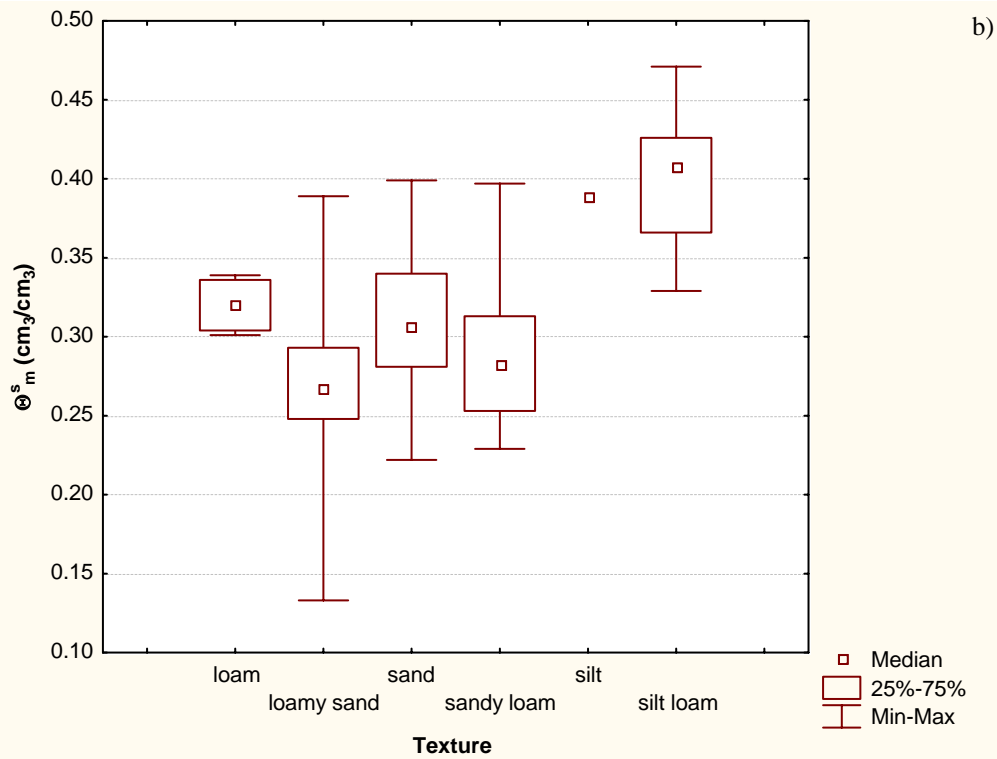
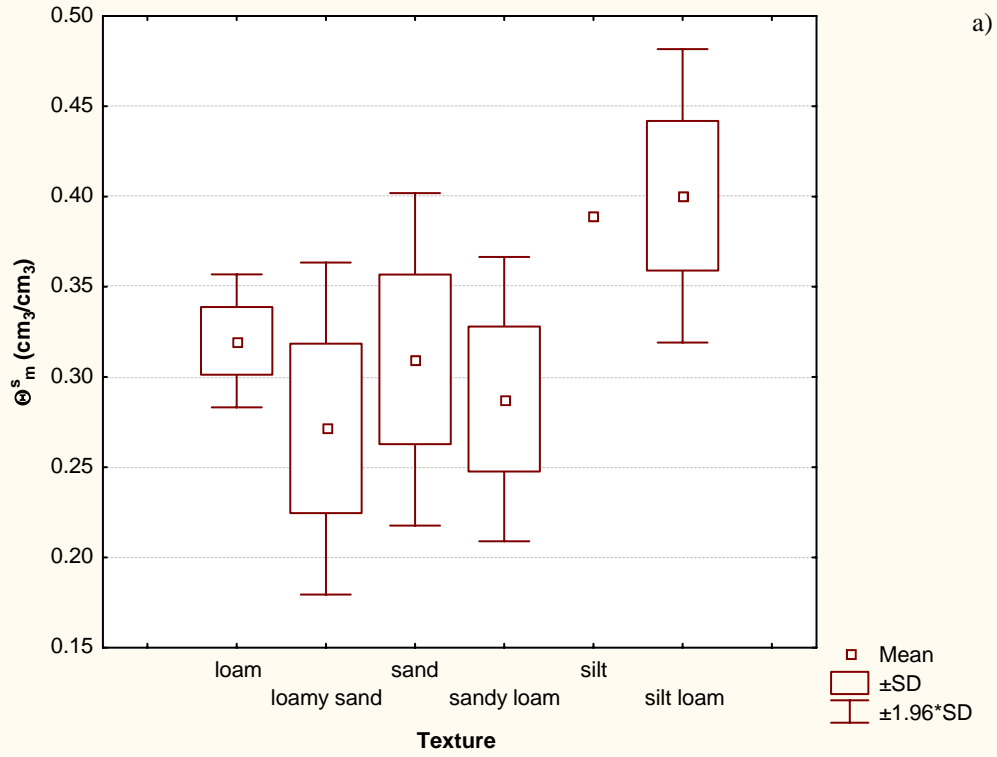


Figure 4.2.6a-b. Categorized box and whisker plots for saturated water content.

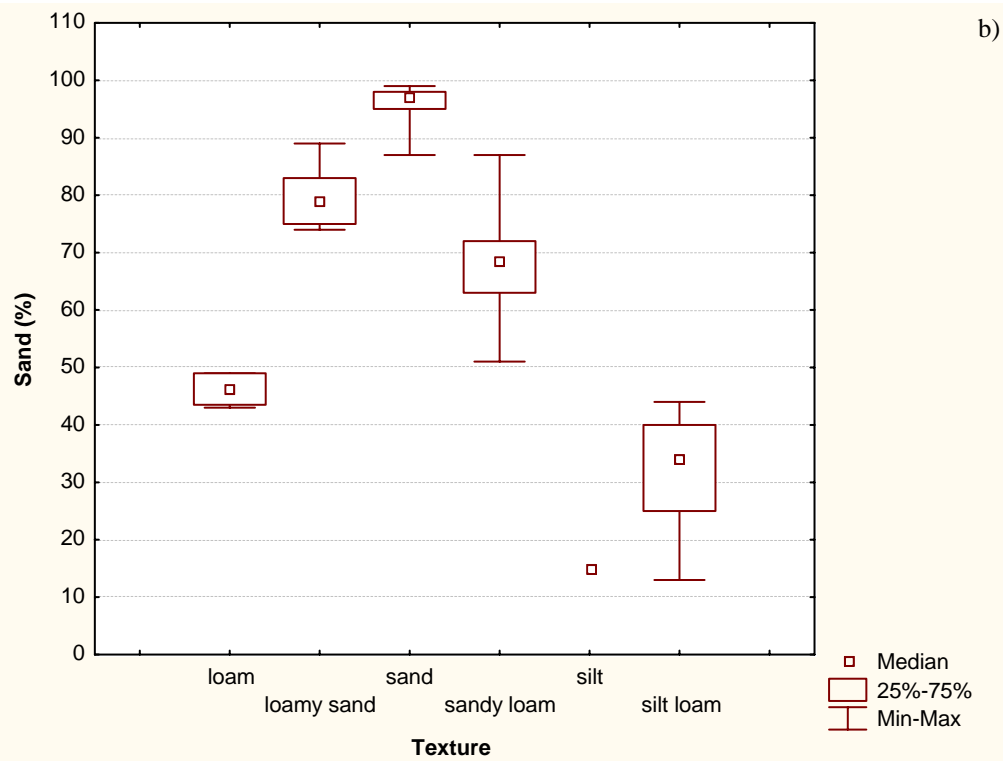
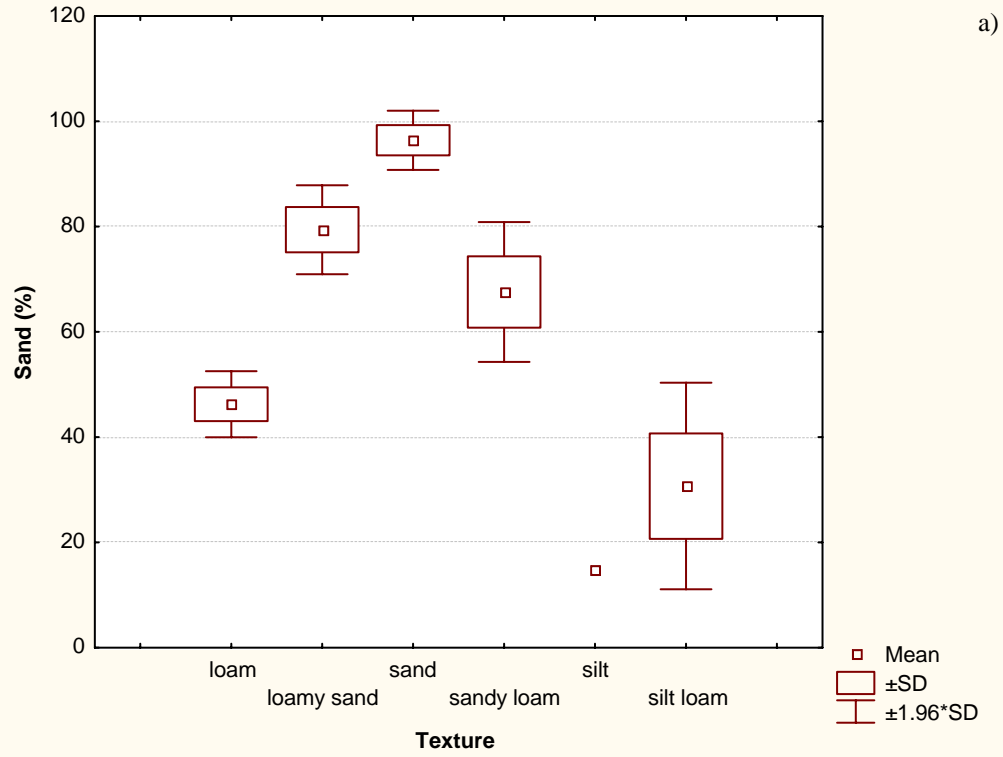


Figure 4.2.7a-b. Categorized box and whisker plots for the sand fraction.

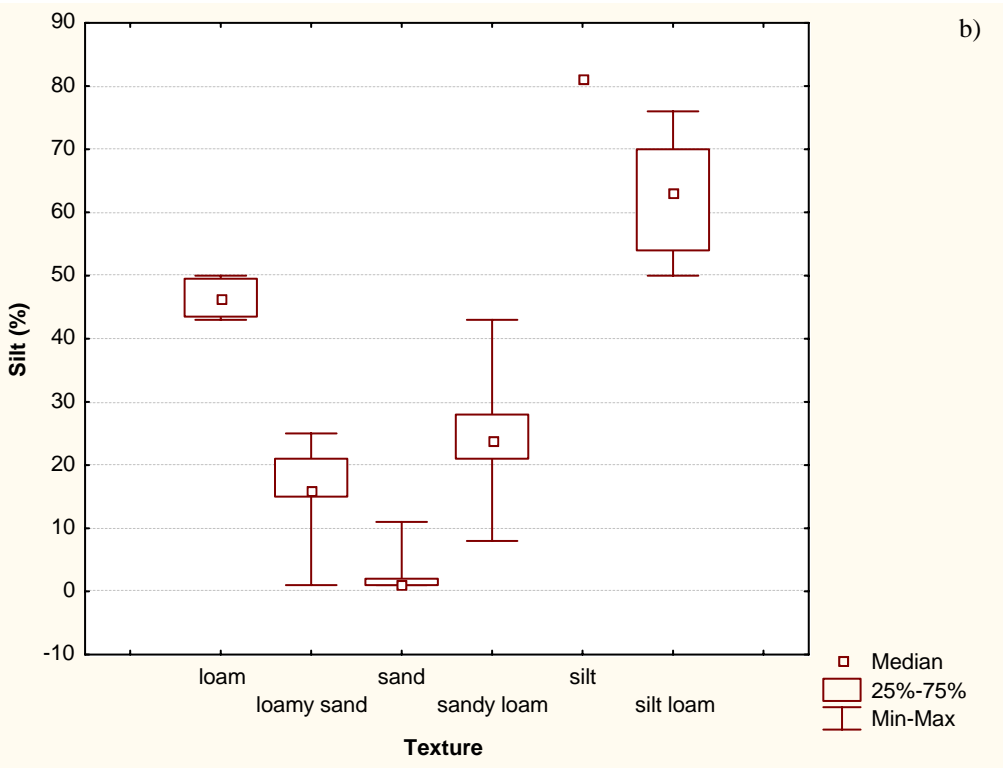
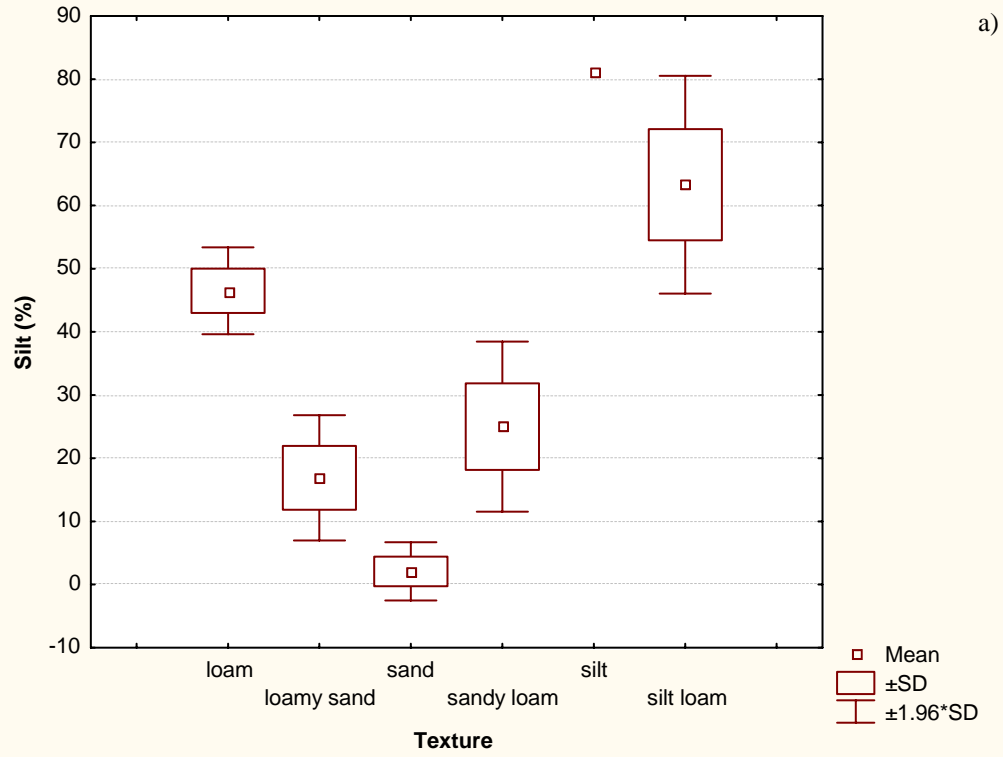


Figure 4.2.8a-b. Categorized box and whisker plots for the silt fraction.

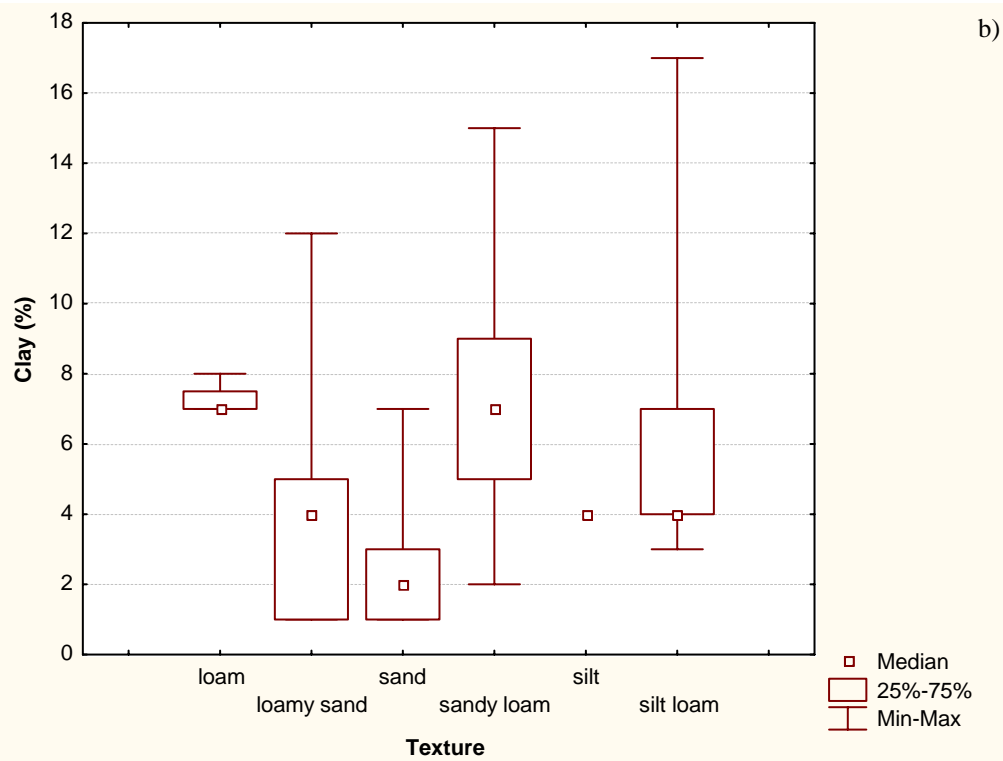
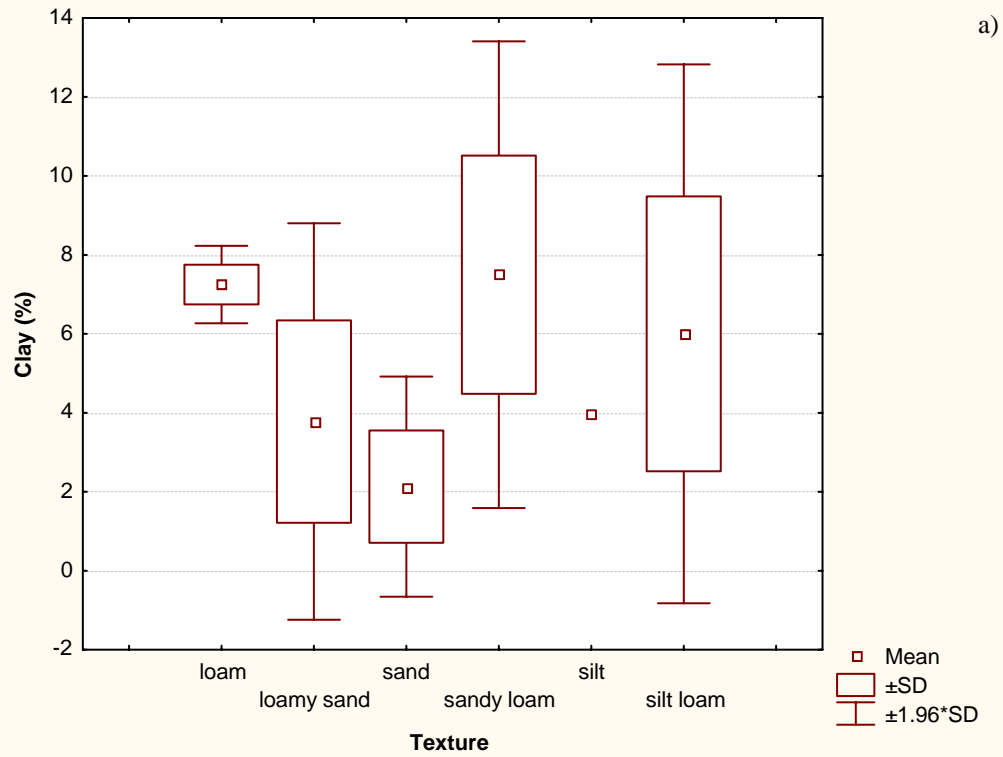


Figure 4.2.9a-b. Categorized box and whisker plots for the clay fraction.

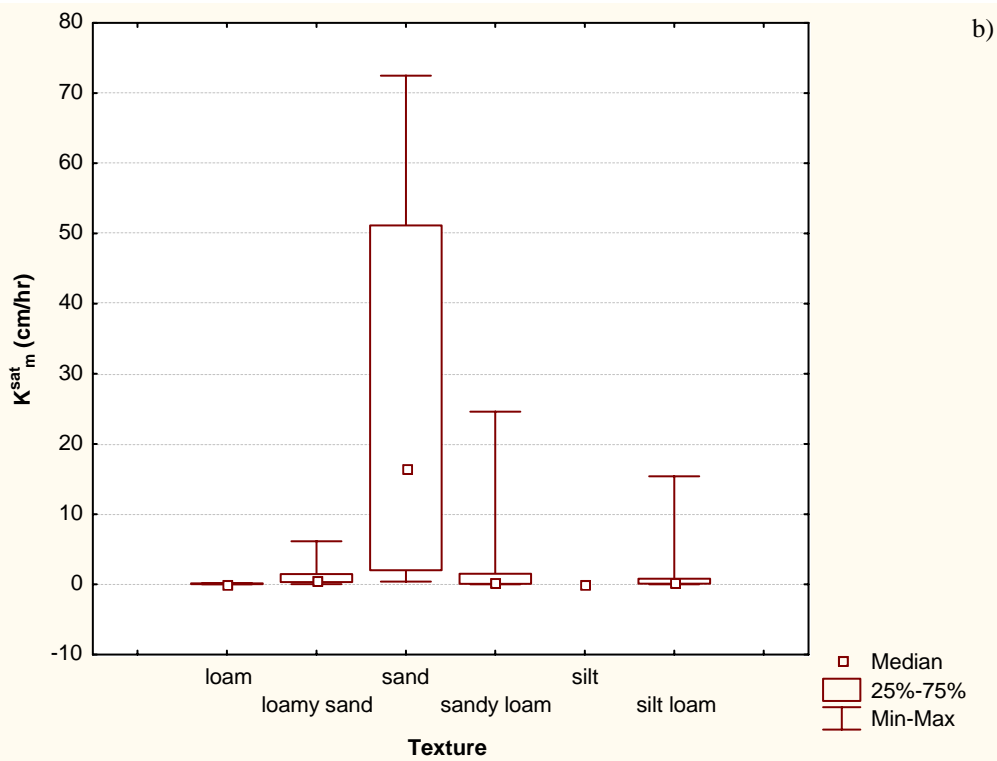
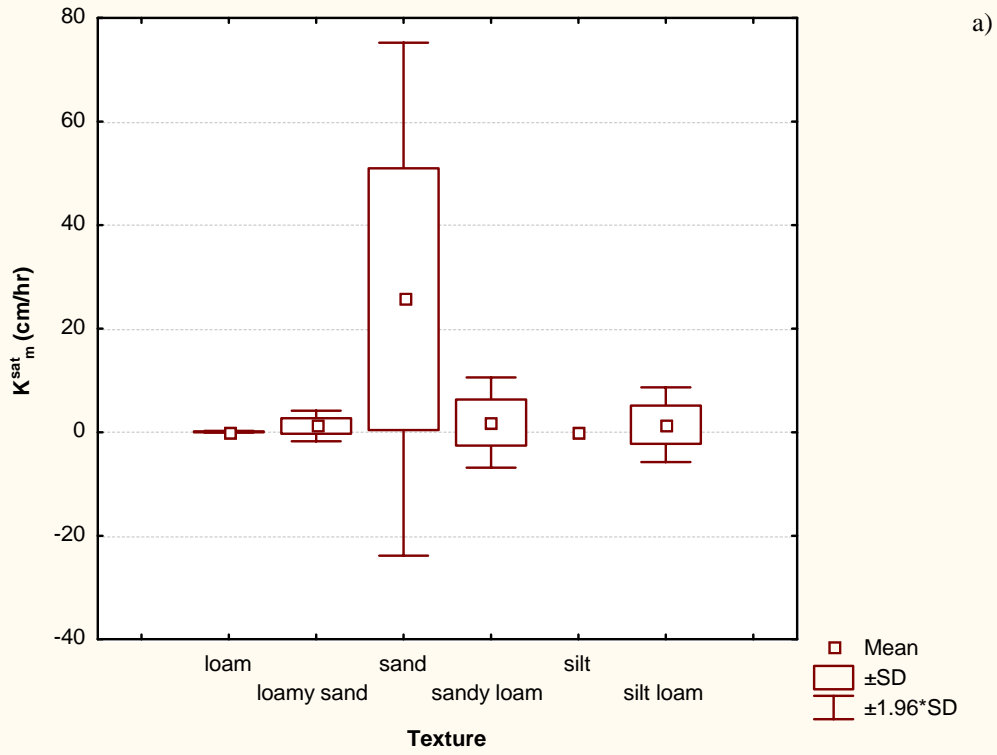


Figure 4.2.10a-b. Categorized box and whisker plots for unsaturated hydraulic conductivity.

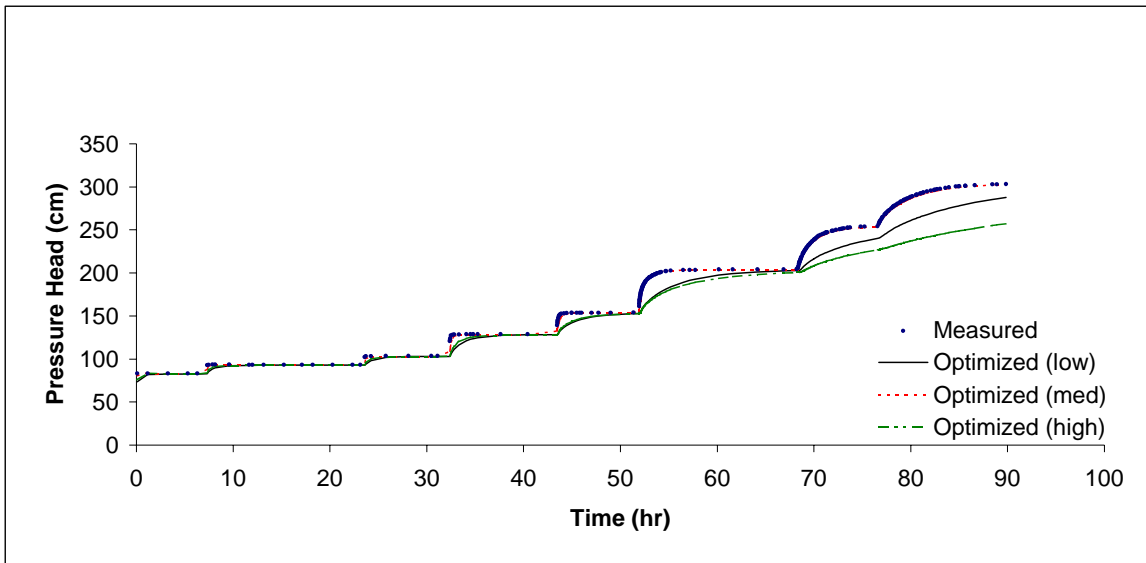
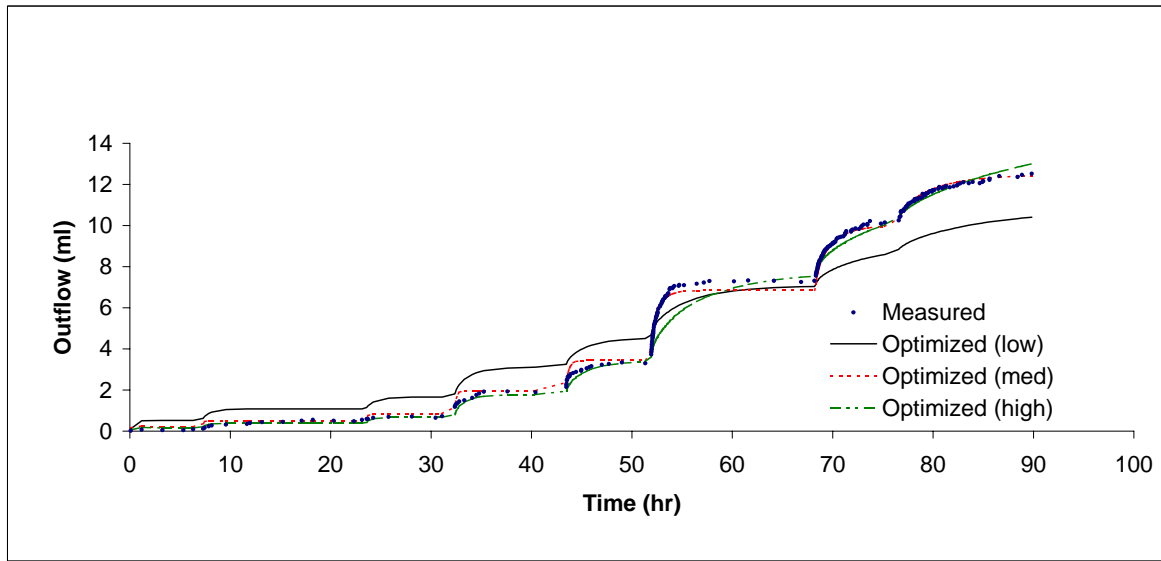


Figure 4.3.1a-b. Multi-step outflow experiment results and optimized curves for a sample with transient data.

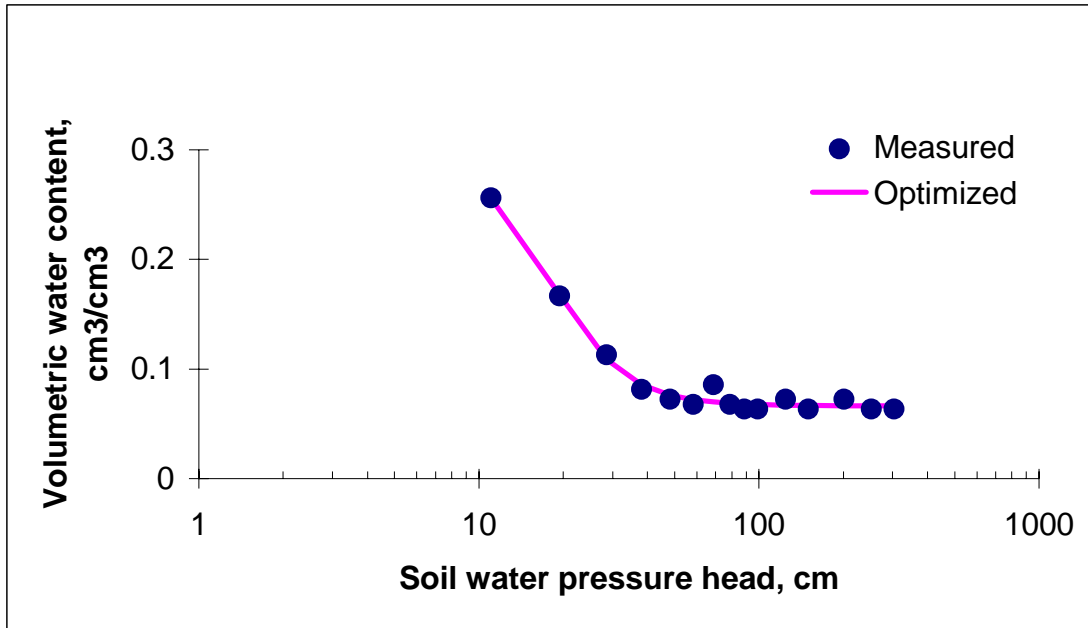
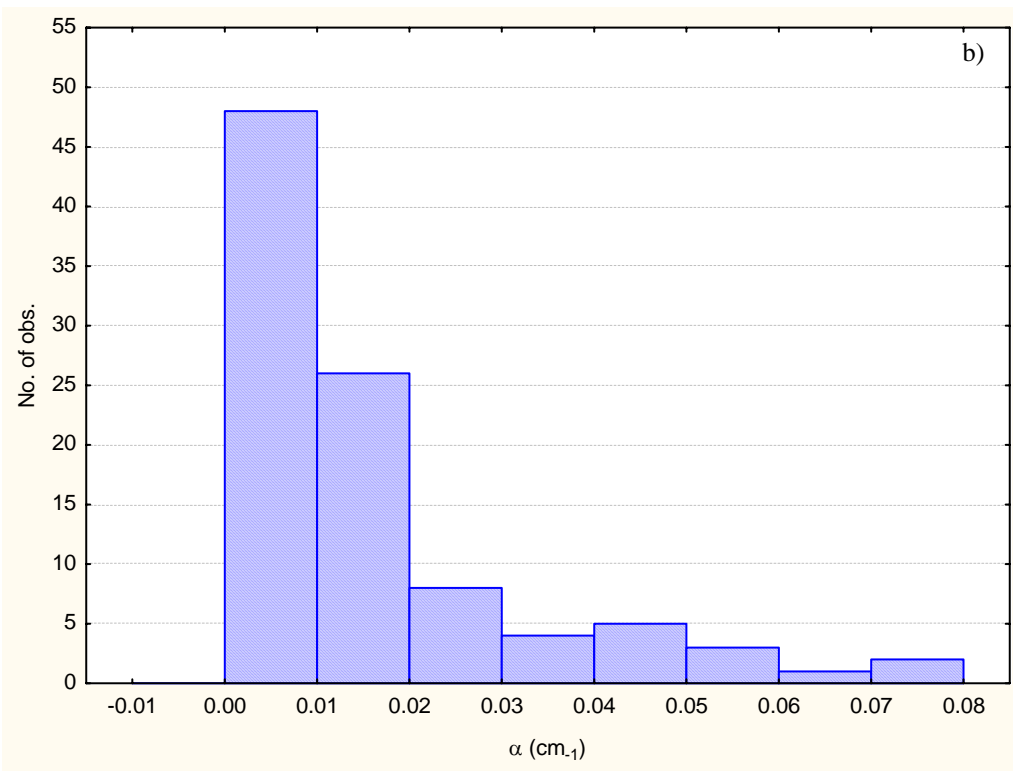
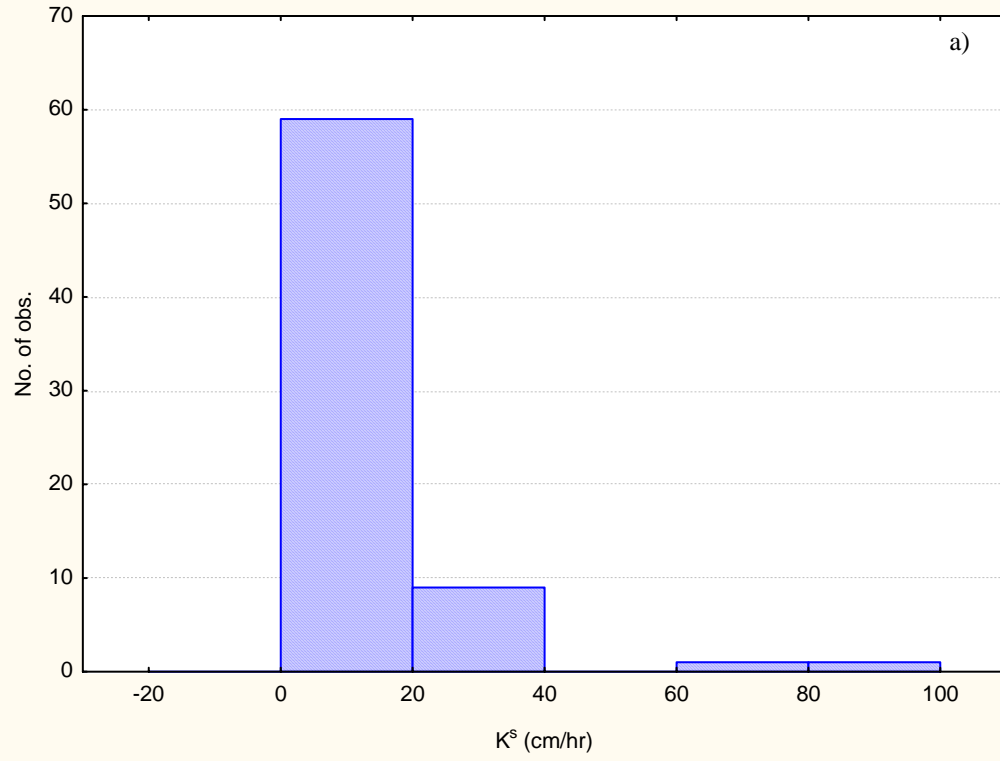


Figure 4.3.2. Multi-step outflow results and optimized curve for a sample with steady state data.



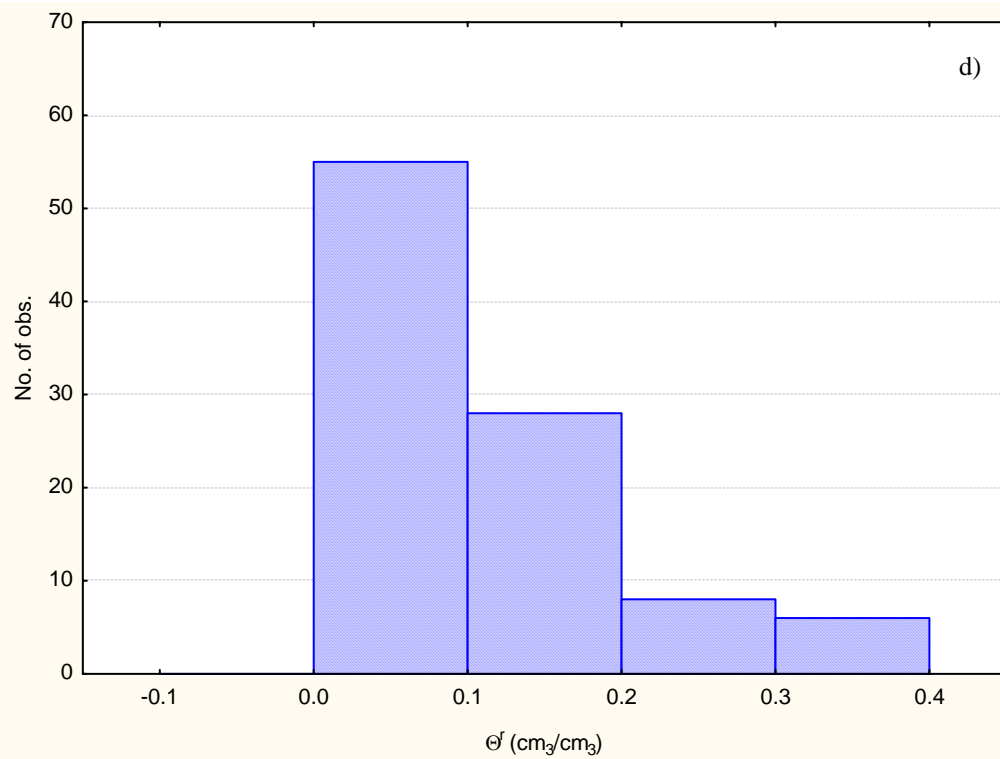
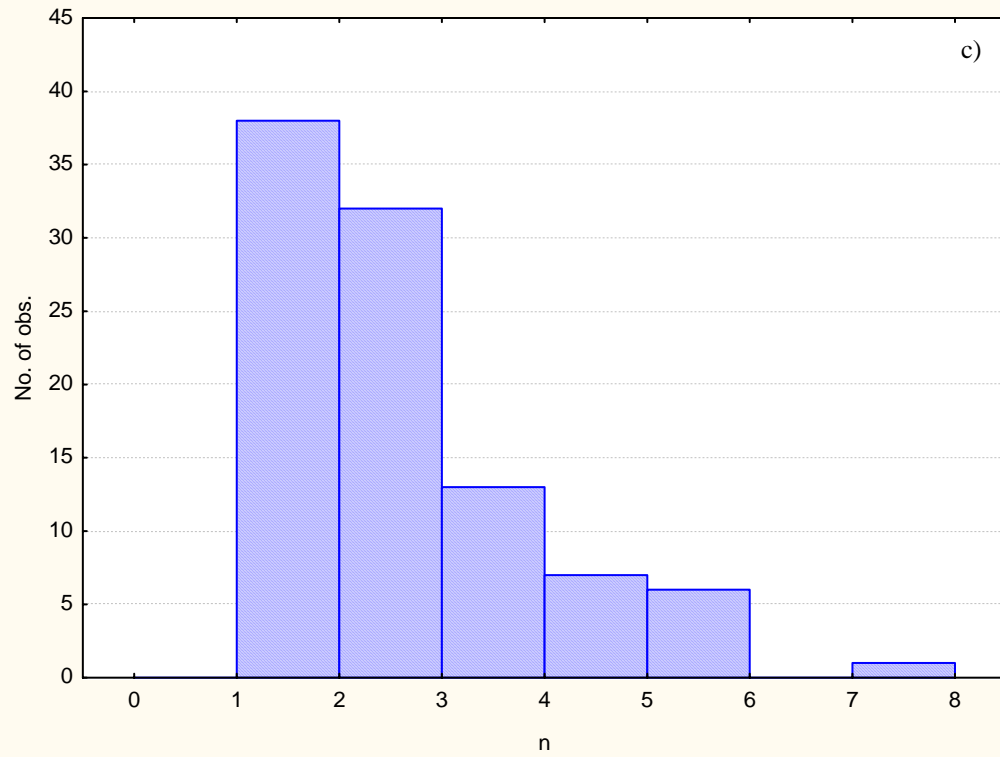
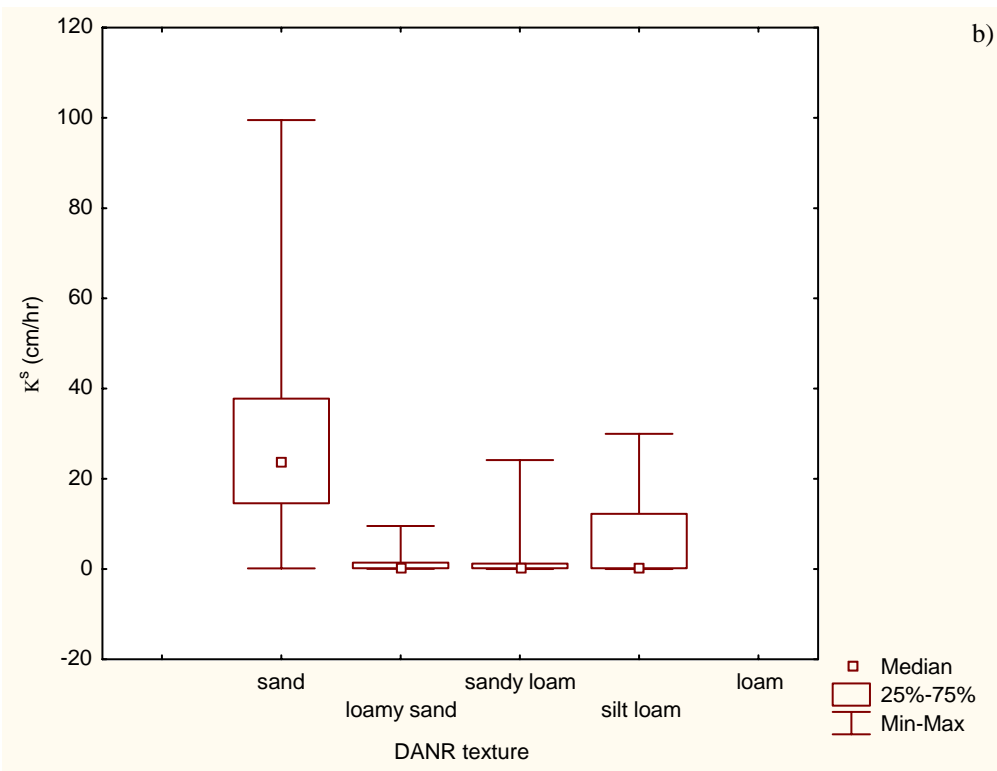
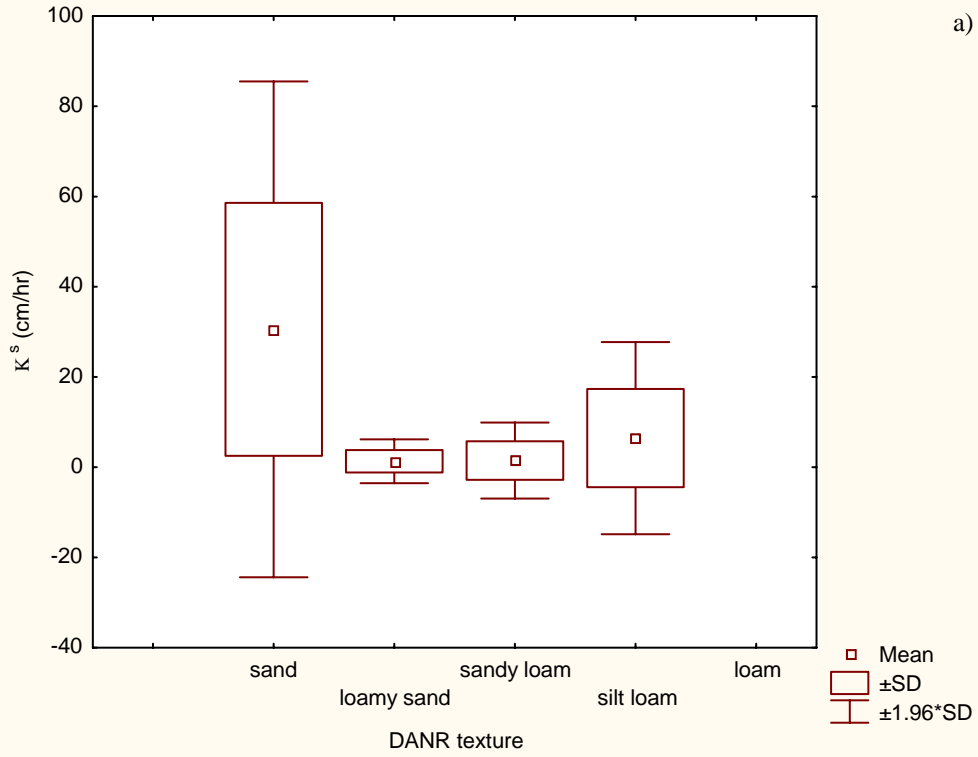
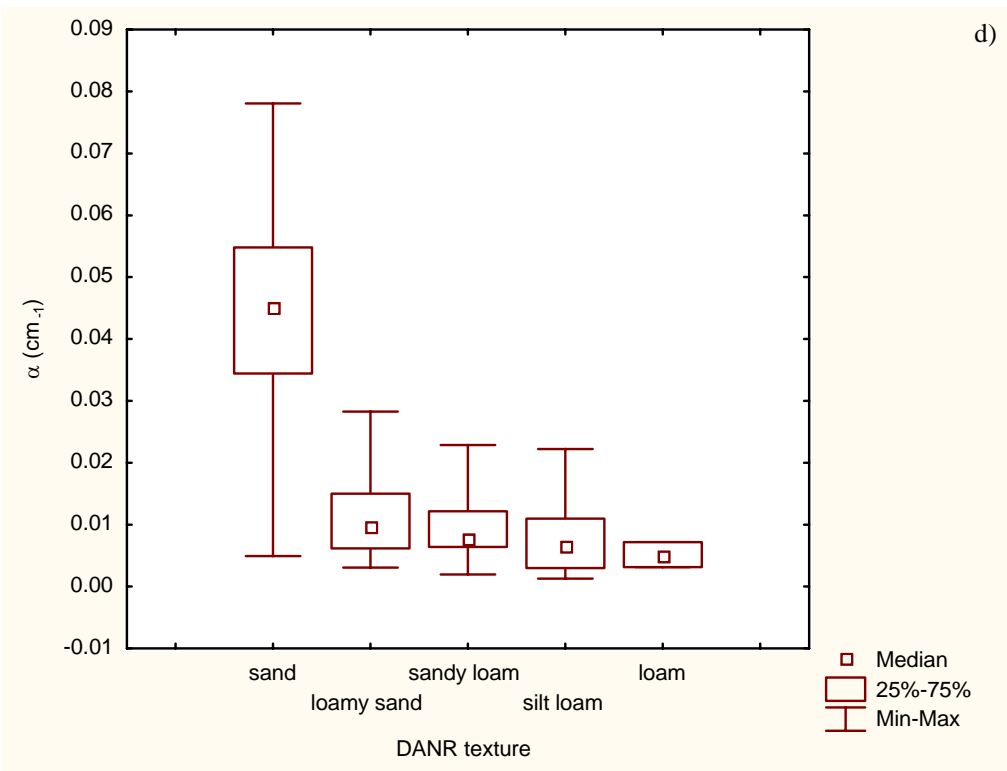
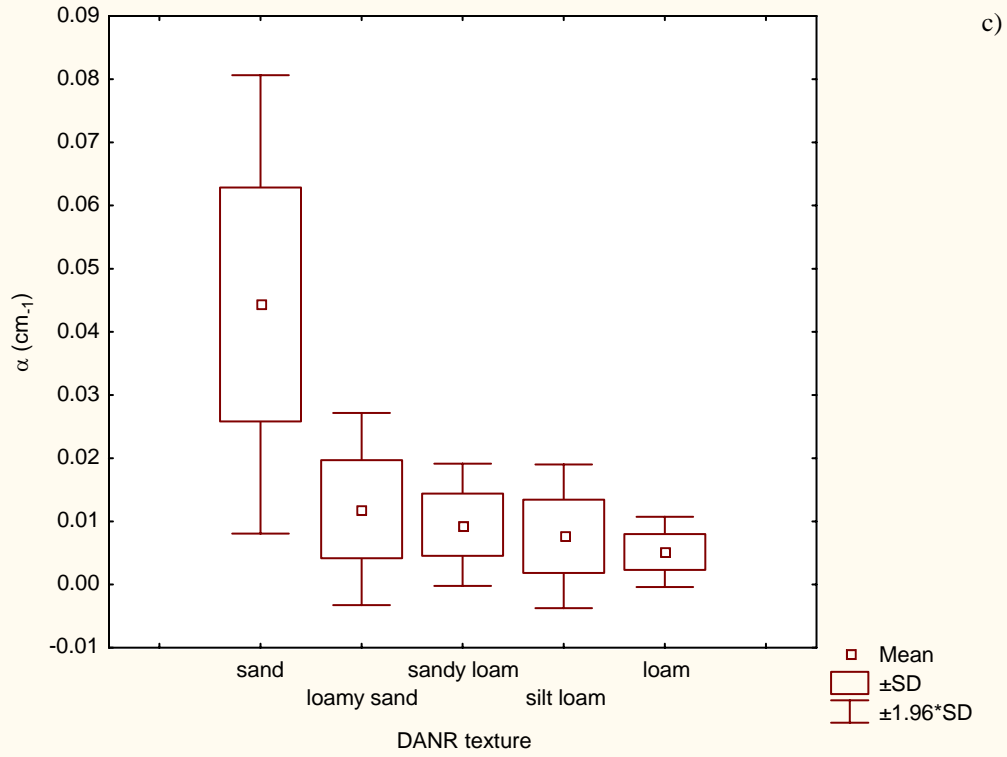
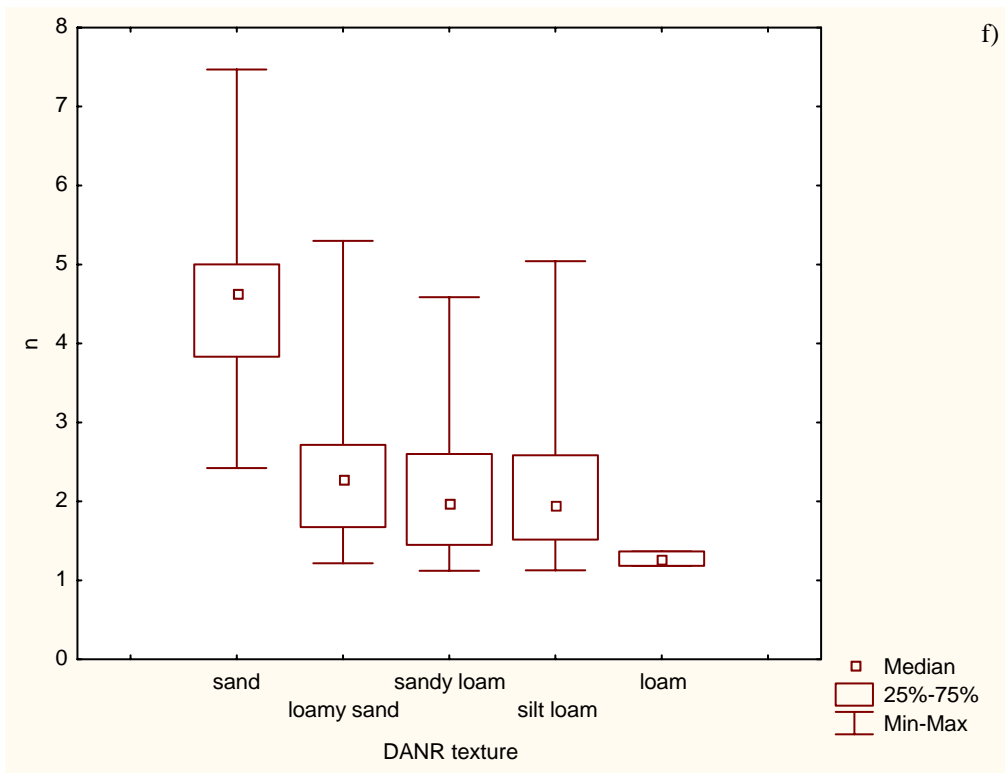
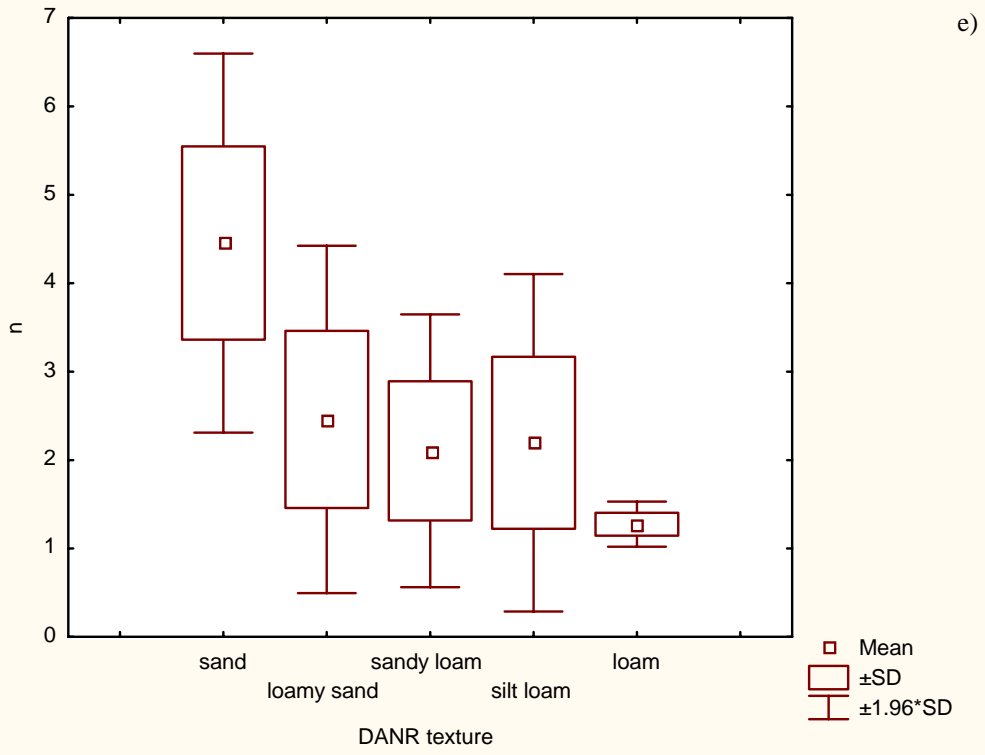


Figure 4.3.3a-d. Histograms for the van Genuchten parameters for the 97 samples.







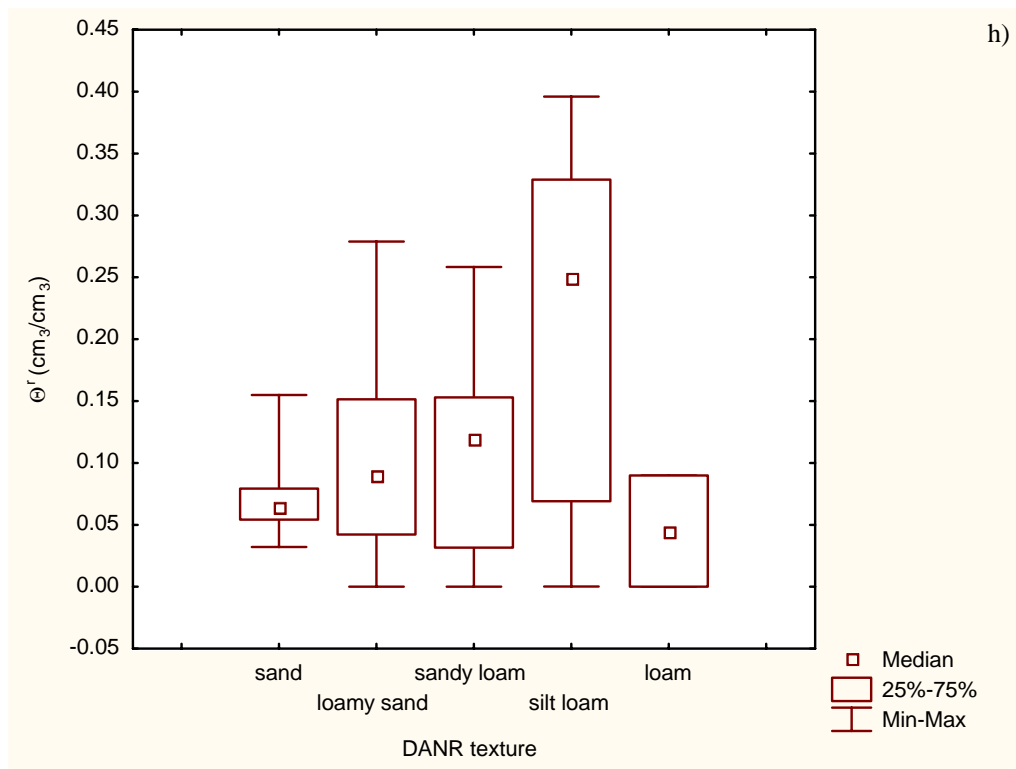
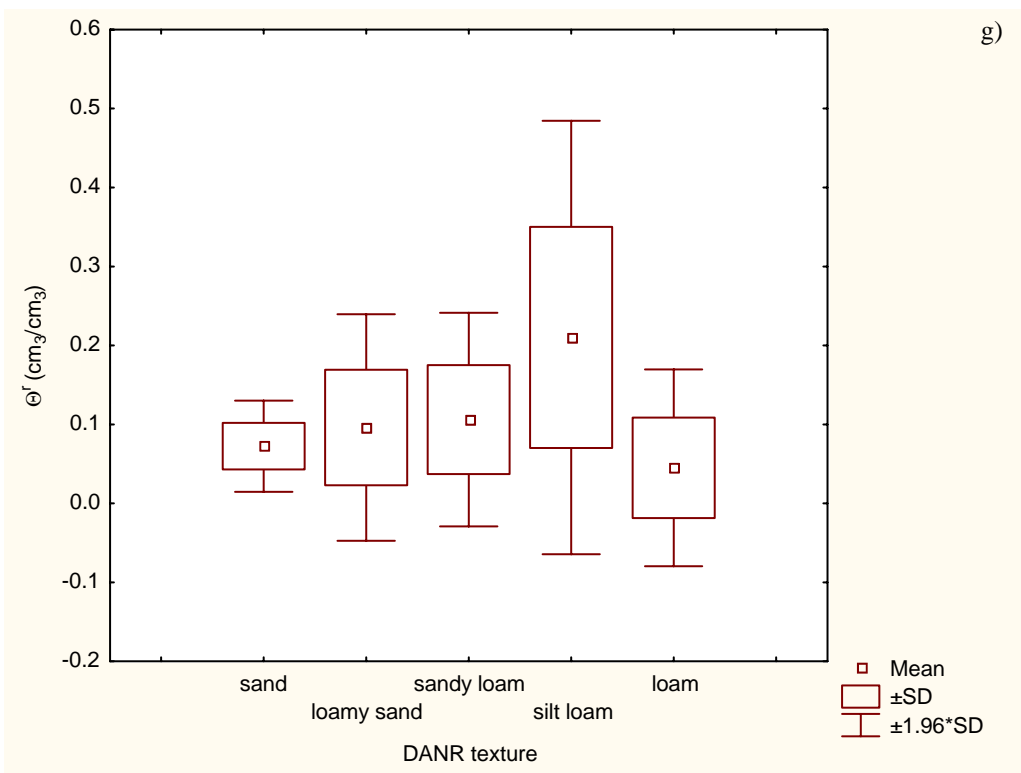
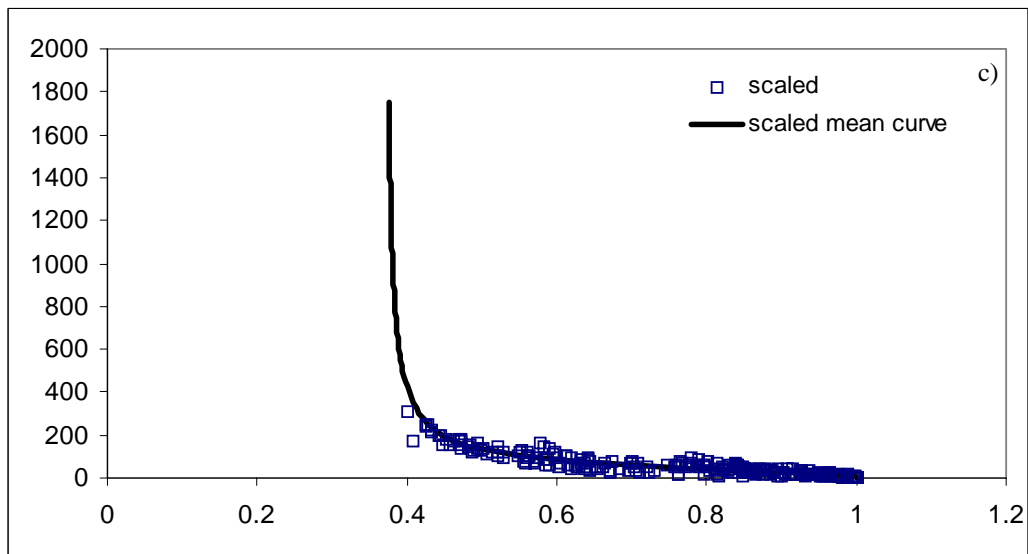
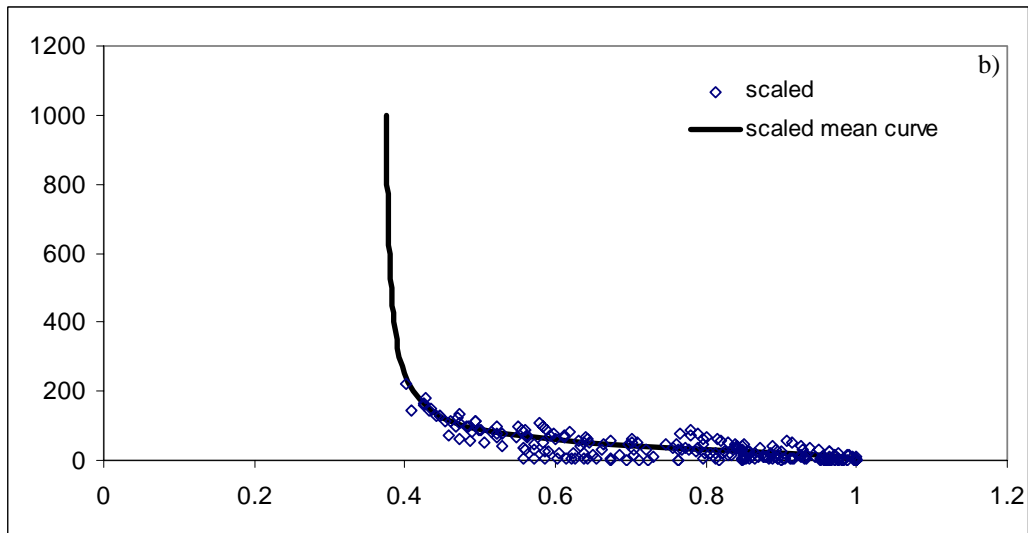
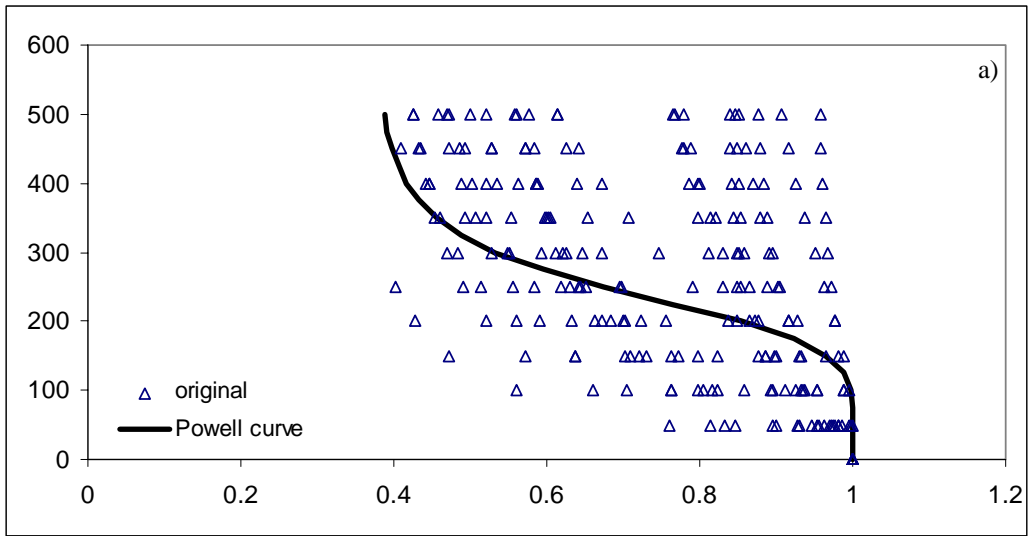


Figure 4.3.4a-h. Categorized box and whisker plot for the van Genuchten parameters.



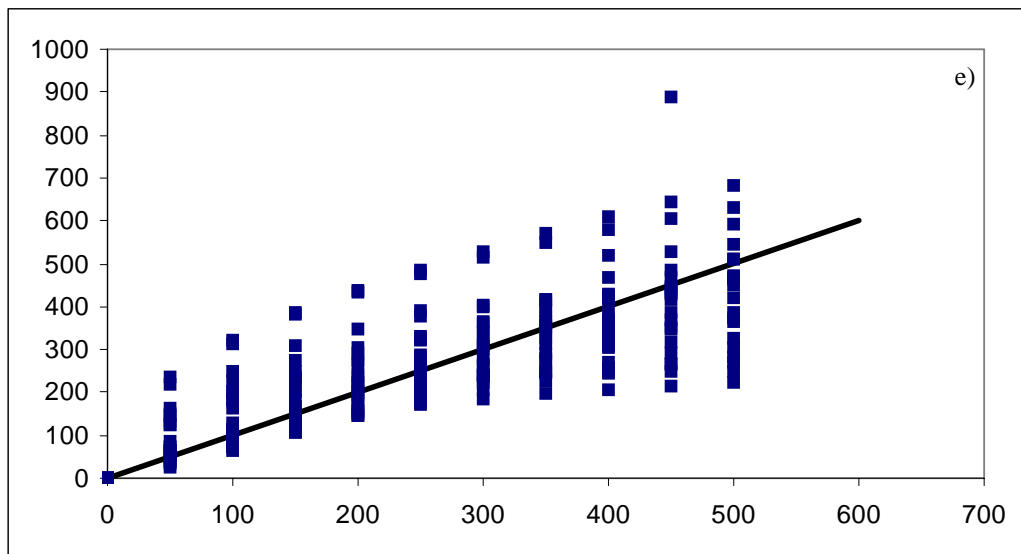
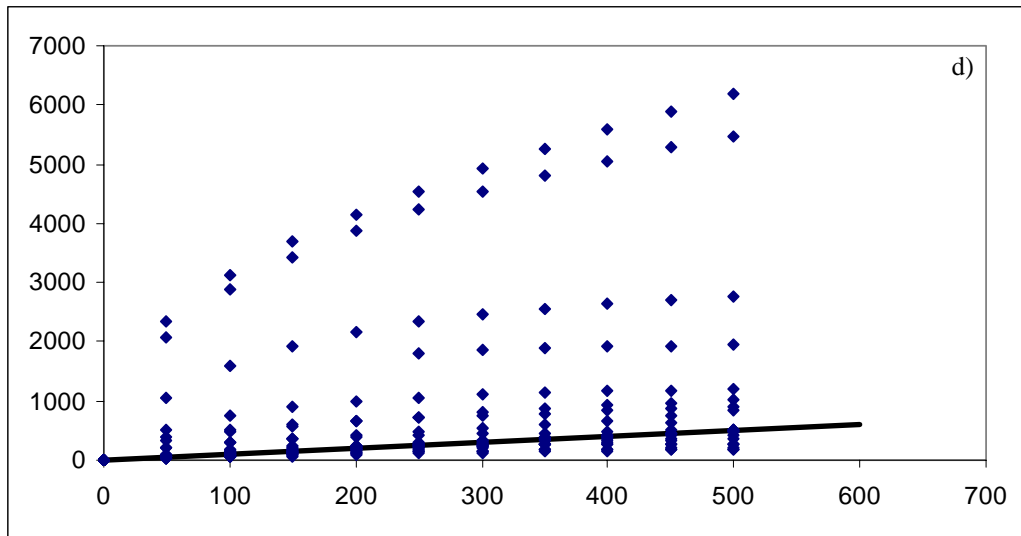
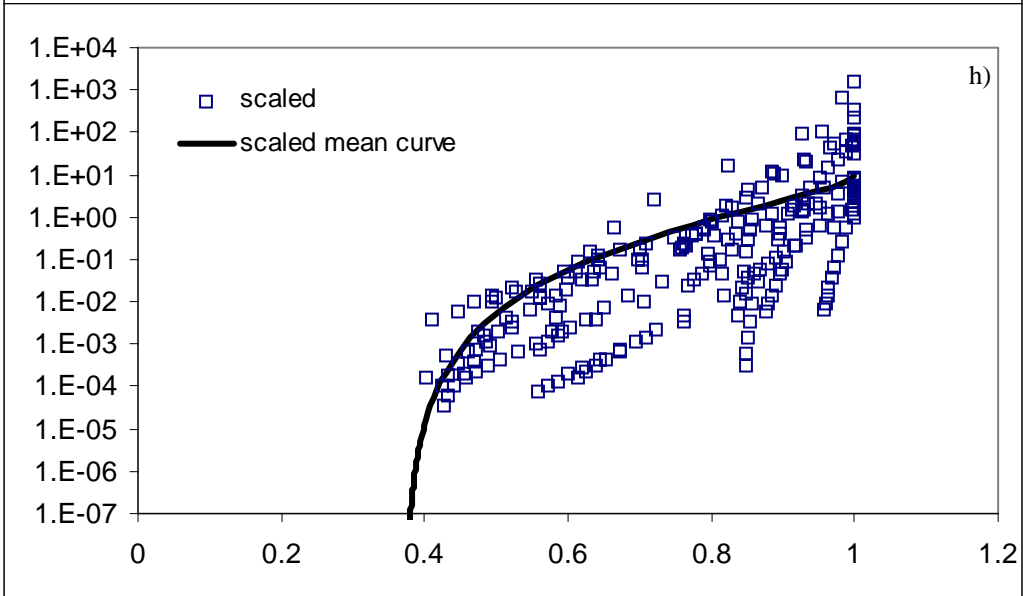
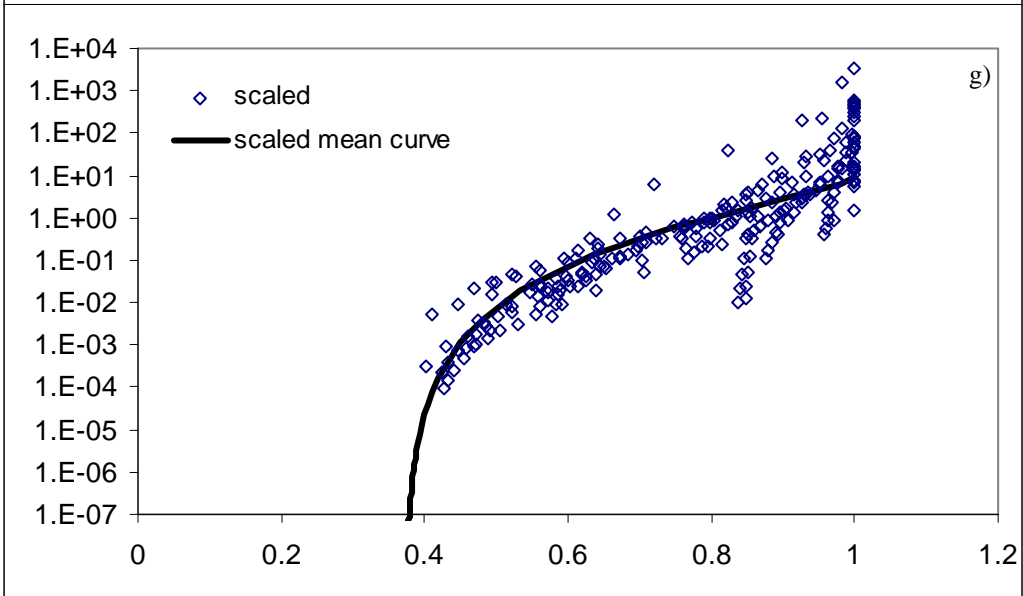
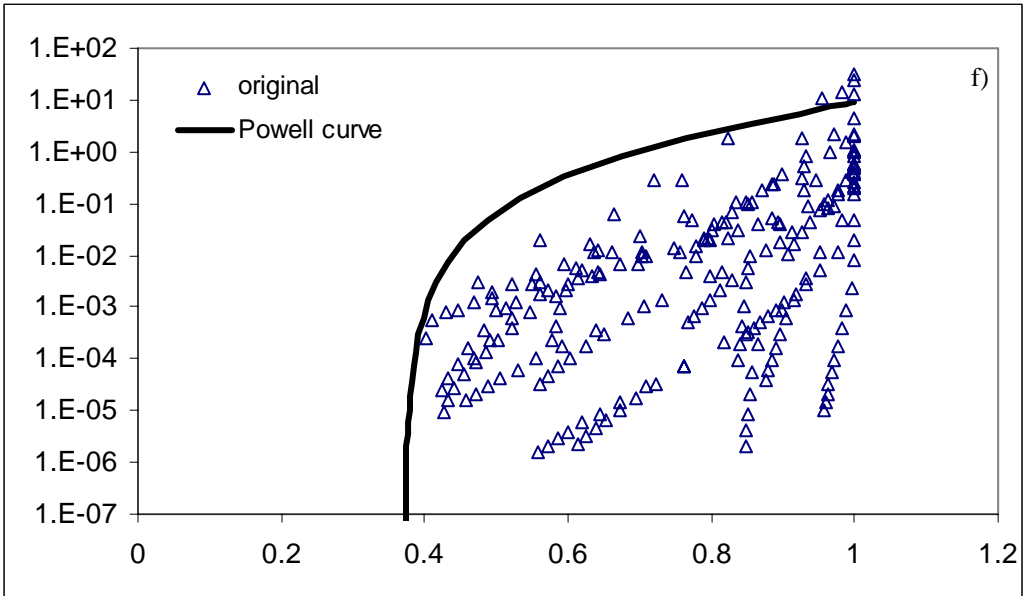


Figure 4.5.1a-e. Soil water retention (a) unscaled, (b) scaled using method 1, and (c) scaled using method 2. Original and de-scaled soil water pressure head using method 1 (d) and method 2 (e). All curves represent Group 1, Population 1.



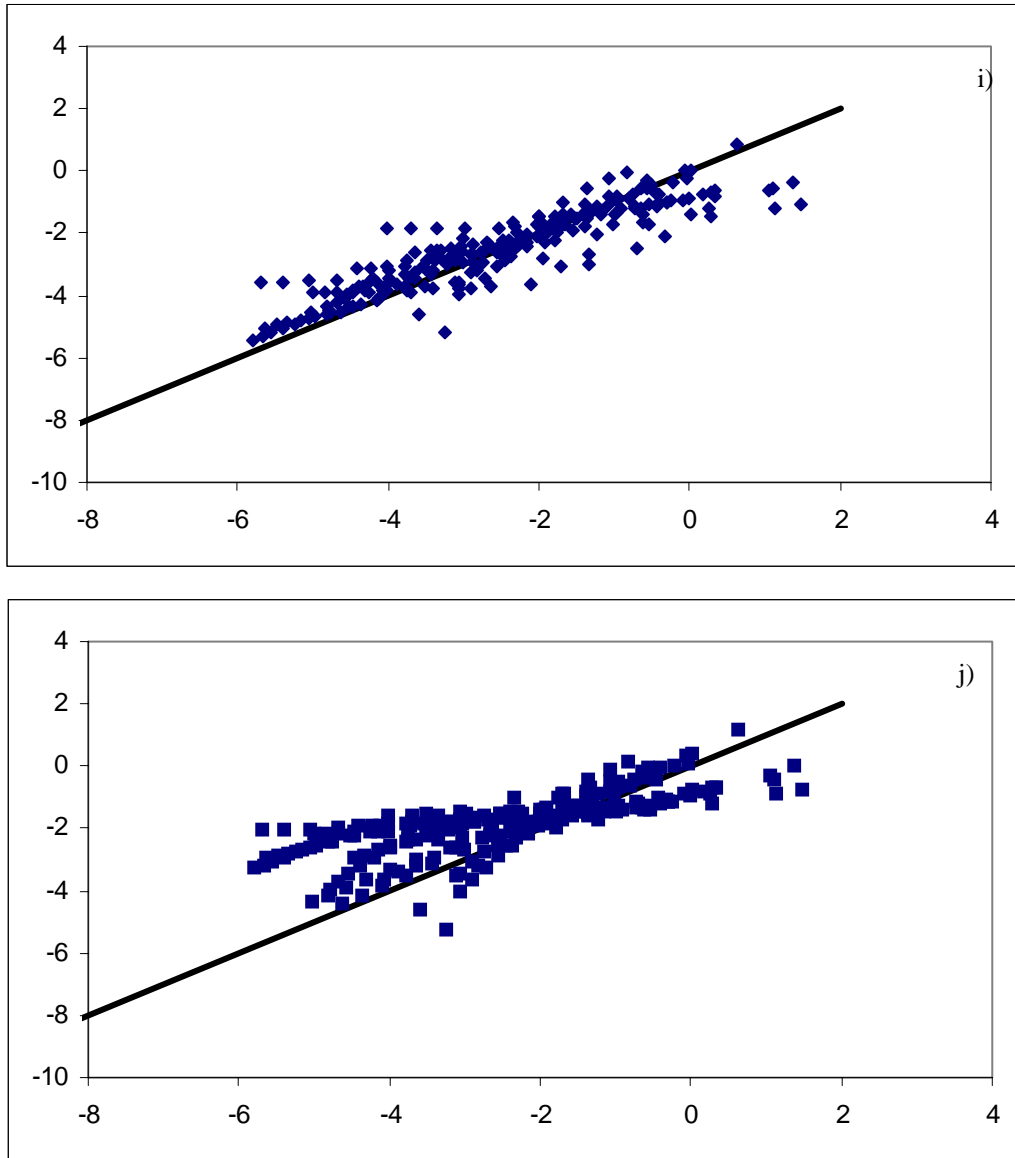
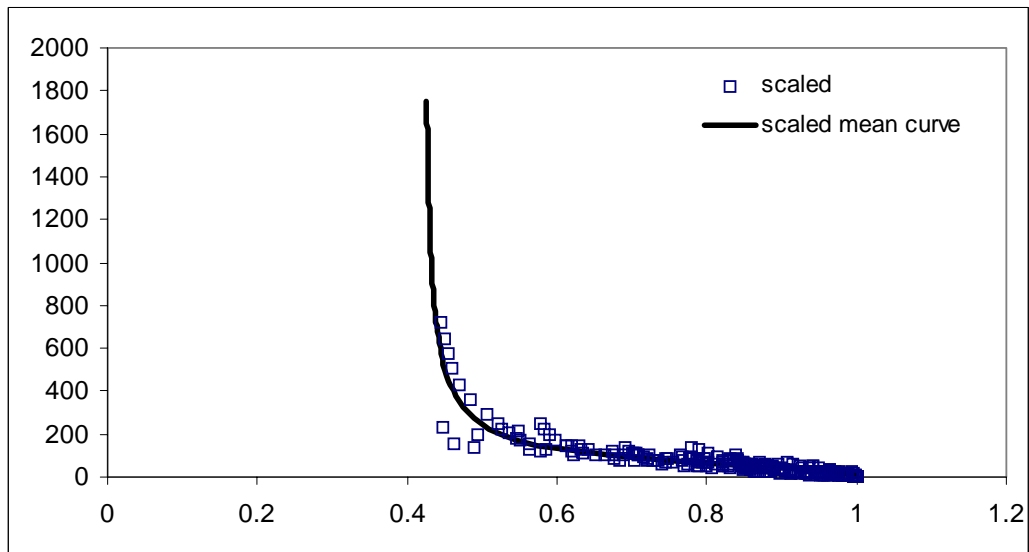
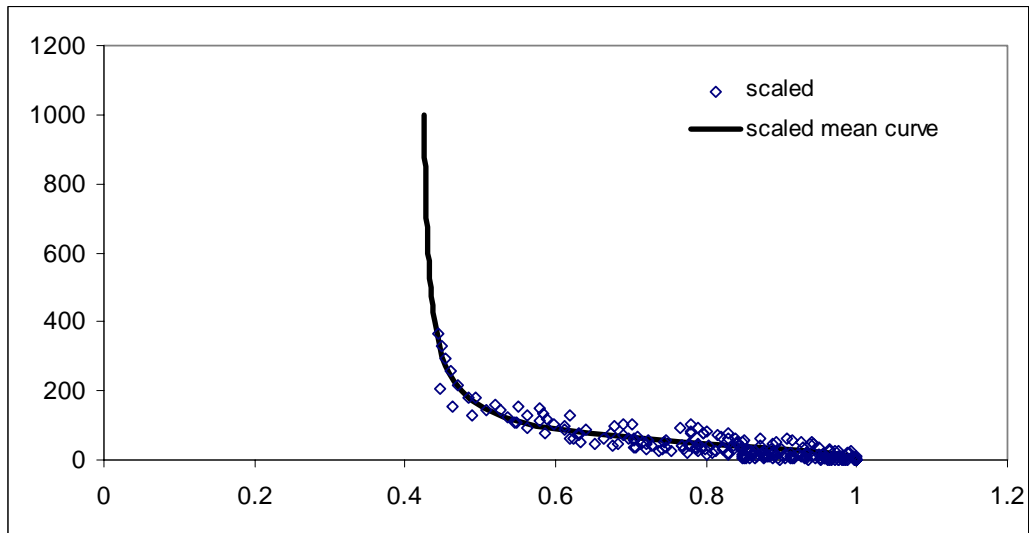
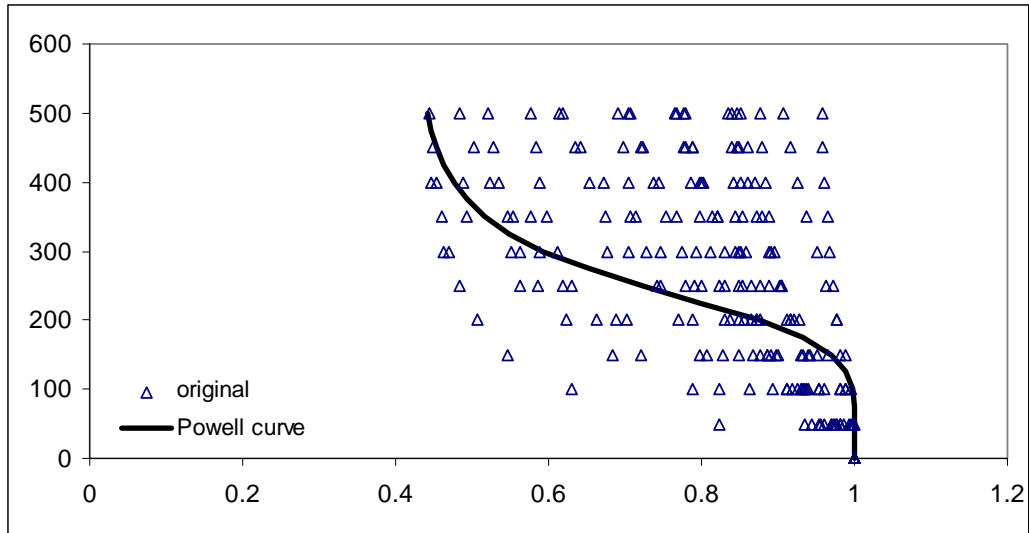


Figure 4.5.1f-j. Unsaturated hydraulic conductivity (f) unscaled, (g) scaled using method 1, and (h) scaled using method 2. Original and de-scaled unsaturated hydraulic conductivity using method 1 (i) and method 2 (j). All curves represent Group 1, Population 1.



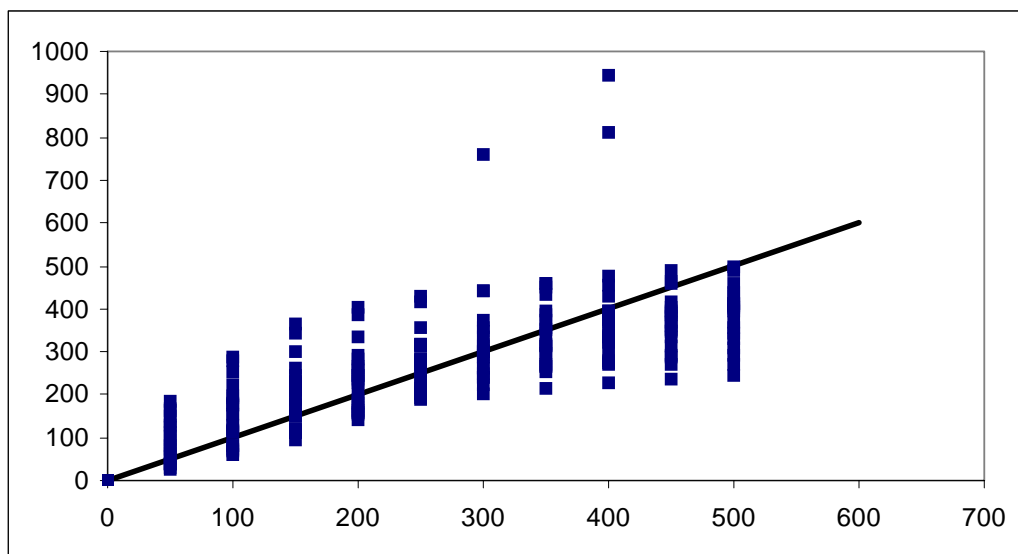
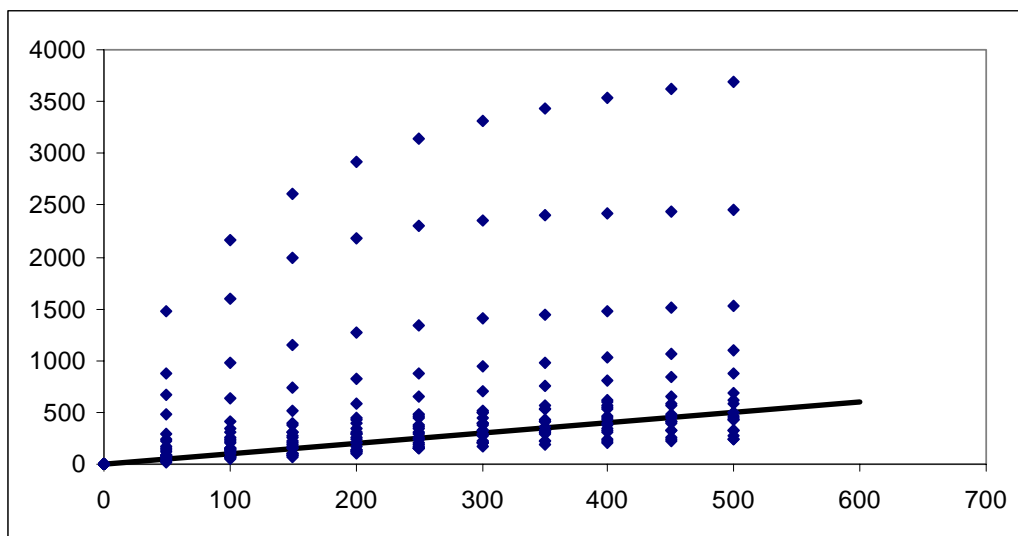
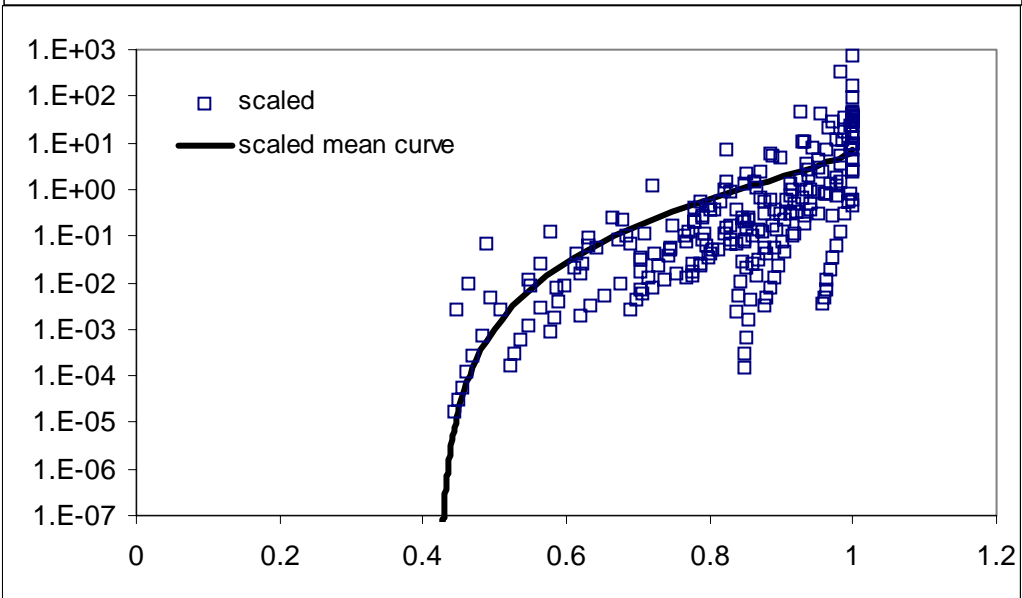
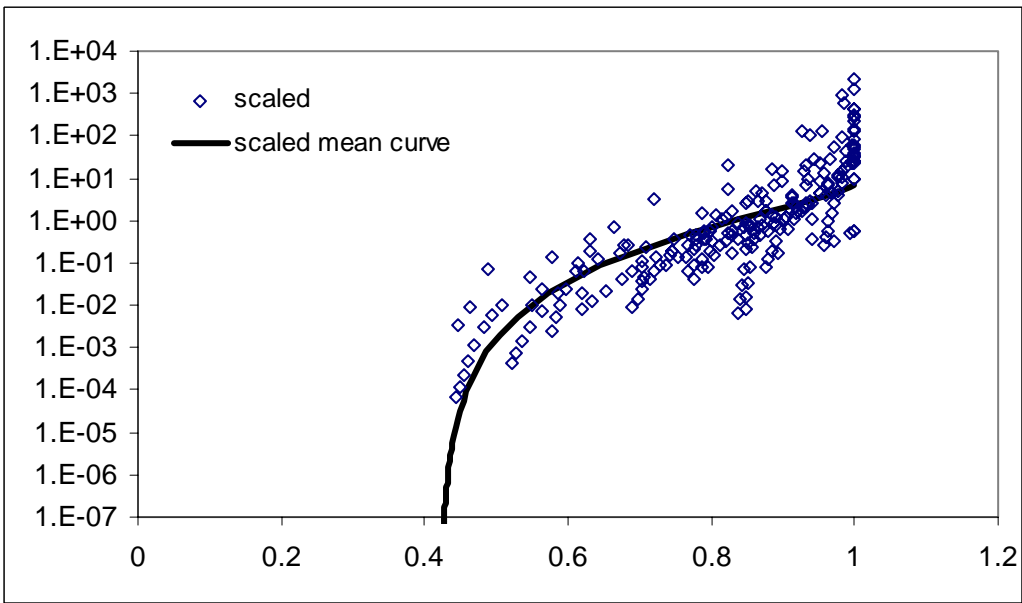
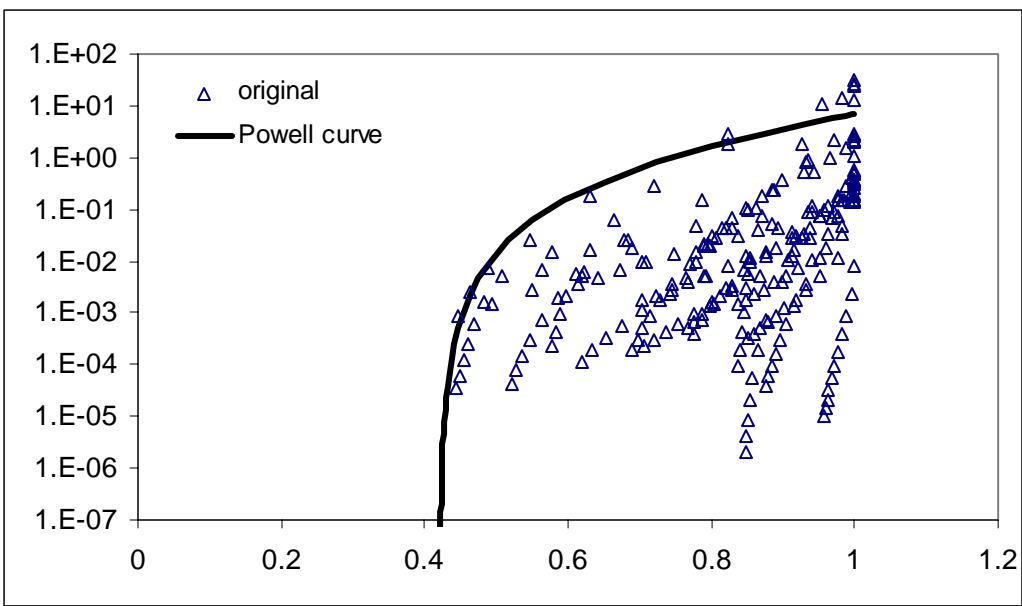


Figure 4.5.2a-e. Soil water retention (a) unscaled, (b) scaled using method 1, and (c) scaled using method 2. Original and de-scaled soil water pressure head using method 1 (d) and method 2 (e). All curves represent Group 2, Population 2.



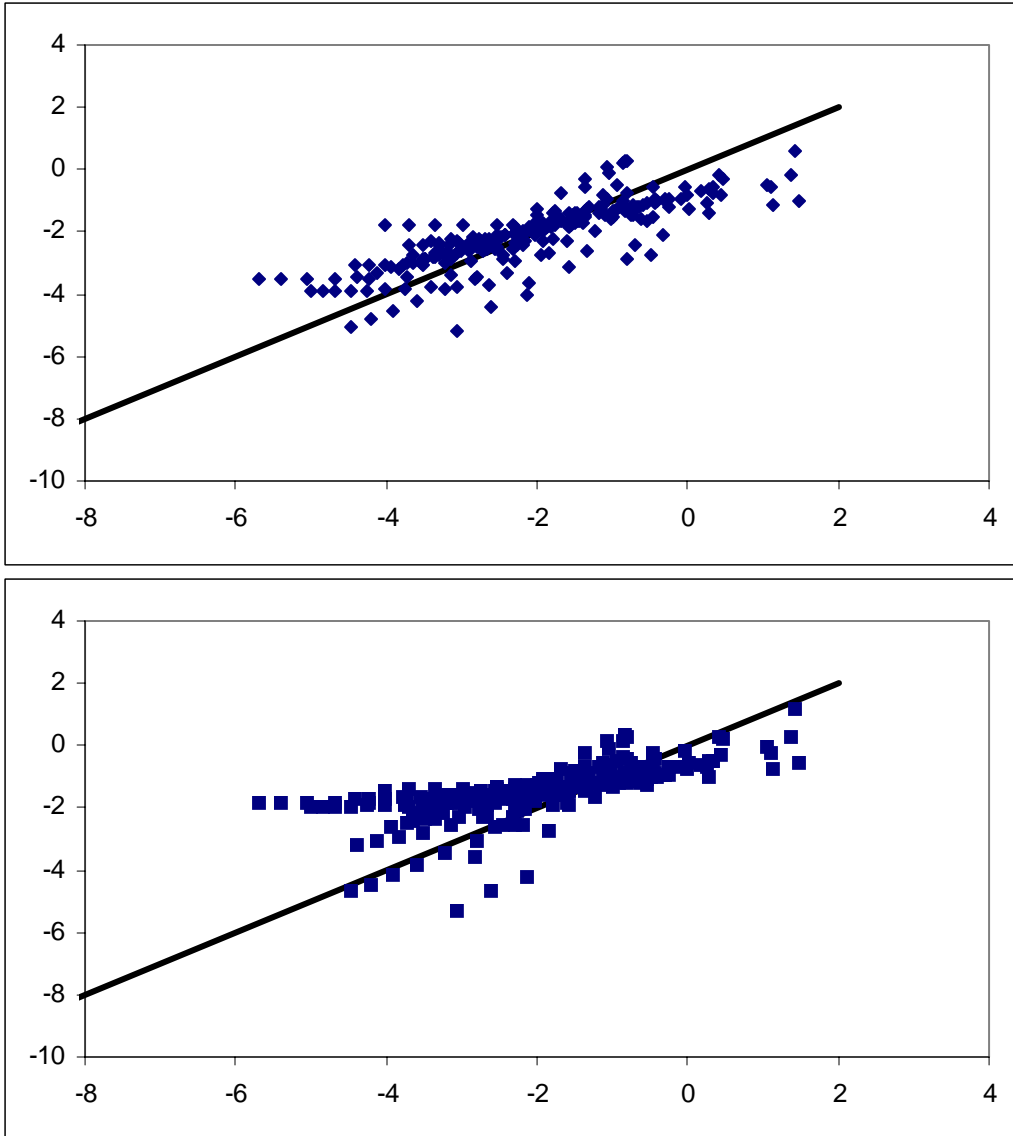
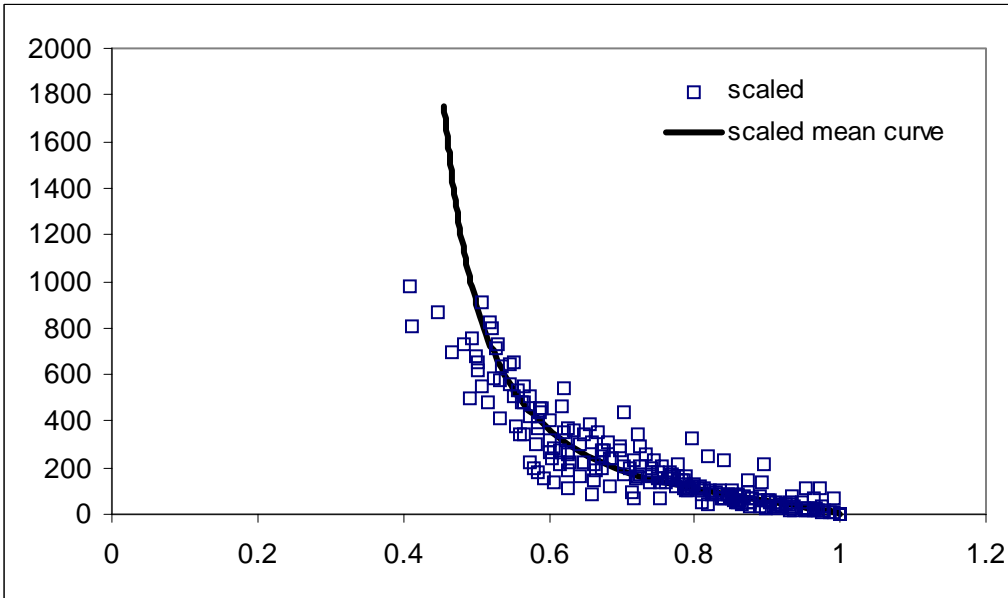
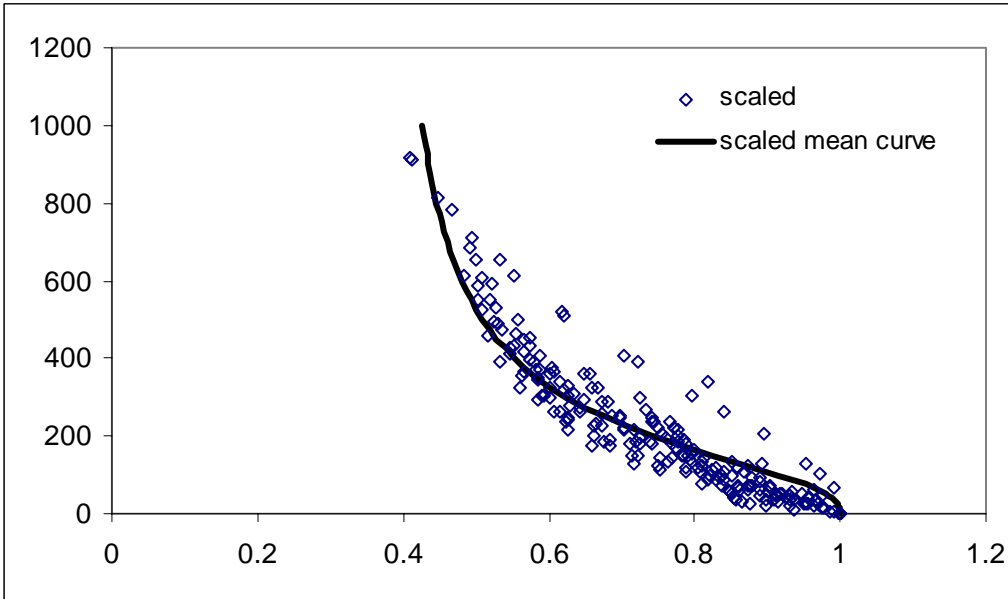
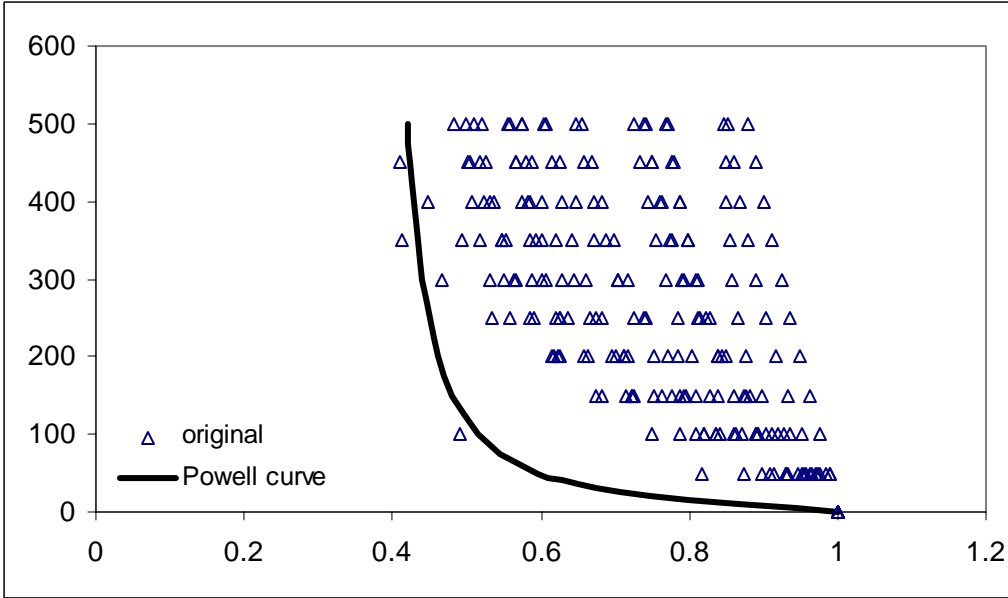


Figure 4.5.2f-j. Unsaturated hydraulic conductivity (f) unscaled, (g) scaled using method 1, and (h) scaled using method 2. Original and de-scaled unsaturated hydraulic conductivity using method 1 (i) and method 2 (j). All curves represent Group 2, Population 2.



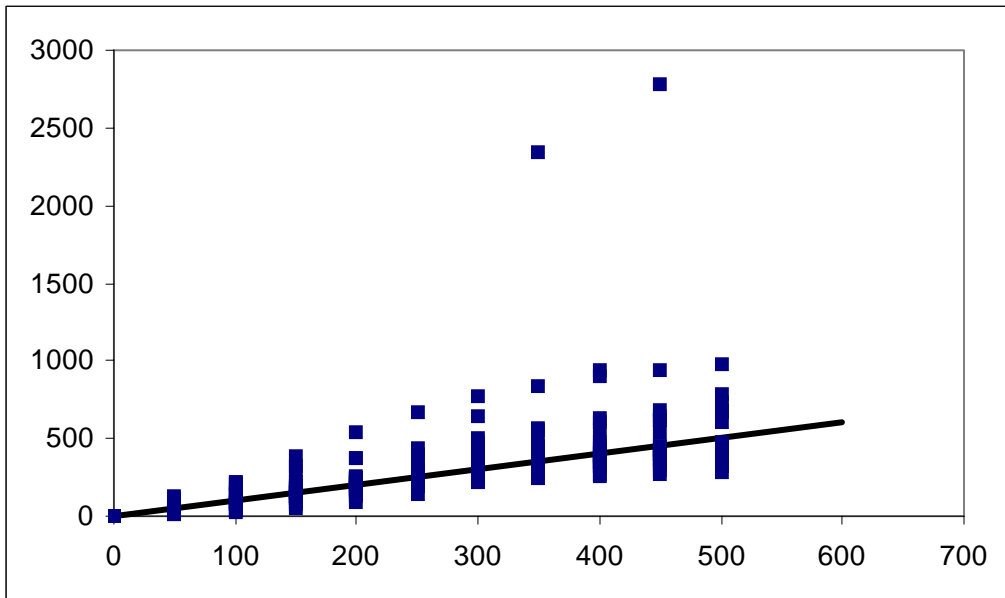
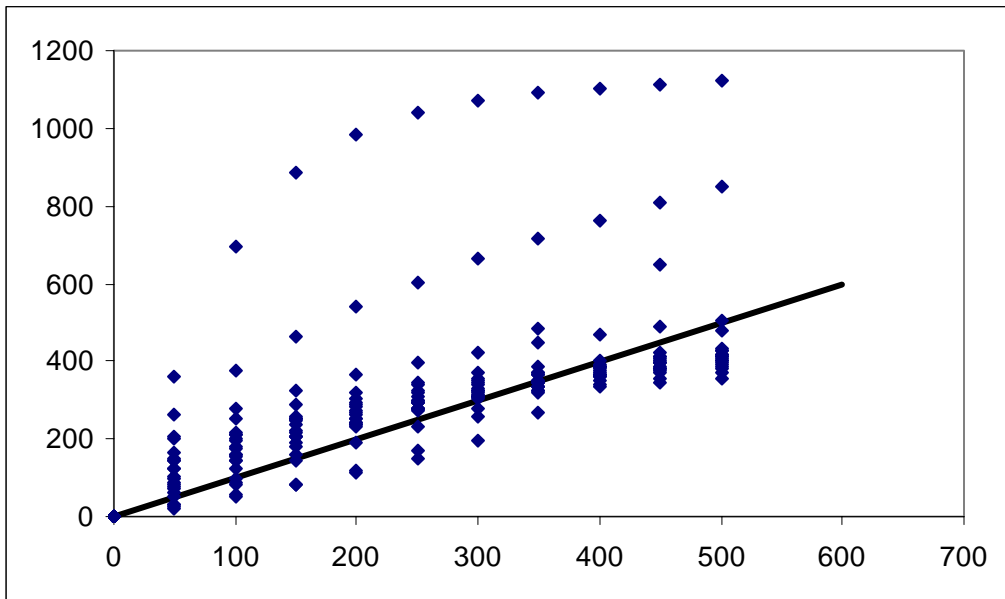
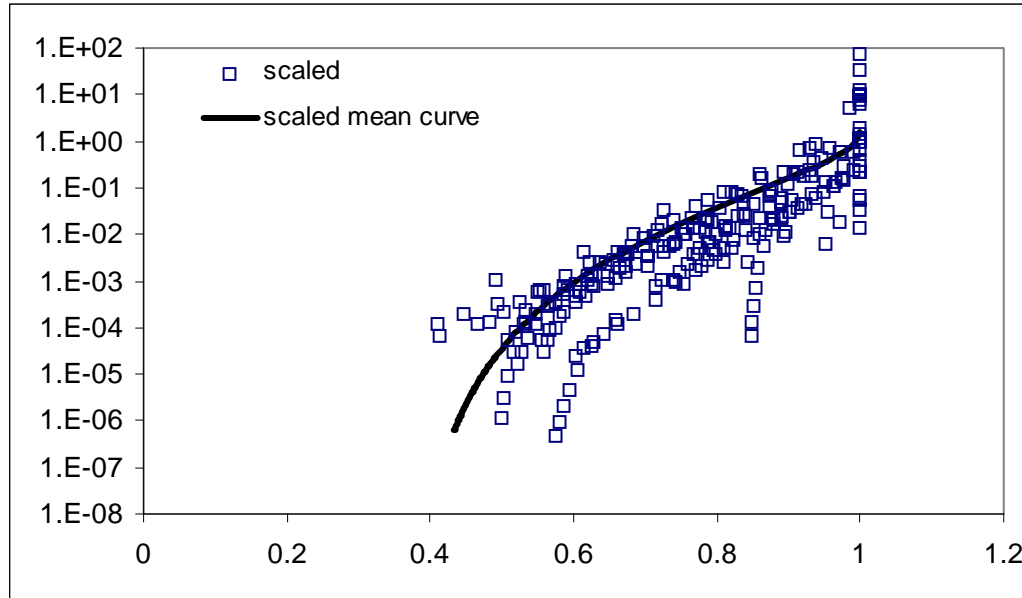
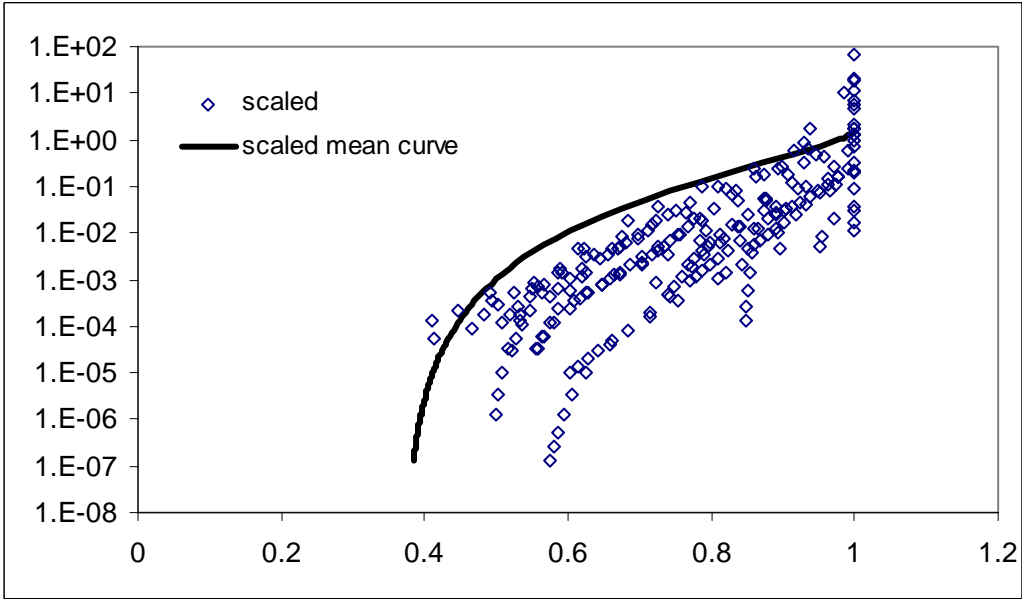
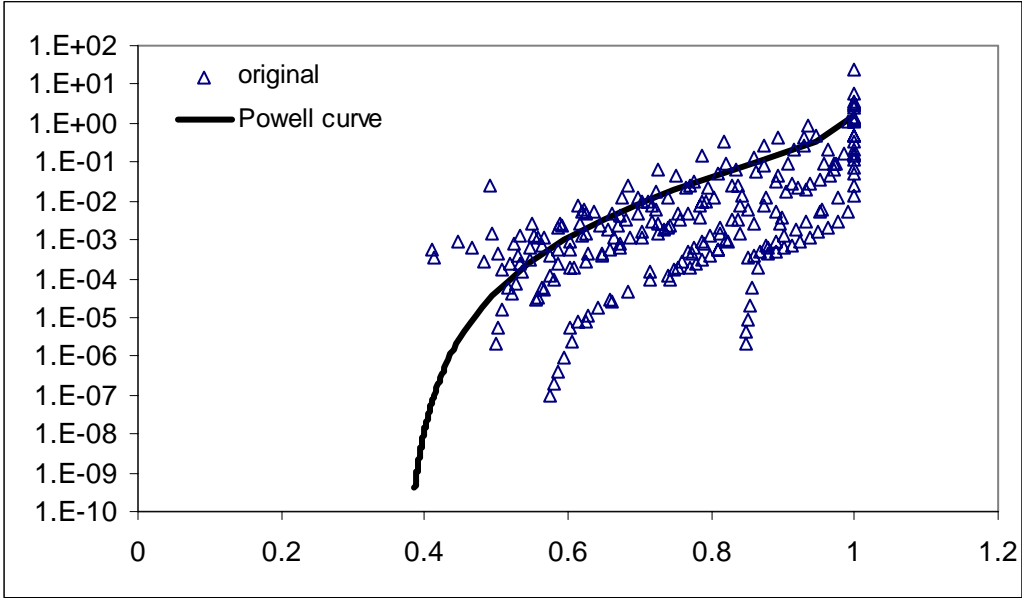


Figure 4.5.3a-e. Soil water pressure head (a)unscaled,(b) scaled using method 1, and (c) scaled using method 2. Original and descaled soil water pressure head using method 1(d) and method 2 (e). All curves represent Group 2, Population 1, subgroup sandy loam.



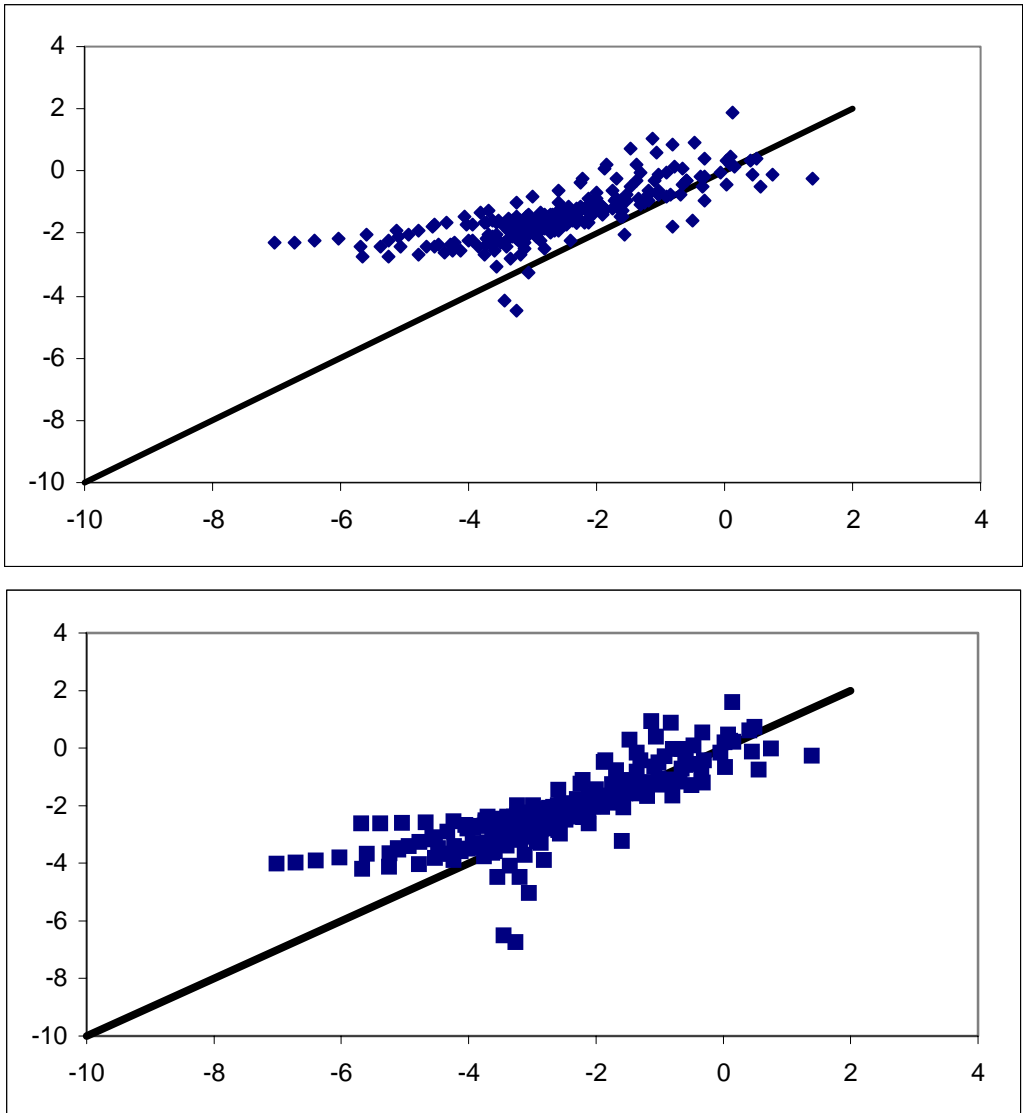
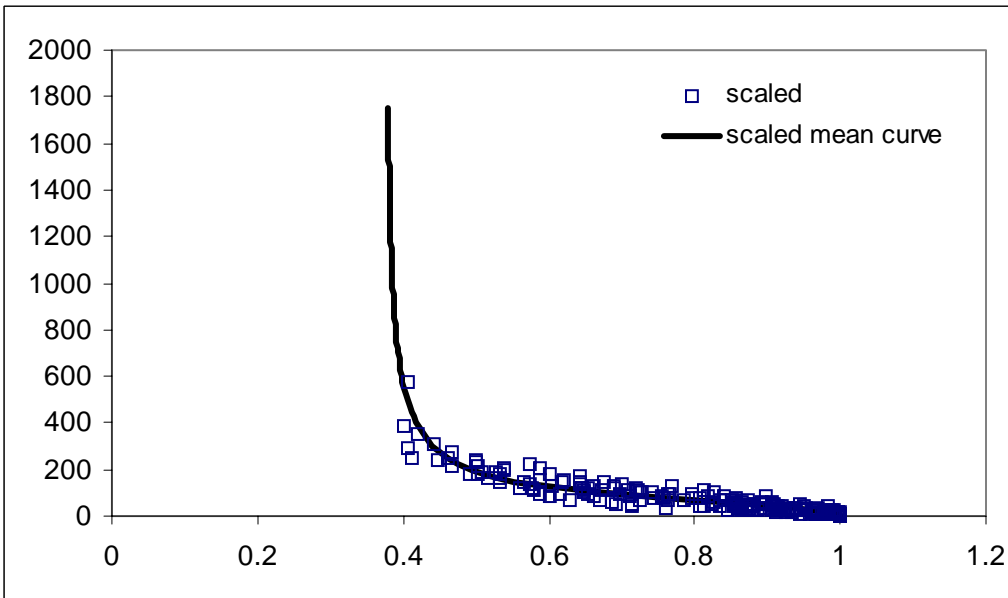
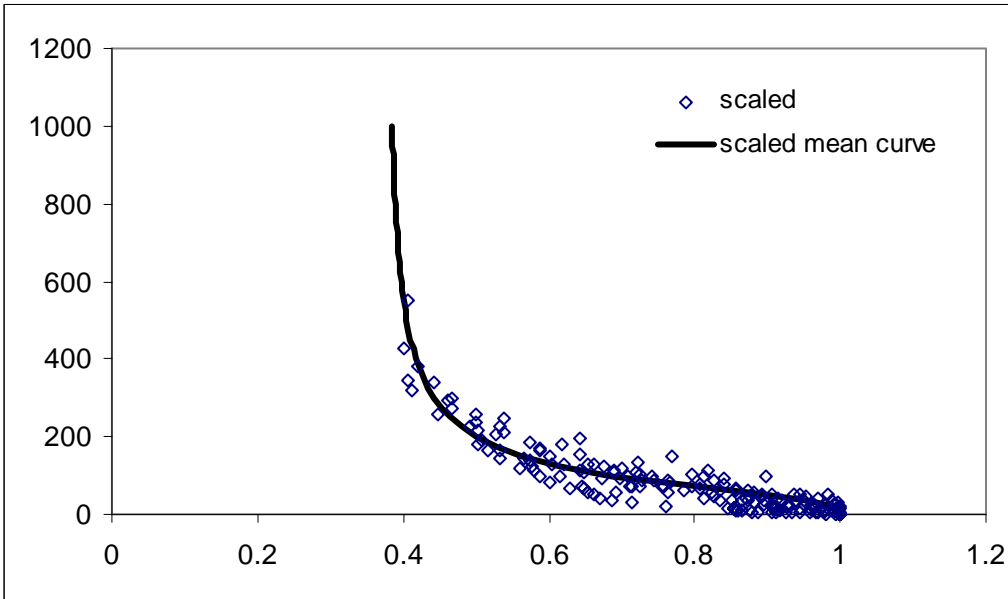
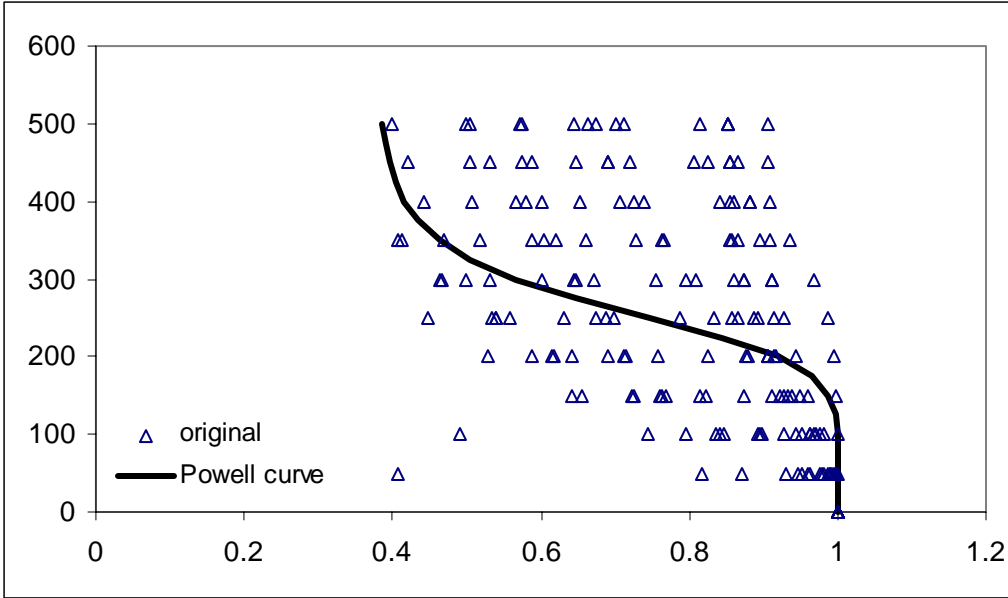


Figure 4.5.3f-j. Unsaturated hydraulic conductivity (f) unscaled, (g) scaled using method 1, and (h) scaled using method 2. Original and de-scaled unsaturated hydraulic conductivity using method 1 (i) and method 2 (j). All curves represent Group 2, Population 1, subgroup sandy loam.



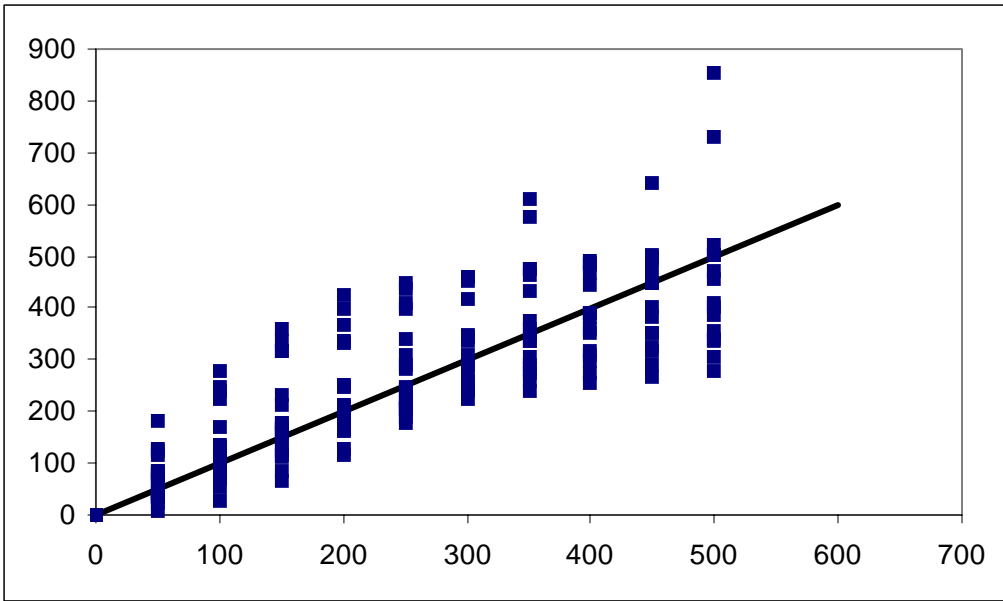
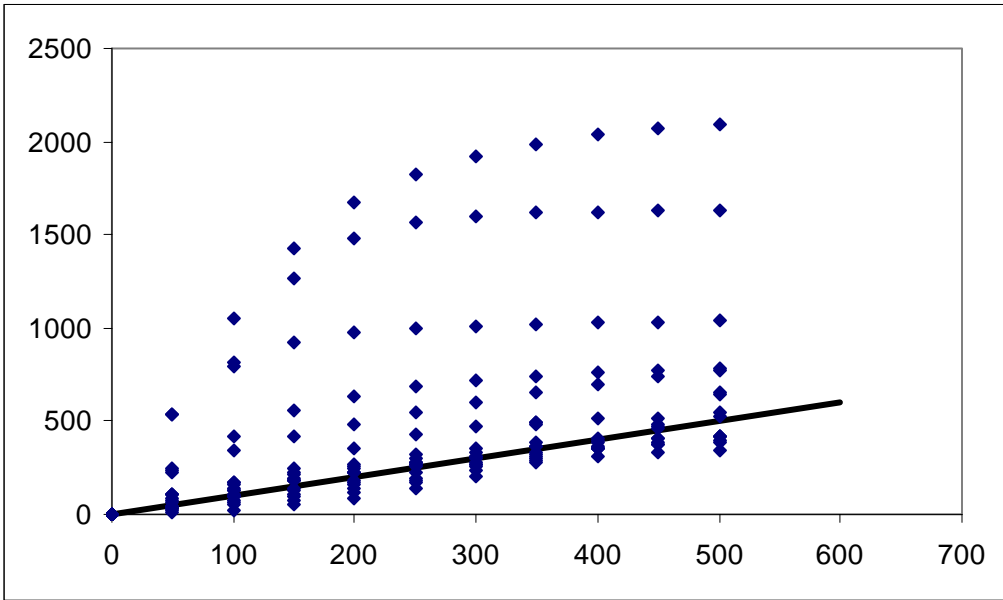
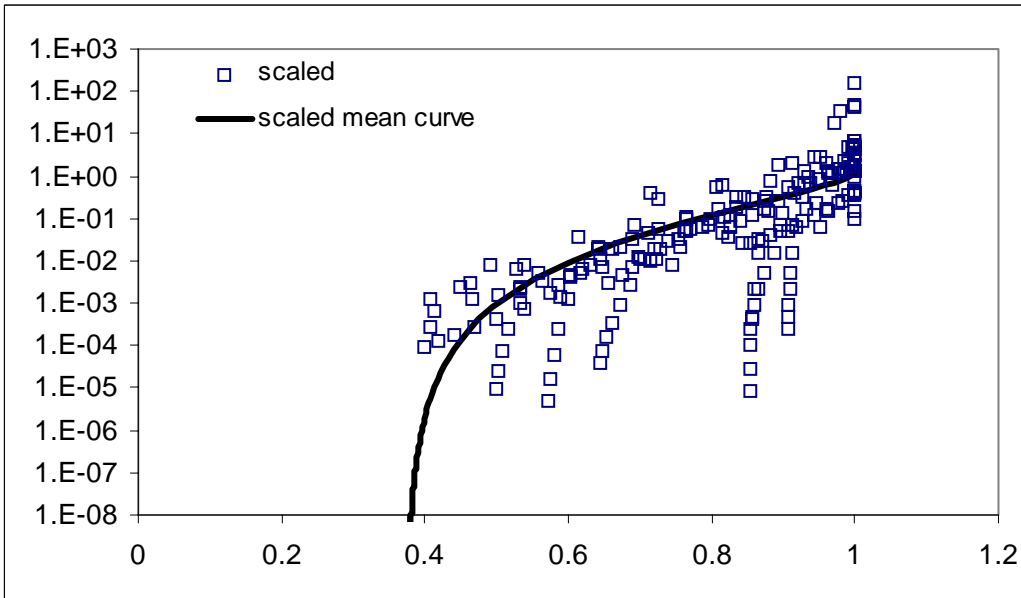
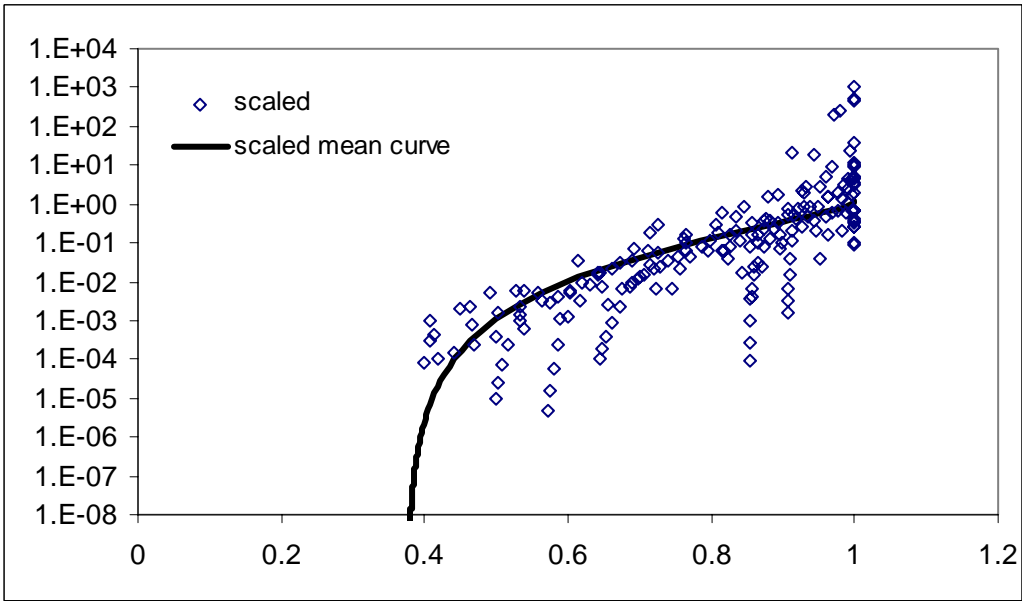
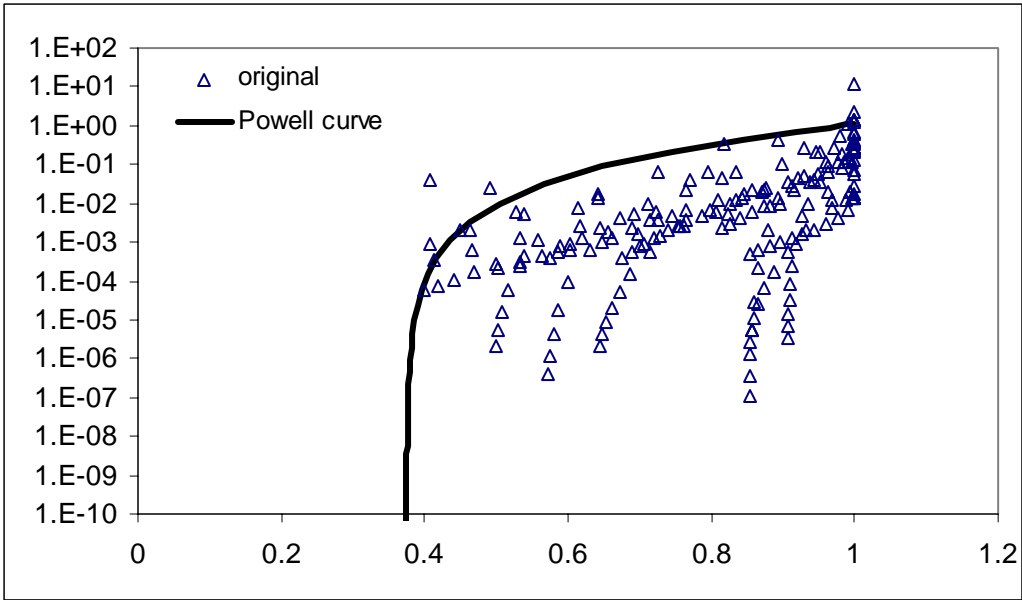


Figure 4.5.4a-e. Soil water pressure head (a) unscaled (b) scaled using method 1, and (c) scaled using method 2. Original and descaled soil water pressure head curves using method 1 (d) and method 2 (e). All curves represent Group 3, Population 1, subgroup sandy loam.



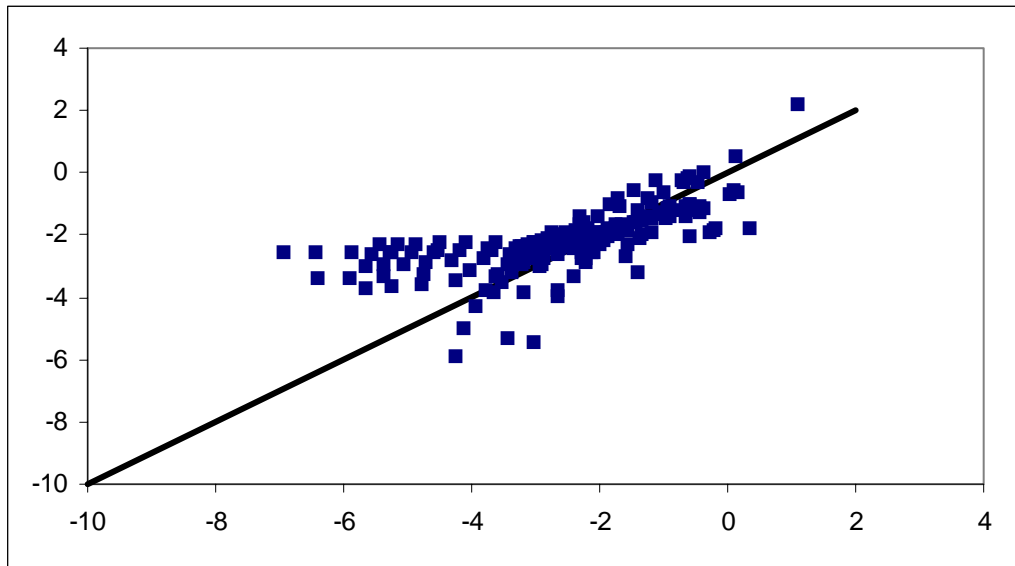
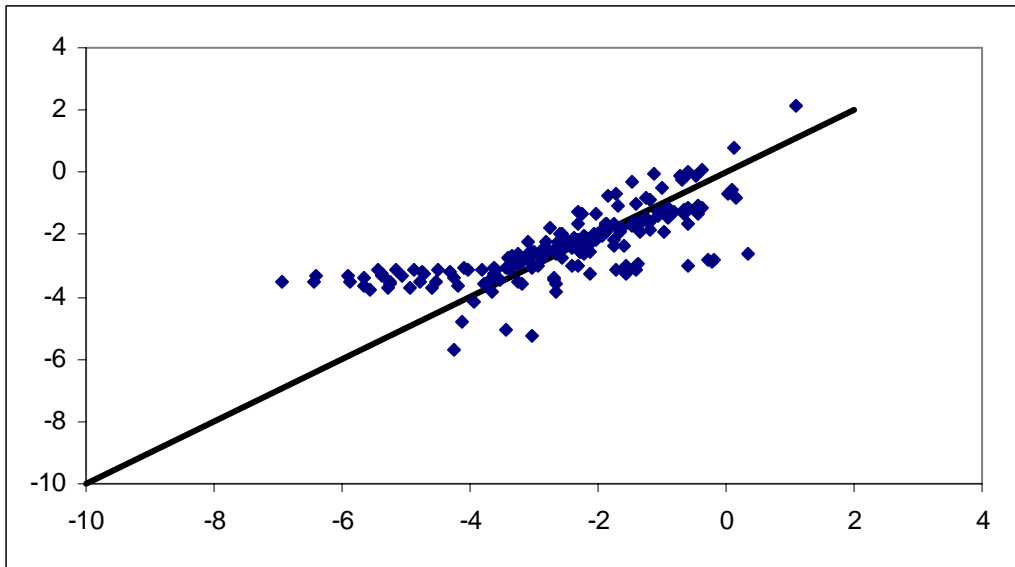
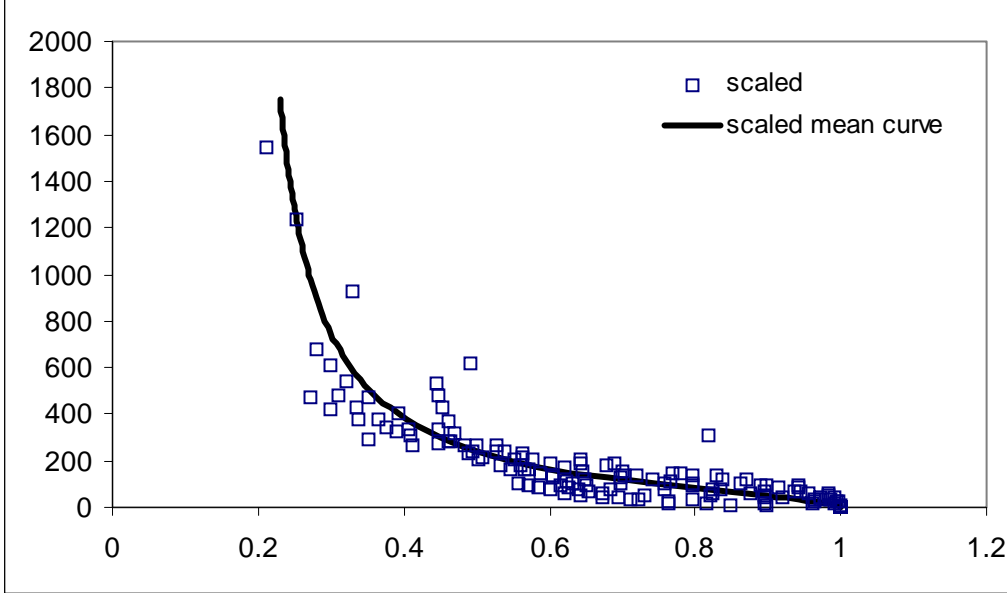
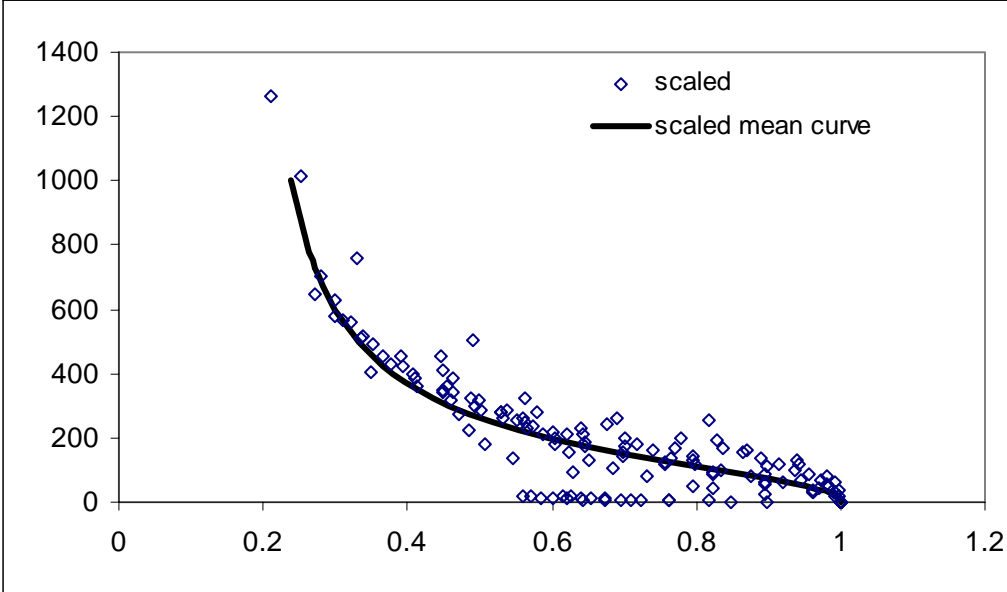
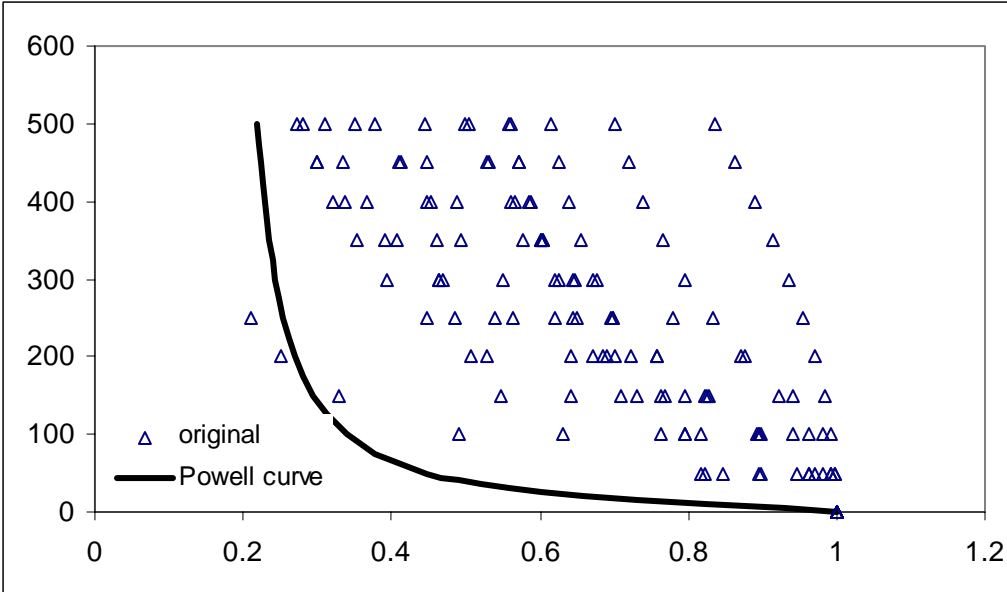


Figure 4.5.4f-j. Unsaturated hydraulic conductivity (f) unscaled, (g) scaled using method 1, and (h) scaled using method 2. Original and descaled unsaturated hydraulic conductivity using method 1 (i) and method 2 (j). All curves represent Group 3, Population 1, subgroup sandy loam.



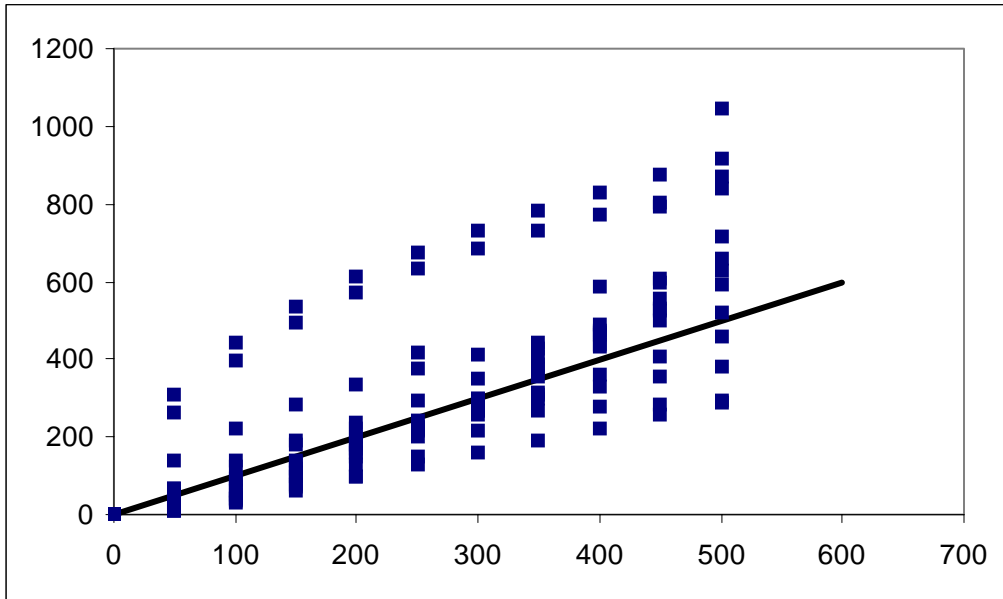
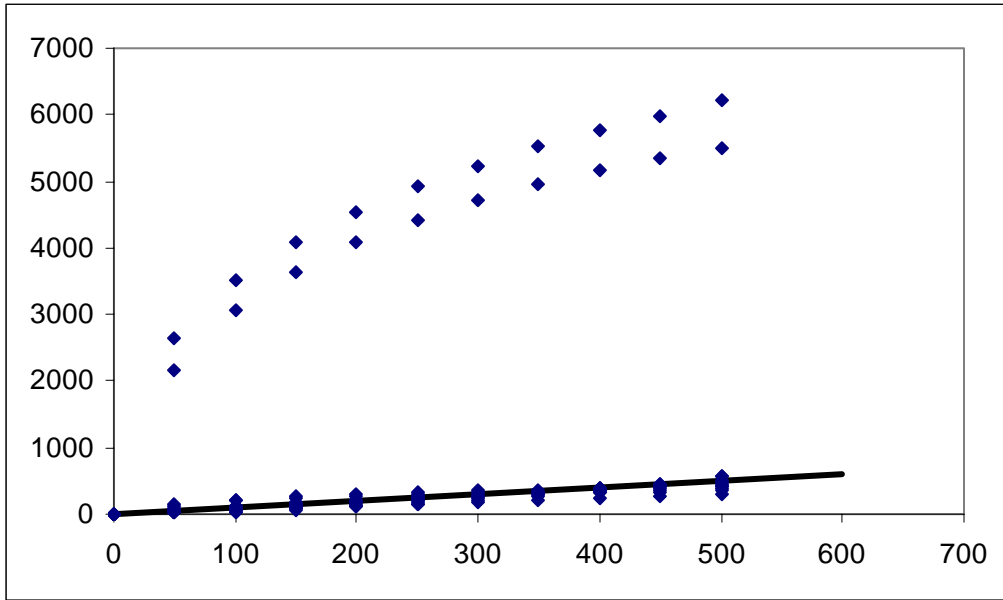
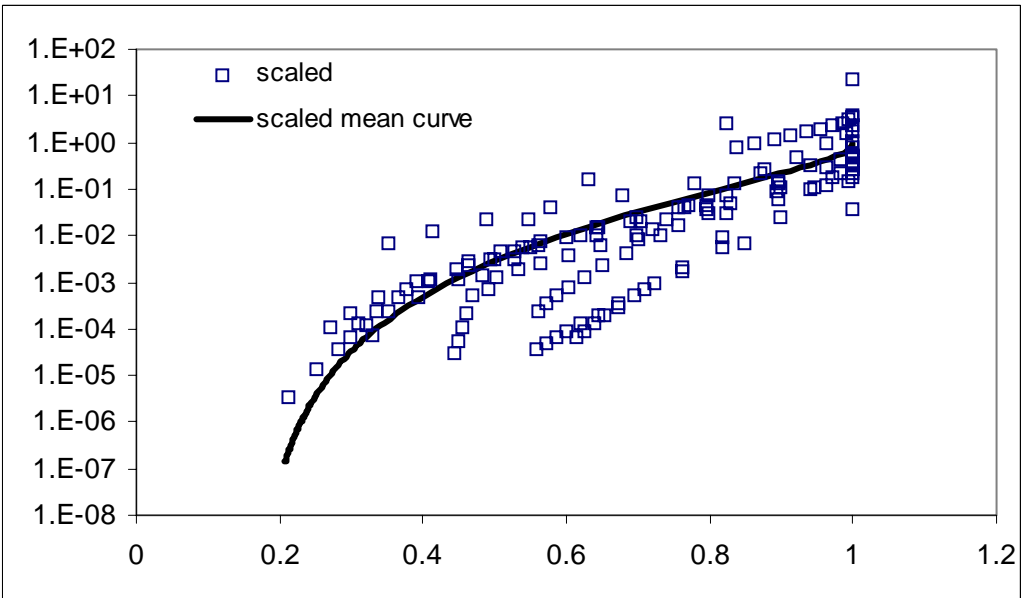
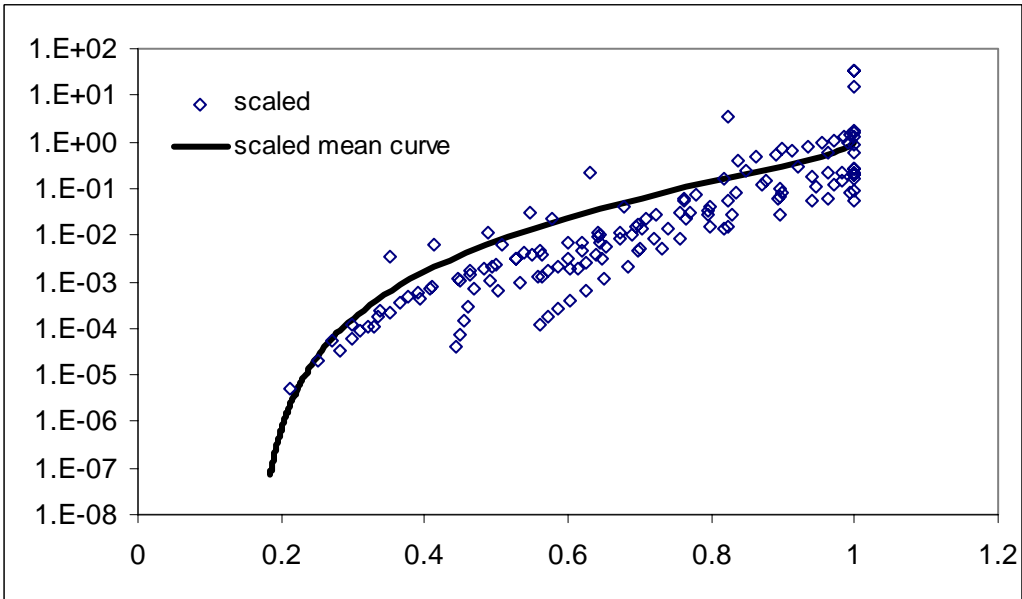
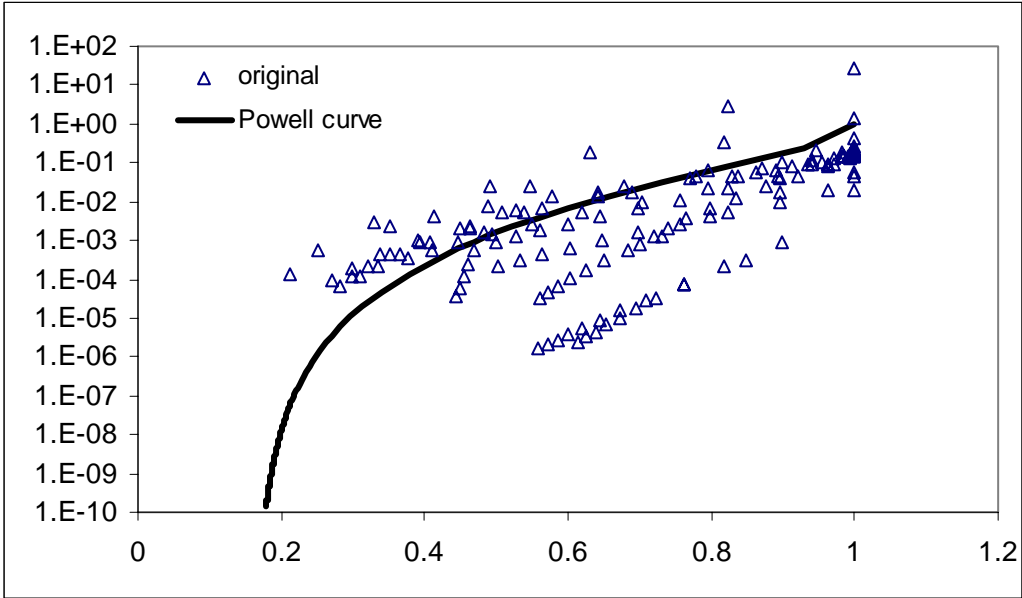


Figure 4.5.5a-e. Soil water pressure head (a) unscaled, (b) scaled using method 1, and (c) scaled using method 2. Original and descaled soil water pressure head curves using method 1 (d) and method 2 (e). All curves represent Group 4, Population 1, subgroup sandy loam.



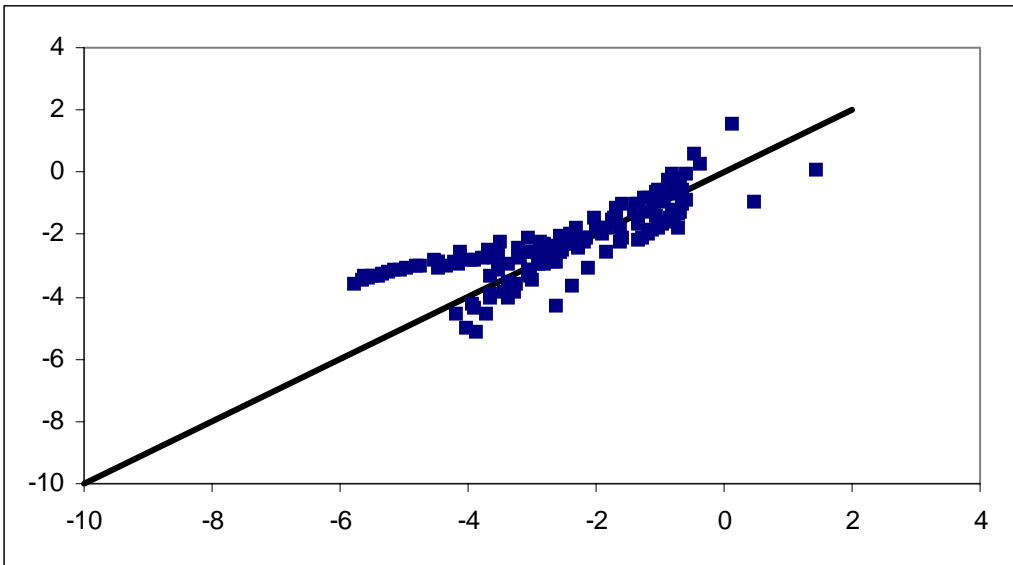
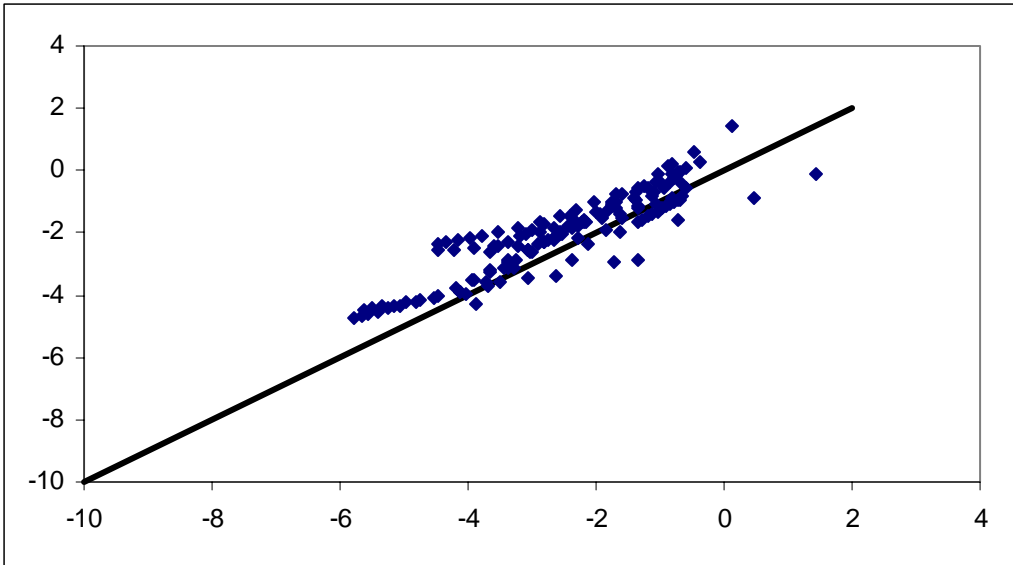


Figure 4.5.5f-j. Unsaturated hydraulic conductivity (f) unscaled, (g) scaled using method 1, and (h) scaled using method 2. Original and descaled unsaturated hydraulic conductivity (i-j) for Group 4, Population 1, subgroup sandy loam.



Photos 1 – 3: The irrigation begins in the afternoon. Prior to this particular irrigation, the flood basin has been mowed and rotovated to 6” depth after a application of potassium bromide (see section 2.6).



Photo 4. Another view of the irrigation pipe.



Photo 5. Overnight, the irrigation water has spread throughout the basin.



Photos 6 and 7. While water is filling the basin in the direction of the arrows, the irrigation is does not completely cover the row basin. The irrigation pipe is shown in the foreground.





Photos 8-11: Additional images of irrigation in other tree row basins (near the end of the irrigation cycle).